Universidade Estadual Paulista
“Júlio de Mesquita Filho”

Faculdade de Ciências Farmacêuticas - FCF

Fernando Roberto Paz Cedeño

Imobilização de celulases e xilanases em óxido de grafeno magnetizado: avaliação cinética e potencial da hidrólise sobre bagaço de cana-de-açúcar

Araraquara
2021

Universidade Estadual Paulista
“Júlio de Mesquita Filho”

Faculdade de Ciências Farmacêuticas - FCF

Imobilização de celulases e xilanases em óxido de grafeno magnetizado: avaliação cinética e potencial da hidrólise sobre bagaço de cana-de-açúcar

Fernando Roberto Paz Cedeño

Tese apresentada ao Programa de Pós-graduação em Alimentos e Nutrição para obtenção do título de Doutor em Alimentos e Nutrição.

Área de concentração: Ciência dos Alimentos

Orientador: Prof. Dr. Fernando Masarin

Araraquara
2021

Imobilização de celulases e xilanases em óxido de grafeno magnetizado: avaliação cinética e potencial da hidrólise sobre bagaço de cana-de-açúcar

Fernando Roberto Paz Cedeño

Tese apresentada ao Programa de Pós-graduação em Alimentos e Nutrição para obtenção do título de Doutor em Alimentos e Nutrição.

Área de concentração: Ciência dos Alimentos

Orientador: Prof. Dr. Fernando Masarin

Araraquara
2021

Immobilization of cellulases and xylanases on magnetized graphene oxide: kinetic evaluation and potential of sugarcane bagasse hydrolysis

Fernando Roberto Paz Cedeño

Thesis presented to the Graduate Program in Food and Nutrition to obtain the title of Doctor in Food and Nutrition.

Concentration area: Food Science

Advisor: Prof. Dr. Fernando Masarin

Araraquara

2021

Paz Cedeño, Fernando Roberto.
P348i Imobilização de celulases e xilanases em óxido de grafeno magnetizado: avaliação cinética e potencial da hidrólise sobre bagaço de cana-de-açúcar / Fernando Roberto Paz Cedeño. – Araraquara: [S.n.], 2021.
226 f. : il.

Tese (Doutorado) – Universidade Estadual Paulista. "Júlio de Mesquita Filho". Faculdade de Ciências Farmacêuticas. Programa de Pós Graduação em Alimentos e Nutrição. Área de Concentração em Ciência dos Alimentos.

Orientador: Fernando Masarin.

1. Material lignocelulósico. 2. Pré-tratamentos. 3. Hidrólise enzimática. 4. Imobilização de enzimas. 5. Óxido de grafeno. 6. Nanopartículas magnéticas. 7. Reutilização de derivado enzimático. I. Masarin, Fernando, orient. II. Título.

Diretoria do Serviço Técnico de Biblioteca e Documentação - Faculdade de Ciências Farmacêuticas
UNESP - Campus de Araraquara

CAPES: 33004030055P6
Esta ficha não pode ser modificada

UNIVERSIDADE ESTADUAL PAULISTA

Câmpus de Araraquara

CERTIFICADO DE APROVAÇÃO

TÍTULO DA TESE: Imobilização de celulases e xilanases em óxido de grafeno magnetizado: avaliação cinética e potencial da hidrólise sobre bagaço de cana-de-açúcar

AUTOR: FERNANDO ROBERTO PAZ CEDEÑO

ORIENTADOR: FERNANDO MASARIN

Aprovado como parte das exigências para obtenção do Título de Doutor em ALIMENTOS E NUTRIÇÃO, área: Ciência dos Alimentos pela Comissão Examinadora:

Prof. Dr. FERNANDO MASARIN (Participaçao Virtual)
Departamento de Engenharia de Bioprocessos e Biotecnologia / Faculdade de Ciências Farmacêuticas - UNESP - Araraquara

Prof. Dr. MICHEL BRIENZO (Participaçao Virtual)
Laboratório de Caracterização de Biomassa / Instituto de Pesquisa em Bioenergia de Rio Claro - UNESP

Prof. Dr. JOÃO RENATO CARVALHO MUNIZ (Participaçao Virtual)
Departamento de Física e Ciência Interdisciplinar / Instituto de Física de São Carlos - USP

Prof. Dr. RODRIGO FERNANDO COSTA MARQUES (Participaçao Virtual)
Departamento de Química Analítica, Físico-Química e Inorgânica / Instituto de Química - UNESP - Araraquara

Araraquara, 16 de março de 2021

Dedico este trabalho à minha esposa Alessandra

e ao meu filho Fernando Davi.

Agradecimentos

À Coordenação de Aperfeiçoamento de Pessoal de Nível Superior - Brasil (CAPES), pela bolsa de doutorado no Brasil e estágio sanduíche na Espanha. O presente trabalho foi realizado com apoio da (CAPES) - Código de Financiamento 001;

Ao Prof. Dr. Fernando Masarin, pela orientação, os ensinamentos e dedicação durante o desenvolvimento da pesquisa;

Ao Prof. Dr. Rubens Monti pelos ensinamentos, e por ter me recebido no Laboratório de Enzimologia;

Aos professores Dr. Avelino Corma, Dra. Sara Iborra e os pesquisadores Dr. José Miguel Carceller e Dra. Karen Arias por ter me recebido e orientado no Instituto de Tecnologia Química da Universitat Politècnica de València;

Ao Prof. Dr. Ricardo Keitel Donato e a pesquisadora Dra. Anna Paula Godoy pelos ensinamentos e apoio durante o estágio no Centro de Pesquisa em Grafeno e Nanomateriais MackGraphe da Universidade Presbiteriana Mackenzie

Ao Departamento de Alimentos e Nutrição e ao Departamento de Engenharia de Bioprocessos e Biotecnologia da Faculdade de Ciências Farmacêuticas (FCF), por toda a infraestrutura e apoio;

À Faculdade de Ciências Farmacêuticas (FCF-UNESP) de Araraquara;

À Seção Técnica da Pós-graduação;

Aos professores, funcionários, técnicos de laboratório, pós-graduandos e graduandos da Faculdade de Ciências Farmacêuticas (FCF) de Araraquara - UNESP e do Instituto de Tecnologia Química da UPV;

Agradecimentos pessoais

A Deus por este presente maravilhoso que é a vida;

À minha esposa, pelo amor, paciência, compreensão e apoio. Obrigado por ser parte da minha vida;

Aos meus pais, por serem modelos de coragem, pelo apoio e amor incondicional. Meu infinito agradecimento;

Aos meus irmãos, aos meus sogros e meus cunhados, pelo apoio, carinho e confiança;

Aos meus amigos e companheiros de laboratório da UNESP e da UPV: Eddyn, Juliana, Leonardo, Johana, Maísa, Lídia, Ismael, José Miguel, Karen, Beatriz, Elena, Hans, Anna, pelos momentos de descontração e pelo auxilio durante a pesquisa;

Aos que aqui não foram citados, mas fizeram parte da minha trajetória e de alguma maneira cooperaram para o desenvolvimento deste projeto;

A todos, muito obrigado;

“...de cierto os digo que todo cuanto pidiereis al Padre en mi nombre, os lo dará. Hasta ahora nada habéis pedido en mi nombre; pedid y recibiréis, para que vuestro gozo sea cumplido.”

Juan 16:23-24

RESUMO

O fracionamento de materiais lignocelulósicos é uma etapa fundamental para a utilização desses recursos na produção de bioprodutos de interesse comercial, como por exemplo, os biocombustíveis; no entanto, na etapa de hidrólise enzimática são encontrados problemas com a estabilidade de enzimas e seu custo. Uma estratégia para contornar este problema é a imobilização de enzimas em suportes sólidos com o objetivo principal de reutilizá-las. **Objetivo:** O objetivo deste trabalho foi estudar a imobilização de celulases e xilanases em óxido de grafeno magnético (OG-NPM) e aplicar o biocatalizador obtido na hidrólise de bagaço de cana-de-açúcar. **Métodos:** O bagaço de cana-de-açúcar foi pré-tratado em diferentes condições. As biomassas obtidas foram caracterizadas quimicamente e estruturalmente. O óxido de grafeno (OG) foi obtido pelo método tradicional de *Hummer's* e a adição de nanopartículas magnéticas foi realizada por co-precipitação de sais de ferro, obtendo o OG-NPM, o qual foi caracterizado estruturalmente. A imobilização de enzimas no OG-NPM foi realizada com os reagentes 1-etil-3-(3-dimetilaminopropil) carbodiimida e N-hidroxissuccinimida (NHS) obtendo-se o derivado (OG-NPM-Enz). O OG-NPM-Enz foi avaliado quanto à estabilidade térmica, de armazenamento, além dos efeitos da temperatura e pH na atividade enzimática. **Resultados:** O bagaço de cana-de-açúcar pré-tratado com sulfito-NaOH (SSB) apresentou maior remoção da lignina, mantendo-se a fração celulósica intacta. Além disso, o SSB apresentou a melhor resposta à hidrólise enzimática de celulose e xilana, em comparação aos bagaços submetidos a outros pré-tratamentos, atingindo conversões de 90%. O OG-NPM-Enz apresentou atividade relativa de endoglucanase, xilanase, β-glucosidase e β-xilosidase de 70%, 66%, 88%, e 70%, respectivamente, após 10 ciclos de atividade de seus respectivos substratos, resultando na maior frequência de *turnover* ($g.g^{-1}.h^{-1}$) quando comparado com reportados na literatura. O tempo de meia-vida ($t_{1/2}$) das enzimas imobilizadas foram superiores do que as enzimas em sua forma livre, com exceção de endoglucanase. Após 45 dias de armazenamento refrigerado, o OG-NPM-Enz apresentou atividades enzimáticas relativas superiores a 65% para todas as enzimas avaliadas. A taxa de hidrólise do SSB utilizando enzimas em suas formas livres foi maior quando comparado com as enzimas imobilizadas, porém, após 72h de hidrólise, as conversões de celulose e xilana em glicose e xilose, respetivamente, foram semelhantes com o uso de enzimas em suas formas livre ou imobilizada. O OG-NPM-Enz foi reutilizado com sucesso em vários ciclos de hidrólise do SSB, resultando em uma eficiência de aproximadamente 80% após o último ciclo. **Conclusão:** Os resultados mostram que a imobilização de celulases e xilanases melhora a estabilidade térmica das enzimas e o derivado obtido tem a capacidade de ser reutilizado na hidrólise do SSB, sendo, portanto, o OG-NPM-Enz um candidato potencial a ser aplicado, por exemplo, em processos de produção de bioetanol em escala piloto e industrial.

PALAVRAS-CHAVE: Material lignocelulósico; Pré-tratamentos; Hidrólise enzimática; Imobilização de enzimas; Óxido de grafeno; Nanopartículas magnéticas; Reutilização de derivado enzimático.

ABSTRACT

The fractioning of lignocellulosic materials is a fundamental step for the use of these resources in the production of bioproducts of commercial interest, such as biofuels; however, in the enzymatic hydrolysis stage, problems with enzyme stability and cost are encountered. An interesting strategy to overcome this problem is the immobilization of enzymes on solid supports with the aim of reusing them. **Objective:** The objective of this work was to study the immobilization of cellulases and xylanases in magnetic graphene oxide (GO-MNP) and to apply the biocatalyst obtained in the hydrolysis of sugarcane bagasse. **Methods:** The sugarcane bagasse was pre-treated under different conditions. The obtained biomasses were characterized chemically and structurally. Graphene oxide (GO) was obtained by the traditional Hummer's method and the addition of magnetic nanoparticles was carried out by co-precipitation of iron salts, obtaining the OG-NPM, which was structurally characterized. The immobilization of enzymes on GO-MNP was performed with the reagents 1-ethyl-3- (3-dimethylaminopropyl) carbodiimide and N-hydroxysuccinimide (NHS) obtaining the biocatalyst (GO-MNP-Enz). The GO-MNP-Enz was evaluated for thermal stability, storage, in addition to the effects of temperature and pH on enzyme activity. **Results:** The sugarcane bagasse pretreated with sulfite-NaOH (SSB) showed a greater removal of the lignin, keeping the cellulosic fraction intact. In addition, SSB showed the best response to enzymatic hydrolysis of cellulose and xylan, in comparison to sugarcane bagasse submitted to other pretreatments, reaching conversions of 90%. The GO-MNP-Enz showed relative activity of endoglucanase, xylanase, β-glucosidase and β-xylosidase of 70%, 66%, 88%, and 70%, respectively, after 10 hydrolysis cycles of their respective substrates, resulting in the greatest frequency turnover ($g.g^{-1}.h^{-1}$) when compared to those reported in the literature. The half-life ($t_{1/2}$) of immobilized enzymes was longer than the enzymes in their free form, with the exception of endoglucanase. After 45 days of cold storage, GO-MNP-Enz showed relative enzymatic activities greater than 65% for all evaluated enzymes. The hydrolysis rate of SSB using enzymes in their free forms was higher when compared to immobilized enzymes, however, after 72 h of hydrolysis, the conversions of cellulose and xylan into glucose and xylose were similar with the use of enzymes in their free or immobilized forms. GO-MNP-Enz was successfully reused in several cycles of SSB hydrolysis, resulting in an efficiency of approximately 80% in the last cycle. **Conclusion:** The results show that the immobilization of cellulases and xylanases improves the thermal stability of the enzymes and the biocatalyst obtained has the ability to be reused in the hydrolysis of the SSB, therefore, GO-MNP-Enz is a potential candidate to be applied, for example, in bioethanol production processes on a pilot and industrial scale.

KEYWORDS: Lignocellulosic material; Pretreatments; Enzymatic hydrolysis; Enzyme immobilization; Graphene oxide; Magnetic nanoparticles; Reuse of enzyme biocatalyst.

LIST OF TABLES

CHAPTER 3

LIST OF FIGURES

3. CHAPTER 2

4. CHAPTER 3

SUMMARY

1. INTRODUCTION

Biofuels represent a topic of great global repercussion due to the current dependence on oil products for energy production and its consequence on the planet's climate changes. In this scenario, Brazil has an excellent opportunity to operate in new energy matrixes associated with the production of fuels and chemicals through renewable sources.

Sugarcane production in Brazil in the 2019/2020 period was around 643 million tons [1]. Sugarcane bagasse (SCB) is an abundant agricultural by-product from sugar-ethanol processing. SCB is usually burned / oxidized by plants for cogeneration of electricity. However, several plants do not have a thermoelectric plant (energy cogeneration) with the capacity to burn / oxidize all the SCB generated in the industry. Thus, excess SCB (around 20% of the amount) can be used for the production of different bioproducts from fractionation by chemical-enzymatic techniques. Several studies show that SCB is an economical and sustainable biomass for obtaining value-added products, such as bioethanol [2–6], biodiesel [7], biobutanol [8,9], biohydrogen [10–12], xylitol [13–16], citric acid [17], succinic acid [18], itaconic acid [19], lactic acid [20], butyric acid [21], gluconic acid [22], furfural [23], oligosaccharides [24–26], reducing sugars [27–29], among others.

Although SCB contains enough cellulose and hemicellulose to be used as a source of sugars for the production of bioproducts, such as bioethanol, this by-product is a highly recalcitrant lignocellulosic material and requires an efficient pretreatment step to guarantee a high conversion of cellulose to glucose, in a second step of enzymatic hydrolysis [30–32]. The recalcitrance

of lignocellulosic materials is related to several factors, including the close association of cellulose with hemicellulose and lignin in the cell wall, making it difficult for enzyme infiltration and action [33].

Biocatalysis processes have been applied in several sectors of biotechnology due to their high specificity, ease of production and conservation of the environment. The use of enzymes in industrial applications may be limited depending on their cost. In addition, maintaining the structural stability of some enzymes during any biochemical reaction is a major challenge [34]. According to Aragon (2013), the immobilization of enzymes in solid materials offers many advantages, among which the reuse of the enzyme, the separation of the product and the increase of enzymatic stability.

Graphene oxide (GO) is a highly versatile chemical platform due to the large surface area it offers, in addition to several chemical groups located on its surface. In this way, GO is a great support for immobilizing enzymes [36]. Recently, some work on GO magnetization, prior to its use as a support for enzyme immobilization, has been carried out, showing great potential for application [37,38].

Sugarcane Bagasse (SCB): main constituents and pre-treatments

Brazil, one of the largest agricultural producers in the world, generates significant amounts of biomass by-products in activities resulting from harvesting and processing products such as rice, cotton, sugar cane, corn and soybeans. Agricultural by-products come from the stage of cultivation of certain species, while agro-industrial by-products result from industrial

biomass processing [39]. Three different solid residues are produced in the processing of sugarcane: straw (during harvest), SCB and filter cake (in the ethanol process) [40,41]. Agro-industrial by-products, such as SCB, have a highly complex structure and chemical composition. The microstructure is linked to low molecular weight substances that include organic and inorganic substances. However, the macrostructure comprises macromolecules: cellulose, hemicellulose and lignin [42]. It is important to emphasize that the components of BCA are closely associated, in order to constitute the cell complex of plant biomass.

Cellulose

The cellulose structure can be classified into three organizational levels. The first is defined by the sequence of cellobiose residues linked by covalent bonds, forming the anhydroglycoside homopolymer that contains glycosidic bonds of the type β-D(1→4) (Figure 1.1), general formula $(C_6H_{10}O_5)n$.

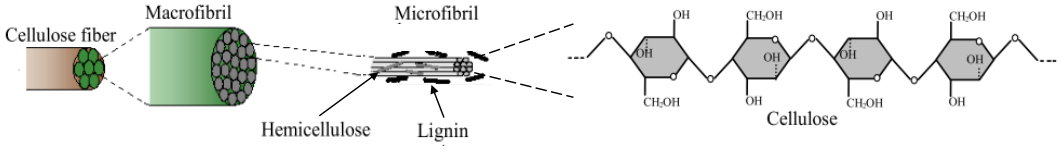

Figure 1.1. Cellulose molecule structure [43].

Figure 1.2 shows the second level that describes the molecular conformation, that is, the spatial organization of the repetitive units, being characterized by the lengths of the bonds and respective angles and by the intramolecular and intermolecular hydrogen bonds. The third level defines the association of molecules, forming aggregates with a given crystalline structure.

These aggregates provide high resistance to tension, making cellulose insoluble in water and in a large number of organic solvents. [44,45].

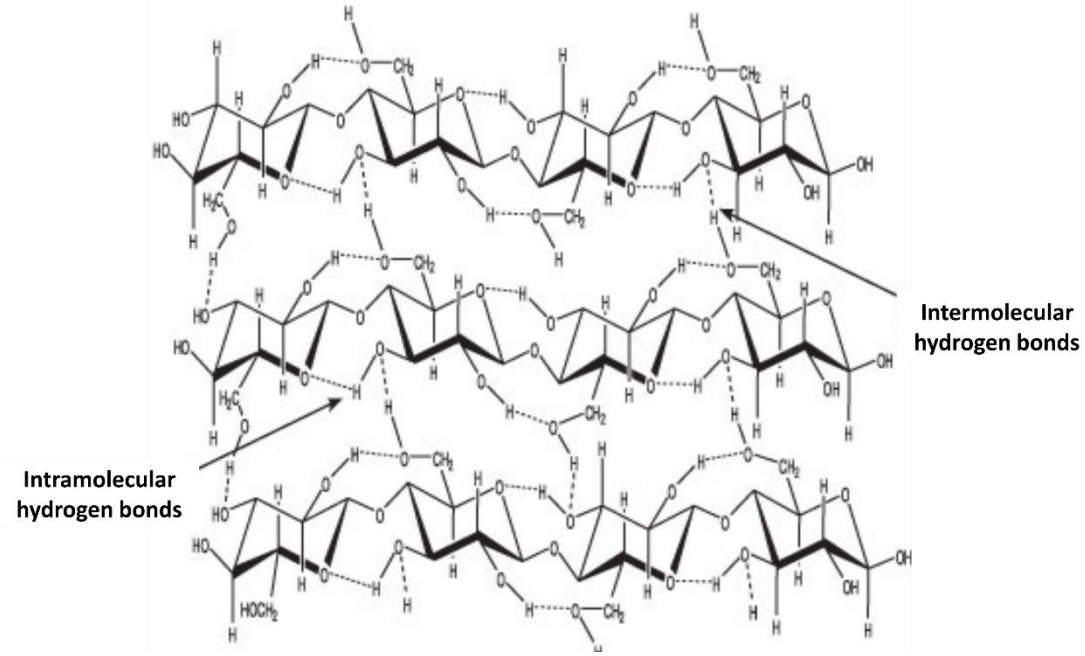

Figure 1.2. Representation of cellulose supramolecular hydrogen bonds [44].

Hemicellulose

Hemicelluloses, also called polioses, are polysaccharides that make up the cell wall of plants, which occupy the second most renewable polymer in lignocellulosic materials, after cellulose. They represent a type of polysaccharide with a lower degree of polymerization (100-200 units) containing pendent groups. The complex structure contains xylose, glucose, mannose, galactose, arabinose, rhamnose, glucuronic acid and galacturonic acid as constituents, in varying amounts, depending on the plant source. [44,46–48]. Hemicelluloses are normally covalently linked to other components of the cell wall of lignocelluloses such as lignin and phenolic compounds [48].

The main hemicelluloses found in plants are xyloglucans (XyG), glucuronoarabinoxylans (GAX) and mannans (MN). Most plants have xyloglucan as the main hemicellulose. However, grasses have glucuronoarabinoxylans (GAX) as their main hemicellulose (Figure 1.3) [48], although they also have, in small proportions, xyloglucans and mannans. In addition to GAX, β-glucans are also found in sugarcane tissues [48,49].

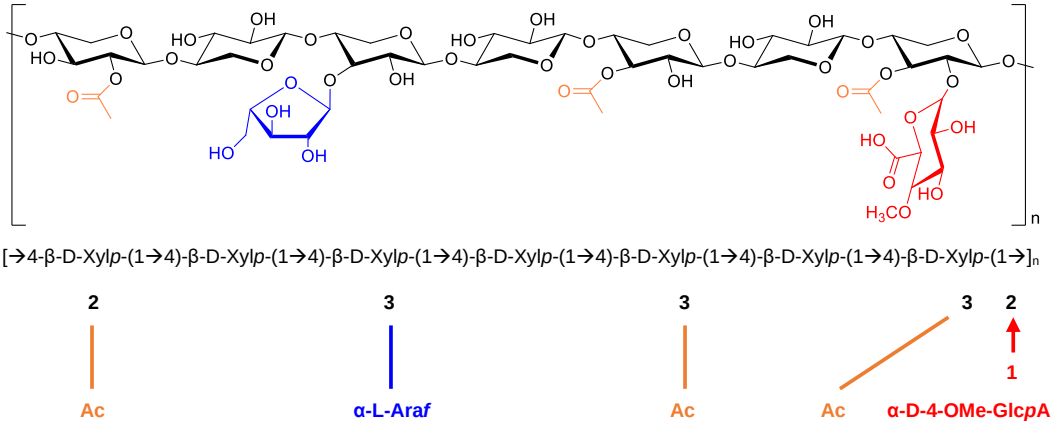

Figure 1.3. Schematic representation of the general structure of the glucuronoarabinoxylan molecule (GAX). Adapted from Ek et al. [50].

Lignin

Lignin is a complex amorphous macromolecule made up of phenylpropane units derived from three basic monomeric units: p-hydroxyphenyl (H), guaiacyl (G), and syringyl (S) that vary in quantity between species and according to the type of tissue in the cells. It is formed by the dehydrogenative polymerization of hydroxycinnamic alcohols (p-coumaryl, coniferyl and synaphyl). Because the polymerization process is random, the lignin macromolecule has a very complex structure, as shown in the model in Figure 1.4 [51].

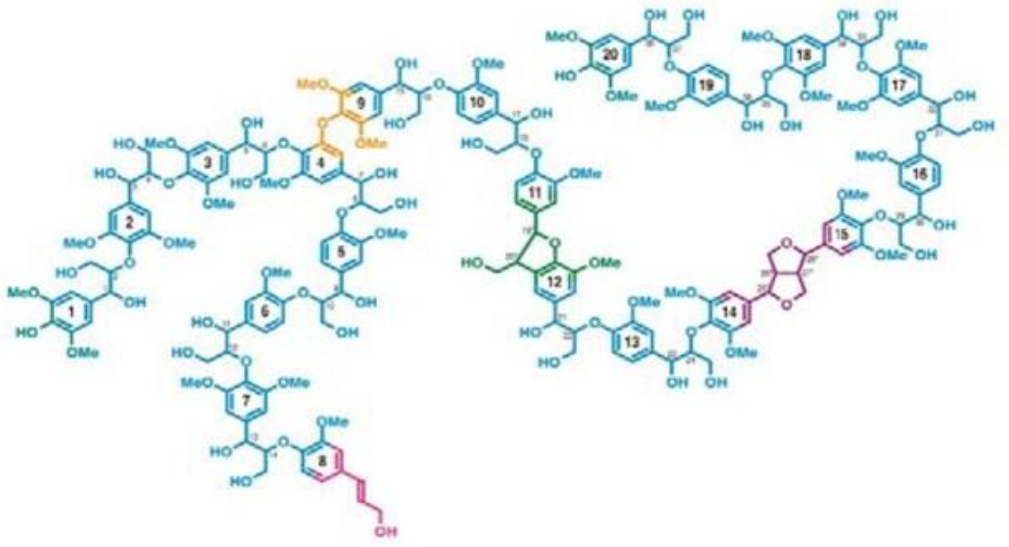

Figure 1.4. Proposed lignin structure model [51].

The structure of lignin is not homogeneous since it has amorphous regions and a globular structure [44,52,53]. The lignin structure hypothesis arises from the polymerization of phenyl radicals (β-O-4 ether bond, which are the most common bonds) formed on the cell wall by oxidative enzymes. Hardwood lignins are predominant in G and S units with traces of H units. Coniferous wood lignins (softwood) are mostly composed of G units [52,54], whereas monocotyledons or grasses (examples: corn straw, straw and SCB) incorporate equivalent amounts of G and S units, together with significantly higher amounts of H units [52].

Lignin in grasses is closely linked to hemicellulose through ferulic and p-cumaric acids. These phenolic acids are linked to the carbon 5 of an arabinose molecule, by an ester-type bond (Figure 1.15). Arabinose (pendant group) is coupled to hemicellulose (xylan) through an ether bond (Figure 1.5) [55].

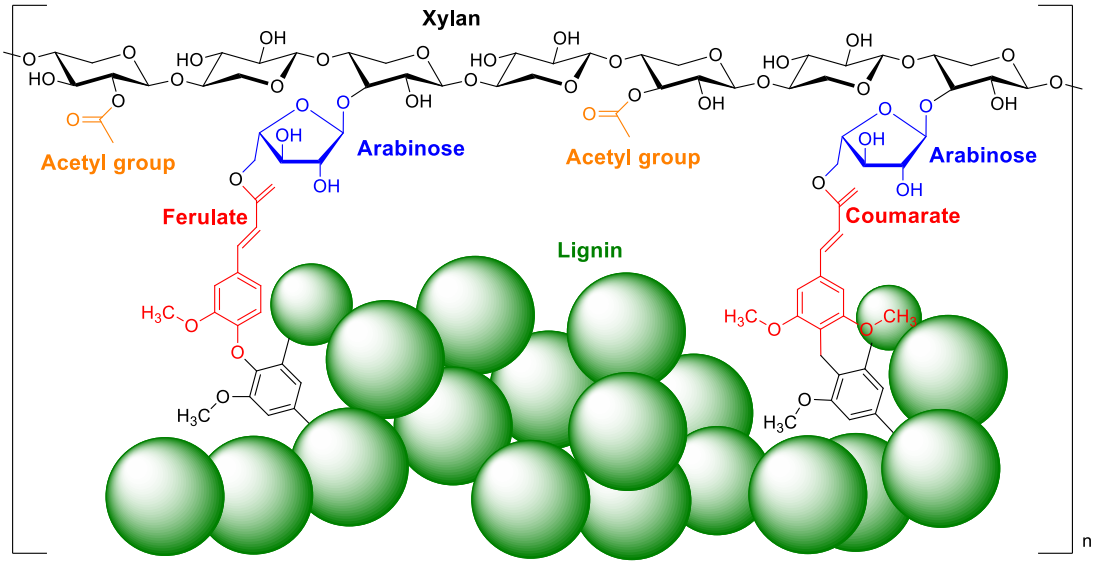

Figure 1.5. Scheme showing residues of ferulate and coumarate coupled to sugarcane bagasse lignin. Adapted from Hatfield et al. [55].

Lignin is connected to phenolic acids through propanoic chains on α-carbon, these bonds being ether-type. Phenolic acids are coupled to lignin via radical processes [55]. However, ferulic and p-cumáric acids are only coupled to monomers (coniferyl and synaphyl alcohols) and not to lignin oligomers, their main function being to act as nucleation points in the lignin biosynthesis in grasses [55]. Xu *et al*., [56] reported that BCA has approximately 1.2-1.3% ferulic acid and 1.6-1.8% p-cumaric acid.

Pretreatments

Pretreatment is one of the most important steps in the conversion of SCB, as it directly affects the efficiency of enzymatic hydrolysis. The main objective of pre-treatment is to cleave the recalcitrant structures of lignin in SCB making cellulose and hemicellulose more accessible to enzymes for efficient conversion into fermentable sugars [57,58]. The efficiency of lignin

removal depends on the type of pre-treatment used and the ideal conditions maintained during it. Pretreatments can be physical, chemical, biological or can be a combination of these methods. Although different pretreatments are available, developing pretreatment with or without little inhibitor formation is a challenge [59].

In the industrial sector, acid hydrolysis is considered the most prominent pre-treatment method. It is usually carried out with diluted solutions of mineral acids, organic acids and sulfur dioxide. The acid cleaves the glycosidic bonds of the polysaccharides which results in the formation of reducing sugars. The most commonly used acids are: sulfuric acid, nitric acid and hydrochloric acid [60].

Alkali-based pretreatments are also widely used to increase cellulose digestibility and remove lignin. Sodium hydroxide and potassium hydroxide are most commonly used, while some other alkalis, such as calcium hydroxide and ammonia, can also be used. This is a delignification process in which part of the lignin and hemicellulose are solubilized. The main reactions of the alkaline pretreatment are: abstraction of a proton from a free phenolic OH found in the aromatic rings of the lignin molecule resulting in the formation of a structure called methylene quinone, which favors the cleavage of the α-aryl ether bond and partial dissolution of lignin; cleavage of ester-like bonds located between hemicellulose and lignin, known as saponification, which leads to the separation of the lignin-carbohydrate complex, and the exposure of cellulose microfibrils increasing the enzymatic digestibility of cellulose [57,58].

Sulphonation of lignin by the action of bisulfite ions (HSO_3^-) is another widely used pretreatment. This process is usually conducted with sodium sulfite and can be in acidic or alkaline conditions. The reaction between a phenylpropane and bisulfite unit under acidic conditions proceeds through protonation of the hydroxyl group followed by the removal of water and addition of the bisulfite ion (Figure 1.6a). In neutral or alkaline conditions, the mechanism is analogous to the reaction in kraft pulping, through the formation of a methylene quinone intermediate followed by the addition of a sulfite ion to the α carbon, making the phenolic OH again protonated and the sulfonated α carbon. The chemical reaction proceeds with the cleavage of the β-aryl-ether bond, between the two aromatic rings culminating in the β-carbon sulfonation and lignin degradation (Figure 1.6b) [61].

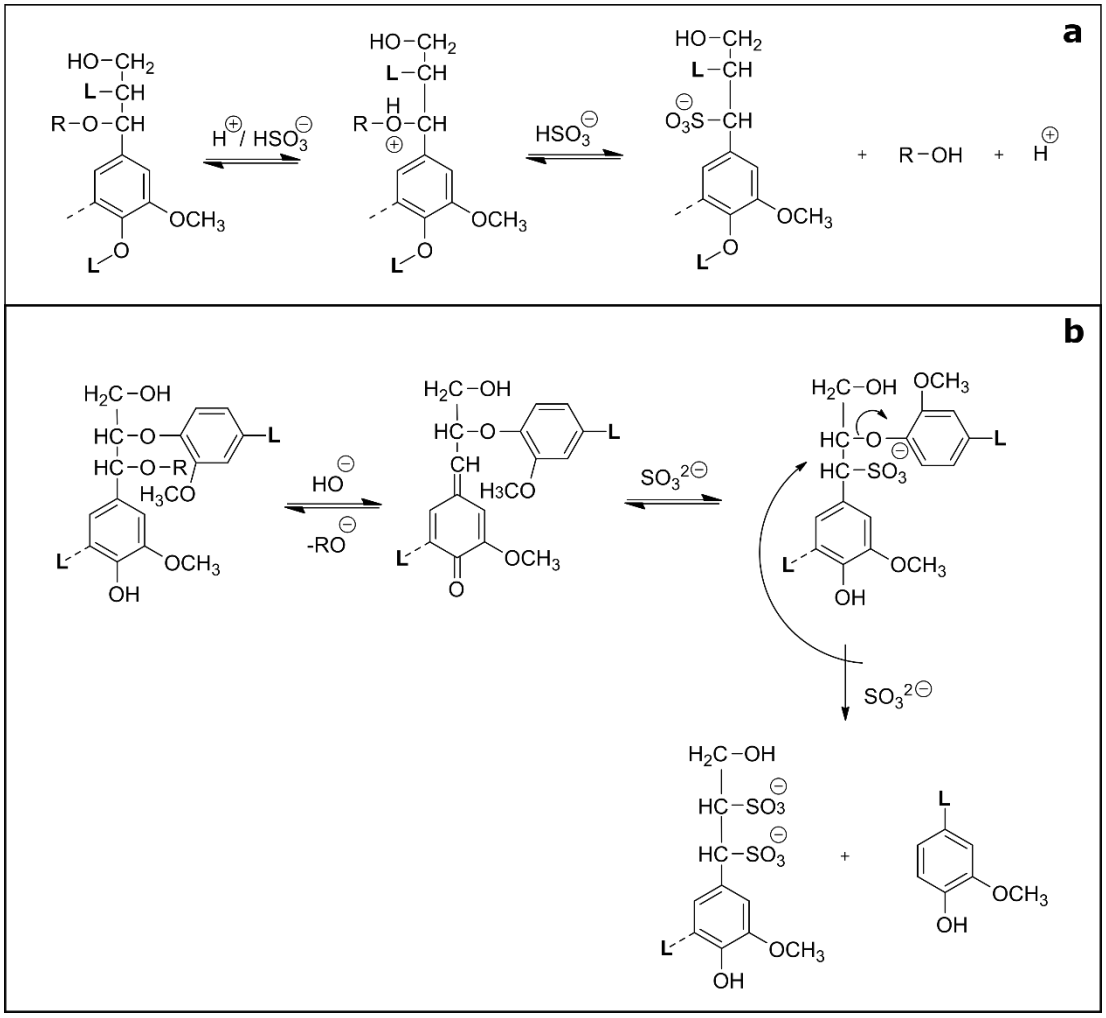

Figure 1.6. Mechanism of lignin sulfonation in pre-treatment in the presence of sulfite / bisulfite ions in (**a**) acidic and (**b**) alkaline conditions [61].

Hydrothermal pretreatment is a pretreatment method in which water as a liquid phase or vapor phase is used. There is no need to add catalyst and alleviates causes of corrosive problems. High-pressure water penetrates directly into biomass and cellulose, removing a substantial part of the hemicellulosic fraction, altering the structure of lignin, but removing very little of this fraction, which is a disadvantage for the efficiency of enzymatic hydrolysis of post-treatment cellulose. The solubilization of hemicelluloses is catalyzed by hydronium ions resulting from the cleavage of the acetyl group (substituting the hemicellulose chain) in acetic acid, in addition to the

autoionization of water. The formation of inhibitors (acetic acid, furfural acid, formic acid, among others) can be reduced by controlling the acidity and temperature of the pre-treatment [58,62].

Enzymes of commercial interest for conversion of lignocellulosic biomass

Cellulases

Cellulases are enzymes that catalyze the hydrolysis of glycosidic bonds of the β-1,4 type present in the cellulose molecule. Cellulases are enzymes applied in the industrial sector and play an important role in the global carbon cycle. They are very diverse in terms of their structure and mode of action. They can be produced by plants, fungi, some bacteria and some animals [63].

Cellulases are currently the third category of industrial enzyme most commercialized worldwide, due to its application in cotton processing, paper recycling, as detergent enzymes, in juice extraction and as additives for animal feed. However, cellulases could become the most commercialized enzymes in the world, if bioethanol, biobutanol or other biofuels obtained by fermenting sugars, become an important transport fuel [64]. Currently, industrial cellulases are almost all produced from fungi of the genus *Trichoderma, Humicola and Aspergillus* [65–68]. This is due to the ability of these organisms to produce extremely high amounts of cellulases with relatively high specific activity and the ability to genetically modify these strains to adjust the set of enzymes they produce, in order to provide an optimal activity for specific uses. [64].

There are three different types of cellulases: endocellulase (EC 3.2.1.4) (also known as endoglucanases), exoglucanase (EC 3.2.1.91) (also known as cellobiohydrolases) and cellobiase (EC 3.2.1.21) (also known as 1,4-β-D-glycosidases or β-glycosidase). All catalytic domains of endocellulases have an open active site and are able to bind to the inside of cellulose molecules and randomly cleave the inside of the chain. In contrast, all exoglucanases have their active sites located in a tunnel. There are two classes of exoglucanases: the first class cleaves the non-reducing end of a cellulose molecule, releasing cellobiose residues. All known exoglucanases in this class are in the GH-6 family. The exoglucanases of the second class cleave the reducing end of the cellulose chain, releasing cellobiose residues. Fungal exoglucanases in this class are in the GH-7 family, while bacterial exoglucanases are in the GH-48 family. [63]. Finally, celobiase is in charge of hydrolysing cellobiosis into glucose. For an efficient hydrolysis of cellulose, the synergistic action of cellulases is necessary (Figure 1.7).

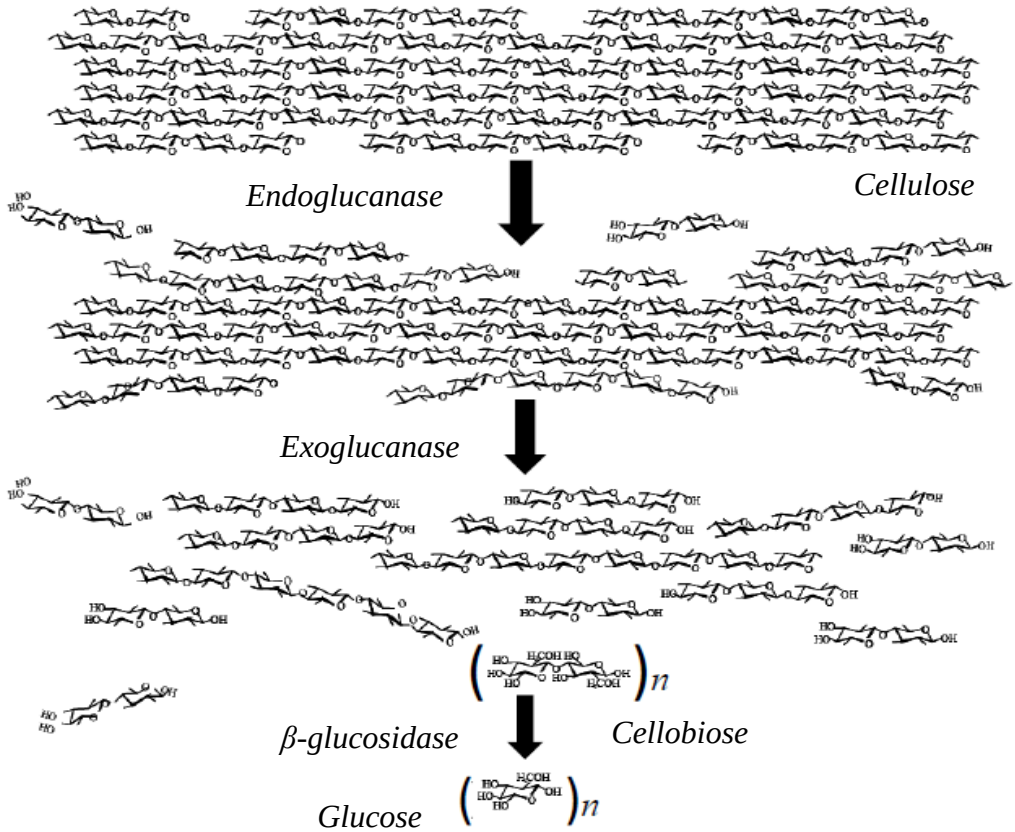

Figure 1.7. Mode of action of enzymes of the cellulolytic complex of *Trichoderma reesei* [69].

Xylanases

Xylanases catalyze the hydrolysis of xylan, which is the second most abundant polysaccharide in hardwoods and grasses and an important component in plant cell walls. There are two enzymes, endoxylanase (EC 3.2.1.8) (also called xylanase) that hydrolyzes the inner part of the xylan chain and 1,4-β-D-xylosidase (EC 3.2.1.37) that hydrolyzes the xylobiosis dimer. These enzymes are produced mainly by microorganisms like bacteria and fungi [66,70–73]. Enzymes participate in the degradation of plant cell walls (together with other enzymes that hydrolyze polysaccharides) and also hydrolyze xylan during the germination of some seeds, for example, in malting

the barley grain. Xylanases can also be found in seaweed, protozoa, crustaceans, insects, snails and seeds of terrestrial plants [72].

The main industrial applications of xylanases are found in the biofuels, cellulose and paper, food and beverage and animal nutrition sectors [74–80]. Due to their biotechnological characteristics, xylanases are most often produced from microorganisms.

Enzyme immobilization

Biocatalysis processes have been widely applied in several sectors of biotechnology due to their high specificity, ease of production and conservation of the environment. The use of enzymes in large quantities is limited depending on the costs of these. In addition, maintaining the structural stability of some enzymes during a catalysis is a major challenge. In order to overcome these limitations, the immobilization of enzymes appears as a promising technique [34]. According to Aragon [35], for practical applications, the immobilization of microorganisms or enzymes in solid materials offers many advantages, among which the possibility of reusing the enzyme, easy separation of the product and increasing the stability of the enzyme. The term "immobilized enzymes" refers to enzymes that are physically confined or located in a specific region of space with retention of their catalytic activities and that can be used repeatedly and continuously [81]. Various materials can be used as a matrix or support system for enzymatic immobilization, usually inert polymers and inorganic materials. The ideal support matrix should have the following properties: inertia, stability, physical strength, ability to increase specificity / activity of the

enzyme, regenerability, ability to reduce product inhibition, ability to prevent unspecific adsorption and bacterial contamination, be inexpensive [34]. Most matrices have only some of the properties mentioned, therefore, the selection of the support matrix for enzyme immobilization should be chosen based on their properties and limitations.

The functions and properties of an immobilized enzyme depend on its own characteristics, the immobilization system and the support material [82]. The characteristic parameters of these three components collectively determine the properties of the immobilized enzyme system. Theoretically, an ideal immobilization method should provide the best immobilization yield, maintaining long-term activity and stability [83]. An enzymatic immobilization method can be based on a chemical reaction or physical adsorption [84]. There are different methods of enzyme immobilization and several factors that affect the performance of immobilized enzymes. The different methods of enzymatic immobilization are grouped as follows: physical adsorption, affinity adsorption, covalent bonding, trapping, encapsulation and cross-linking.

Covalent bonding, one of the most studied immobilization methods, involves the irreversible coupling of enzymes to an appropriate support. This method, therefore, is the most stable form of immobilization. There is a wide range of chemical bonding mechanisms and water-insoluble support materials that can be functionalized for covalent immobilization of enzymes. This wide range of options provides great flexibility in designing an immobilized enzyme system with specific desired properties. Physical parameters such as load distribution, hydrophobic / hydrophilic ratio and separation of the spacer arm

can be conveniently modified [84]. The covalent binding of enzymes depends heavily on the chemical properties of the support materials and on the natural or grafted functional groups in the enzyme molecules. Thus, to ensure efficient enzymatic recovery by covalent immobilization, the binding reaction conditions must not compromise the enzymatic activity. Despite the strong covalent bond, this type of immobilization has some disadvantages, for example, cost of the method and loss of enzyme activity due to enzymatic rigidity that can result from the multipoint bond [85,86].

Graphene oxide (GO)

Graphite oxidation has been studied for more than a century, with the study of B.C. Brodie in 1859 being available in the literature as the first example [87]. Typically, graphite reacts with strong oxidizing agents, such as potassium permanganate ($KMnO_4$) and concentrated sulfuric acid (H_2SO_4), followed by purification and exfoliation in water, which results in a yellow colloidal dispersion, as reported by Hummers [88]. Graphite oxide has a structure in the form of layers of atomic thickness similar to that of graphite, but the plane of the carbon atoms in graphite oxide is linked to several groups that contain oxygen, which not only expand the distance between the layers, but they also make them hydrophilic. These oxidized layers can be exfoliated in water or organic solvents under sonication. When the exfoliated material contains only one or a few layers of carbon atoms, such as graphene, this material is called graphene oxide (GO) [89]. Thus, GO is a single atomic layer material that comprises molecules of carbon, hydrogen and oxygen obtained

by oxidizing graphite crystals that are cheap and abundant, being dispersible in water and easy to process. (Figure 1.8). In addition, GO can be (partially) reduced to graphene by removing oxygen-containing groups. In this way, recovering a conjugated structure. The reduced GO can be considered a type of chemically derived graphene [90].

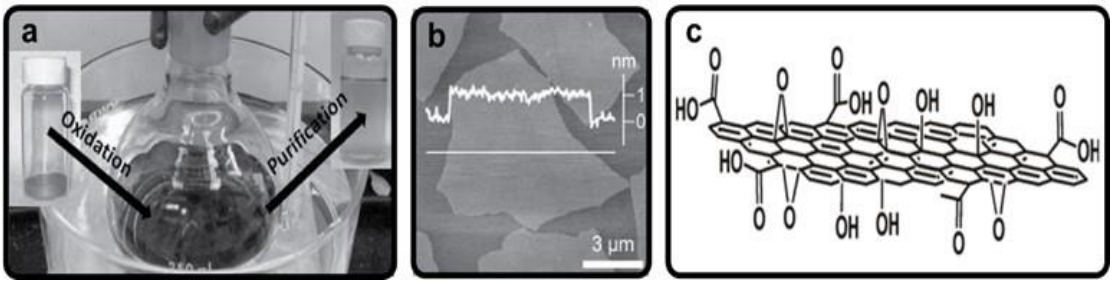

Figure 1.8. (a) Synthesis of graphene oxide (GO) (**b**) Atomic force microscopy of a GO sheet of the obtained colloidal dispersion. (**c**) Schematic model of the GO [36,91].

GO's abundance of chemical features makes it a highly versatile chemical platform for creating graphene-based materials. As shown in Figure 1.8b (the thickness profile of atomic force microscopy) the thickness of the layers of the GO is in the order of 1 nm, the thickness scale being typical of these molecules. On the other hand, the length of the GO molecule is on the order of micrometers, which is the typical length scale of colloidal particles. Therefore, depending on the length scale in question, the GO can be treated as a molecule or colloidal sheet [91].

Graphene oxide properties

One of the advantages of GO is its easy dispersibility in water and other organic solvents, as well as in different matrices, due to the presence of

oxygen molecules that act with functional groups. This property is very important when mixing GO with ceramic or polymeric matrices. The functionalization of GO can fundamentally change its physicochemical properties. The resulting chemically modified graphenes can potentially become more adaptable for many applications. There are many ways in which GO can be functionalized, depending on the desired application. For optoelectronics, bio-devices or drug-delivery systems, it is possible to replace amines with the organic covalent functionalization of graphene to increase the dispersibility of chemically modified graphenes in organic solvents [90].

Surface modification of graphene oxide

Covalent and non-covalent functionalization are the two approaches used for surface modification of carbon materials. In covalent functionalization, functional groups containing oxygen, including carboxylic groups at the extremities and epoxy / hydroxyl groups at the basal plane, can be inserted to alter the surface functionality of the GO. In addition, isocyanate treatment can be used to reduce the hydrophobicity of GO by forming amide and carbamate esters in the carboxyl and hydroxyl groups, respectively. Consequently, the isocyanate modified GO rapidly forms a stable dispersion in polar aprotic solvents, culminating in exfoliated graphene films with a thickness of 1 nm. This dispersion also facilitates the intimate mixing of the GO film with matrix polymers, providing a new synthesis path to form graphene nanocomposites and polymers [90]. Figure 1.9 shows the functionalization of graphene and its derivatives with avidin-biotin, peptides, nucleic acids, proteins, aptamers, small

molecules, bacteria and cells through physical adsorption or chemical conjugation. Functionalized graphene biosystems with unique properties have been used to build biological platforms, biosensors and bio-devices [92].

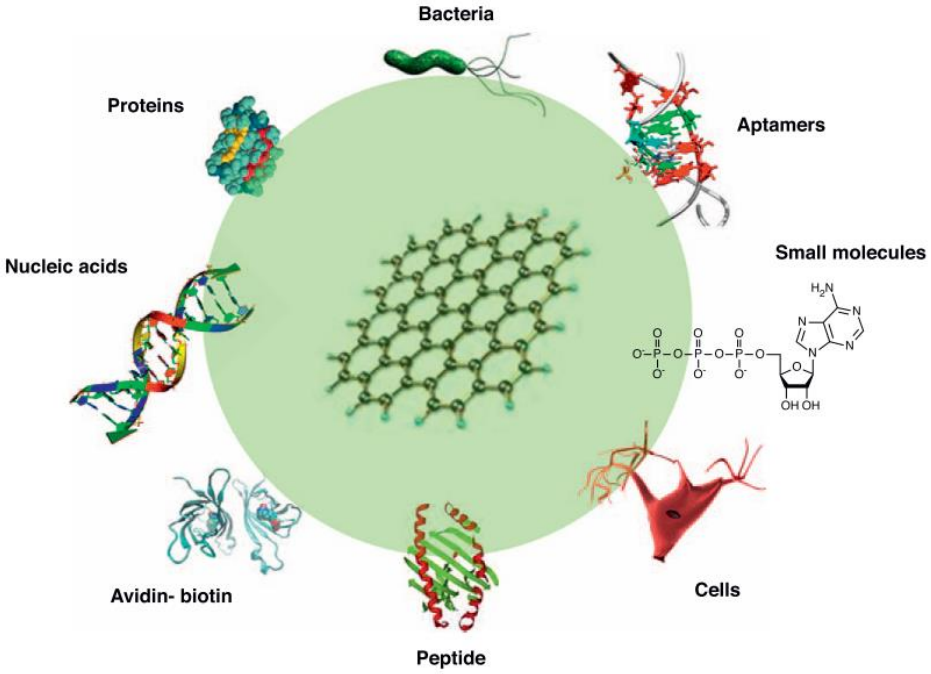

Figure 1.9. Graphene functionalized with avidin-biotin, peptides, nucleic acids, proteins, aptamers, small molecules, bacteria and cells through physical adsorption or chemical conjugation [92].

Graphene and OG have been linked with several proteins, which results in biosystems with unique properties. It was verified that the horseradish peroxidase and lysozyme can be spontaneously immobilized in an individual GO film, as it is enriched with oxygen-containing groups, which allows immobilizing enzymes without surface modifications or coupling reagents [36].

Magnetization of graphene oxide

Since the discovery of the first magnetic nanoparticles, several types of applications have been developed in drug administration [93], detection

methods [94], medicine and catalysis [95–97]. Magnetic nanoparticles (MNP) can be formed from iron oxide III (Fe_3O_4) and iron oxide II (Fe_2O_3). These nanomaterials are famous for their magnetic characteristic which, in recovery, can be quickly separated from the media by an external magnet [37]. Doustkhah and Rostamnia [37] showed that Fe_3O_4 nanoparticles can be bonded to the surface of the OG by coprecipitating Fe^{2+} and Fe^{3+} in alkaline solution over the addition of ammonia at 80 °C (Figure 1.10).

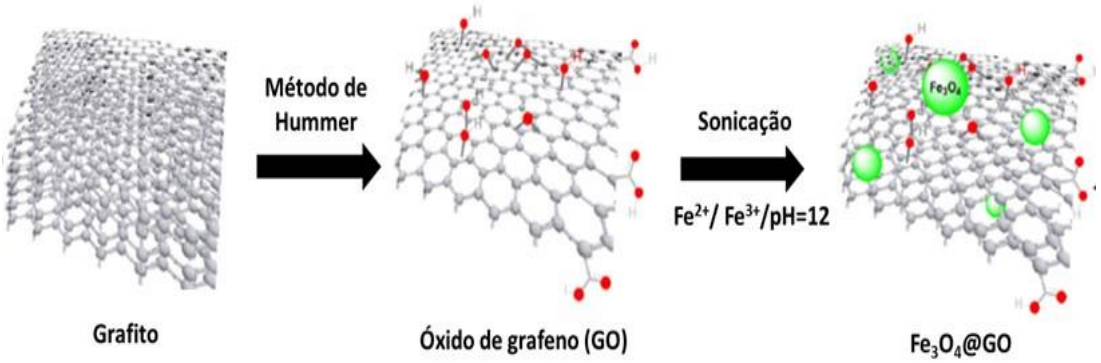

Figure 1.10. Schematic route for the synthesis of graphene oxide with magnetic nanoparticles (GO-MNP) [37].

Immobilization of enzymes in graphene oxide as a support

The incredibly large specific surface area (accessible from both sides), the abundant functional groups containing oxygen, such as epoxy, hydroxyl and carboxyl groups and the high solubility in water make GO a very promising material for many applications [98,99]. However, to date, few studies on the binding of biomacromolecules, such as enzymes, to GO have been reported in the literature. [36].

Zhang [36] et al*.,* demonstrated that GO films can be used as supports to immobilize the horseradish peroxidase enzyme. The functional groups on

the surface of the GO cause the enzyme immobilization to occur quickly through electrostatic interaction without making any previous modifications to the material. The flat surface of the GO allows to see the immobilized enzyme “in situ” using atomic force microscopy, as shown in Figure 1.11.

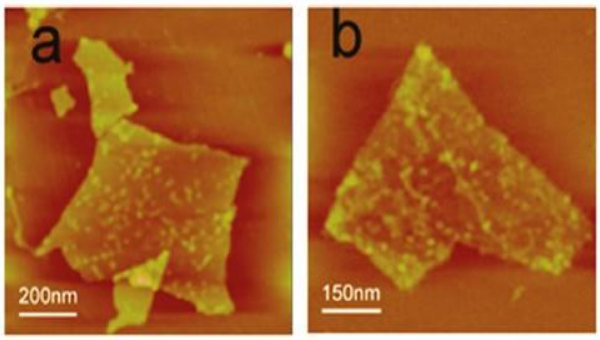

Figure 1.11. Atomic force microscopy images of horseradish peroxidase linked to graphene oxide with (**a**) low enzyme load and (**b**) high enzyme load. [36].

Heidarizadeh [38] et al., covalently immobilized porcine pancreas lipase on the surface of magnetically separable GO (GO-MNP), functionalizing its surface using (3-aminopropyl) triethoxysilane (APTES) and carbon disulfide (CS_2), as shown in Figure 1.12.

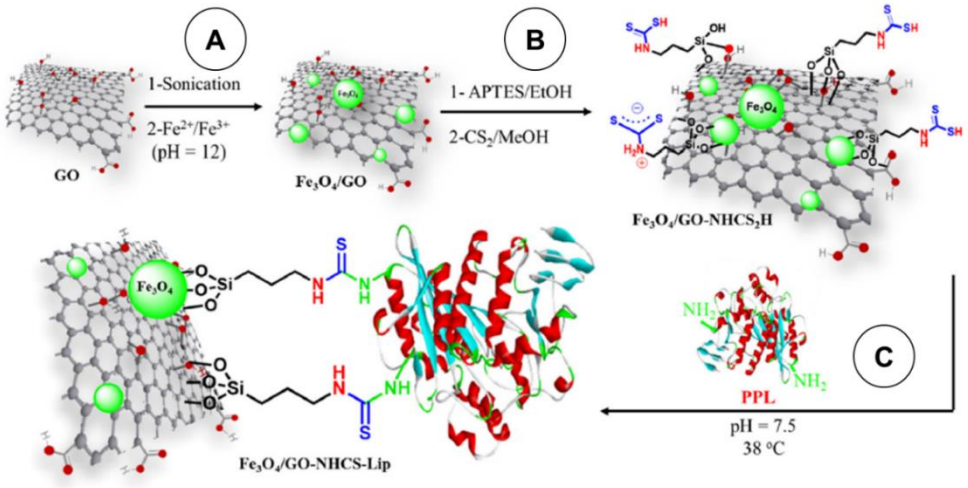

Figure 1.12. (A) Magnetization procedure and **(B)** functionalization of graphene oxide. **(C)** Lipase immobilization [38].

OBJECTIVE

The main objective of this study was to evaluate the immobilization of cellulases and xylanases in graphene oxide decorated with magnetic nanoparticles (GO-MNP) and to study the potential of hydrolysis of pre-treated sugarcane bagasse (SCB). A seguir apresentamos os objetivos específicos que foram estabelecidos para atingir a meta do estudo:

- Evaluate the effect of different pretreatments on chemical composition of sugarcane bagasse (SCB);
- Assess the effect of pretreatments in response to enzymatic hydrolysis of SCB;
- Evaluate the synthesis of magnetized graphene oxide (GO);
- Examine the structure of magnetic graphene oxide (GO-MNP);
- Assess the immobilization of cellulose and xylan enzymes on the surface of the GO-MNP;
- Determine the stability parameters of previously immobilized cellulases and xylanases;
- Evaluate the reuse of immobilized enzymes through hydrolysis of specific substrates for cellulases and xylanases;
- Assess the enzymatic hydrolysis of cellulose and xylan from SCB pretreated and the potential for reuse of the biocatalyst obtained;

2. CHAPTER 1

Evaluation of the effects of different chemical pretreatments in sugarcane bagasse on the response of enzymatic hydrolysis in batch systems subject to high mass loads

Article published in October 2020 in Renewable Energy.

DOI: 10.1016/j.renene.2020.10.092

Evaluation of the effects of different chemical pretreatments in sugarcane bagasse on the response of enzymatic hydrolysis in batch systems subject to high mass loads

Fernando Roberto Paz-Cedeno, Lucas Ragnini Henares, Eddyn Gabriel Solorzano-Chavez, Mateus Scontri, Flávio Pereira Picheli, Ismael Ulises Miranda Roldán, Rubens Monti, Samuel Conceição de Oliveira and Fernando Masarin*

São Paulo State University (UNESP), School of Pharmaceutical Sciences (FCF), Department of Bioprocess Engineering and Biotechnology. Araraquara-SP, Brazil. 14800-903.

(*) corresponding author

Email addresses:
FRPC: fernando.paz@unesp.br
LH: lucas_henares@hotmail.com
EGSC: eddynsch04@hotmail.com
MS: mateus.scontri@unesp.br
FPP: flavio.picheli@unesp.br
IUMR: imiranda_3@hotmail.com
RM: rubens.monti@unesp.br
SCO: samuel.oliveira@unesp.br
*FM: fernando.masarin@unesp.br

ABSTRACT

In the present study, SB was subjected to different pretreatments. The pretreated SB was characterized chemically and structurally and was enzymatically hydrolyzed using a commercial enzyme preparation. In addition, enzymatic hydrolysis of pretreated SB at high-solid loads in Erlenmeyer flasks and bioreactors was evaluated. Pretreatment with sulfite-NaOH was the most efficient for removing lignin while keeping cellulose intact. In addition, sulfite-NaOH pretreatment presented the best response to the enzymatic hydrolysis of cellulose and xylan, reaching conversions of 90%. The increase in consistency (≥ 10%) in the enzymatic hydrolysis of SB pretreated with sulfite-NaOH showed a loss of cellulose and xylan conversion efficiencies of approximately 28% and 37%, respectively. However, enzymatic hydrolysis with a consistency of 20% resulted in a maximum rate of glucose and xylose formation of 8.5 and 3.0 $g.L^{-1}.h^{-1}$, respectively, and an enzymatic hydrolysate containing 80 and 33 $g.L^{-1}$ of glucose and xylose, respectively. The enzymatic hydrolysis assay in a bioreactor with 20% consistency promoted faster liquefaction of SB, resulting in a higher maximum rate of glucose production (10.6 $g.L^{-1}.h^{-1}$). The increase in the concentration and rate of formation of fermentable sugars in the enzymatic hydrolysate can partially avoid steps of concentration of the hydrolysate, resulting in less energy consumption. This results in greater productivity of the bioproducts obtained from the hydrolysate, such as cellulosic ethanol (2G ethanol).

KEYWORDS: Lignocellulosic biomass; Alkaline pretreatment; Biomass hydrolysis; High consistency; Cellulase, Xylanase.

HIGHLIGHTS

- Pretreatment of sugarcane bagasse with sulfite-NaOH efficiently removed lignin while keeping cellulose intact.
- Pretreatment with sulfite-NaOH had the strongest effect on the enzymatic hydrolysis of sugarcane bagasse.
- The enzymatic hydrolysis of sugarcane bagasse pretreated with sulfite-NaOH under high consistency resulted in a hydrolysate rich in fermentable sugars.
- When enzymatic hydrolysis was performed in a bioreactor, the maximum rate of glucose formation increased.

INTRODUCTION

The most abundant renewable sources are vegetable biomasses that constitute the softwoods, hardwoods, and grasses and can be found directly in nature or as byproducts generated in different sectors of agribusiness. The production of biofuels from renewable raw materials is important for reducing the climatic impact of our dependence on fossil fuels. Brazil is the world leader in terms of the use of energy from renewable energy sources, which represents approximately 45% of the total energy consumption in Brazil. There is already a large amount of ethanol produced in the country from sucrose and/or

sugarcane molasses, which represents 18% of all energy produced in the country [1–5].

Brazil, one of the largest agricultural producers in the world, generates significant amounts of biomass byproducts from harvesting and processing. According to the National Company of Supplying [6], from 2019 to 2020, 642.7 million tons of sugarcane were obtained, and ethanol production from sugarcane was 34 billion liters, accounting for 95.5% of total ethanol production in Brazil. The main byproduct in sugar-alcohol processing is sugarcane bagasse (SB). For each ton of sugarcane harvested and processed, approximately 270 kg of SB is generated (currently equivalent to 178 million tons per year) [7].

SB is a lignocellulosic material formed by cellulose, hemicellulose, and lignin, whose pretreatment is essential for breaking down the cell wall, resulting in greater access to hydrolytic enzymes. Pretreatment can be chemical (acidic, basic, or oxidative), physical (steam explosion or hydrothermal), or a combination of these [8–10]. Alkaline pretreatments combined with sodium sulfite (Na_2SO_3) stand out, as it has the capacity to sulfonate lignin, making cellulose and xylan more accessible to enzymes. Na_2SO_3 dissolved in aqueous medium results in the formation of hydrosulfite (HSO_3^-) and hydroxide (OH^-) ions [8]. OH^- ions subtract a proton from a phenolic OH present in aromatic lignin rings, forming an intermediate (methylene quinone) that is attacked in α carbon by HSO_3^- ions, making phenolic OH again protonated and sulfonating α carbon. The chemical reaction proceeds with the cleavage of the β-aryl-ether bond between the two aromatic rings, resulting in the sulfonation

of the β carbon and consequent dissolution/degradation of the lignin [8,9,11,12].

Cellulases and xylanases are enzymes that constitute a complex capability of hydrolyzing lignocellulosic materials, and consist of endoglucanase (EC 3.2.1.4), which hydrolyzes all the internal bonds and type β-1,4-glycosides of the cellulosic fiber, releasing cello-oligosaccharides (COS), exoglucanase, or cellobiohydrolase (EC 3.2.1.91), which hydrolyze the crystalline region of cellulose. This results in the release of a cellobiose molecule, β-glucosidase (EC 3.2.1.21), which hydrolyzes soluble oligosaccharides (COS and cellobiose) in glucose. The synergistic action of these three enzymes is necessary to effectively cleave cellulose into glucose, which is a raw material for the production of bioproducts of commercial interest, such as ethanol [13–16]. Xylanase are enzyme complexes consist of endoxylanase (EC 3.2.1.8), which randomly hydrolyzes β-1,4-xylosidic linkages in the xylan main chain, releasing xylooligosaccharides (XOS) and β-xylosidase (EC 3.2.1.37), which hydrolyzes short-chain XOS to xylobiose then xylose. Xylose can be applied in the production of dietary sugars, such as xylitol [17–20].

The enzymatic hydrolysis of cellulose at a high mass load (or high consistency) has the advantage of promoting the formation of a hydrolysate containing high concentrations of glucose and avoiding concentration steps, resulting in saving energy and increasing bioprocess productivity. Nevertheless, high glucose concentrations have significant inhibitory effects on the activity of cellulases [21–24]. In addition, the high consistency in the

enzymatic hydrolysis of cellulose also presents problems of mass transfer that reduce the reaction rates. Both problems prevent the complete hydrolysis of cellulose.

However, these problems (enzyme inhibition and mass transfer limitation) can be minimized with the use of suitable bioreactors and impellers, which promote adequate mixing and homogenization of the reaction medium. Therefore, the impellers must be carefully designed to allow efficient agitation in reaction media containing high mass loads and to avoid adherence of material in the bioreactor wall and impeller [22,23].

Within the scope of the guidelines presented in this introduction, the objective of this study was to select a chemical pretreatment for SB based on the efficiency of enzymatic hydrolysis carried out in a flask and stirred tank bioreactor under high consistency conditions.

MATERIAL AND METHODS

Sugarcane bagasse pretreatment

SB was obtained from a local sugar-alcohol plant, oven dried at 40°C for 48 h, and stored appropriately until use. For the pretreatments, 50 g (dry basis) of SB was placed in a 1.5 L reactor (AU/E-20, ®Regmed) and the reaction medium corresponding to each pretreatment was added (Table 2.S1). The mass ratio of NaOH and KOH was 5% (5/100 g of SB, dry basis) and that of Na_2SO_3 was 10% (10/100 g of SB, dry basis) [9]. The reactor was set to operate at a temperature of 140°C and a stirring speed of 4 rpm for 30 min. The obtained material was washed with tap water until a neutral pH was

obtained, oven dried at 40°C for 24 h, and stored until use. The yield of pretreatment was determined by gravimetry (percentage in relation to initial mass and mass after pretreatment, dry basis).

Chemical composition

The chemical composition of untreated and pretreated SBs was determined by milling the SBs using a knife mill and a sieve of 20 mesh (0.84 mm screen). SBs were subjected to ethanol (95%, v/v) extraction for 6 h in *Soxhlet* apparatus, and extractive content was determined by gravimetry [16]. Structural carbohydrates and lignin contents were determined by acid hydrolysis. Briefly, 0.3 g of SB (dry basis) was mixed with 72% H_2SO_4 (w/w) for 1 h at 30°C and then with 4% H_2SO_4 (w/w) for 1 h at 121°C. The hydrolysate was filtered through porous glass filters (Schott #3, Germany), and the material retained was washed with distilled water, dried, and weighed. This material corresponds to insoluble lignin. An aliquot of the filtrate was used to determine soluble lignin by spectrophotometry at 205 nm [16]. The filtrate was passed through a 0.45 µm membrane and a Sep-Pak C_{18} cartridge then injected into a high-performance liquid chromatography (HPLC) system to determine the structural carbohydrates. Chromatographic analyses were performed using an HPX87H column (Bio-Rad, Hercules, CA, USA) at 60°C with 0.005 M H_2SO_4 at 0.6 $mL.min^{-1}$. Detection was performed using a refractive index detector at 60°C (Shimadzu, model C-R7A) [16,25]. Cellulose and hemicellulose contents in the SB were calculated from glucose, xylose, arabinose, and acetic acid (Sigma-Aldrich) data. The statistical differences among the cellulose,

hemicellulose, and lignin contents obtained in the different pretreatments were evaluated using Tukey's test (Minitab 19.1 software) with a significance level of 0.05.

Structural characterization

The SBs were air dried, milled, and screened through a 0.84 mm screen. The samples were then dried in an air circulation oven at 50°C for 12 h, homogenized, and stored. The dried samples were subjected to infrared analysis using attenuated total reflection with a Fourier transform infrared (ATR-FTIR) spectrometer (Platinum-ATR Alpha; Bruker) with a single reflection diamond module at 25°C. X-ray diffractograms (XRDs) of the dried samples were obtained at 25°C within an angle range of 5° to 70°2θ (Bragg Angle) and a scan speed of 2° min^{-1}. The equipment used was a Siemens Kristalloflex diffractometer, running at a power output of 40 kV with a current of 30 mA and Kα Cu radiation (λ = 1.5406 Å). The crystallinity index (CrI) of the samples was calculated from the XRD by the deconvolution method (curve fitting). For peak fitting, PeaKFit software version 4.12 was used, assuming Gaussian functions to approximate each peak [26–29]. The CrI was calculated using Equation 1 as follows:

$$CrI(\%) = \left[\frac{A_C}{A_C + A_A}\right] . 100\% \qquad \textbf{(1)}$$

In Equation (1): A_C is the area of the crystalline region, and A_A is the area of the amorphous regions.

Enzyme activity assays

Commercial enzymatic preparation Cellic CTec 2 (®Novozymes) was used in this study for enzymatic hydrolysis of untreated and pretreated SB. The following enzyme activities were determined:

Total cellulases were measured according to the method described by Ghose [30]. A strip of Whatman N°1 filter paper was placed in a tube with 1 mL of 0.05 M sodium acetate buffer (pH 4.8). Then 0.5 mL of enzymatic preparation was added to the tubes. After 1 h at 50°C, the reaction was stopped by adding 3 mL of 3,5-dinitrosalicylic acid reagent (DNS). The readings were taken in a spectrophotometer at 540 nm.

Endocellulase was measured using the methodology described by Tanaka et al. [31]. Accordingly, 0.9 mL of 0.44% (w/v) sodium carboxymethylcellulose (≥ 95%; Carbosynth, USA) solution was placed in a tube, and 0.1 mL of properly diluted enzymatic preparation was added. After 1 h in a water bath at 50°C, the reaction was stopped by adding 1.5 mL of DNS, boiling for 5 min, and cooling. The readings were taken in a spectrophotometer at 540 nm.

Exoglucanase was measured using the methodology described by Tanaka et al. [31]. Accordingly, 0.9 mL of 0.5% (w/v) Avicel (≥ 90%; Sigma-Aldrich) in 0.05 M sodium acetate buffer at pH 5 was placed in a tube, and 0.1 mL of properly diluted enzymatic preparation was added. The suspension was incubated for 2 h at 50°C. At the end of the reaction, 1.5 mL of DNS was added, boiled for 5 min, and cooled. The tubes were centrifuged at 12200 x*g* and the supernatant readings were taken in a spectrophotometer at 540 nm.

Xylanase was measured according to the methods of Bailey et al. [32]. Tubes were placed in a water bath at 50°C and 0.9 mL of 1% (w/v) xylan (≥ 90%; Sigma-Aldrich) solution buffered with 0.05 M sodium acetate at pH 5.0 was added to 0.1 mL of properly diluted enzymatic preparation. After 5 min, the reaction was stopped by adding 1.5 mL of DNS, boiling for 5 min, and cooling. The readings were taken in a spectrophotometer at 540 nm.

β-glucosidase and β-xylosidase were measured according to the method described by Tan et al. [33]. In following this method, 0.8 mL of 0.1% (w/v) 4-nitrophenyl β-D-glucopyranoside (≥ 98%; Sigma-Aldrich) or 4-nitrophenyl β-D-xylopyranoside (≥ 98%; Sigma-Aldrich) solution was added to 0.2 mL of properly diluted enzymatic preparation. The reactions were stopped by adding 2 mL of 10% (w/v) $NaHCO_3$, and the respective absorbance was read at 410 nm.

Enzymatic hydrolysis of sugarcane bagasse

Untreated and pretreated SBs were subjected to enzymatic hydrolysis using Cellic CTec 2. The reactions were carried out in Erlenmeyer flasks at a consistency of 5% (w/v) in 0.05 M sodium acetate buffer (pH 4.8) at 45°C and 150 rpm, with an enzyme load of 13.2 FPU (total cellulases) per gram of SB (dry basis). In the case of SB pretreated with sulfite-NaOH, consistency of 2%, 5%, 10%, 20%, and 30% (w/v) were used. In addition, enzymatic loads of 3.3, 13.2, and 30.0 FPU (total cellulases) per gram of SB (dry basis) were used at a consistency of 20% (w/v). Also, a hydrolysis assay was performed in a bioreactor equipped with an impeller (Figure 2.S5). This assay was performed

with 20% consistency (200 g of SB and 1000 mL of reaction medium) and 12.4 FPU (total cellulases) per gram of SB (dry basis) at 45°C and 150 rpm. An Erlenmeyer flask assay was performed simultaneously with the bioreactor assay under the same conditions (10 g of SB in 50 mL of reaction medium). Table 2.S2 presents the enzymatic activity of endoglucanase, exoglucanase, β-glucosidase, xylanase and β-xylosidase equivalent to each total cellulases load used in the enzymatic hydrolysis. Aliquots were periodically withdrawn from the reaction medium and injected into a HPLC system to determine and quantify monomeric sugars (see the chemical composition section). Cellulose and xylan conversions were calculated according to Equation 2 as follows:

$$\delta = \left[\frac{(glucose\ or\ xylose)\cdot f}{m}\right] \cdot 100\% \qquad \textbf{(2)}$$

In Equation (2):

- δ = cellulose or xylan conversion into glucose or xylose, respectively (%);
- *glucose or xylose* = mass of glucose or xylose, respectively (g);
- *f* = hydrolysis factor of 0.9 and 0.88 for cellulose and xylan ($g.g^{-1}$);
- *m* = initial dry mass of cellulose or xylan (g).

Kinetic parameter estimation

The glucose and xylose concentration data obtained during enzymatic hydrolysis were interpreted using a mathematical model applicable to the enzyme kinetics under study. This model was based on saturation kinetics, as the sugar concentration during enzymatic hydrolysis increases over time,

reaching an asymptotic final value, as described by Equation (3) [34–37] as follows:

$$C = C_{max}(1 - e^{-kt}) \qquad \textbf{(3)}$$

In Equation (3):

- C = sugar concentration ($g.L^{-1}$);
- C_{max} = asymptotic maximum sugar concentration ($g.L^{-1}$);
- k = kinetic constant of sugar accumulation (h^{-1});
- t = hydrolysis time (h).

Estimation of C_{max} and k parameters was performed using Origin software (OriginPro, 2017). The statistical difference among the C_{max} values estimated for each hydrolysis assay was evaluated by Tukey's test (Minitab 19.1 software) with a significance level of 0.05. Although the value of the determination coefficient (R^2) is rigorously correct for quantifying the predictive capability of linear models, this indicator was used here, as first approximation, to evaluate the fit quality of the nonlinear mathematical model given by Equation (3).

RESULTS AND DISCUSSION

Evaluation of different chemical pretreatments on sugarcane bagasse

SB biomass was subjected to different chemical pretreatments in an alkaline medium to determine the efficiency of removing the lignin fraction, in addition to the effect on the removal of cellulose and hemicellulose fractions.

Lignin provides rigidity and protection to plant cell walls. Therefore, reducing the lignin content in the material facilitates the catalytic action of cellulases and xylanases over cellulose and hemicellulose [9,16]. The chemical composition of the SBs after the different chemical pretreatments is shown in Figure 2.1 and Table 2.1.

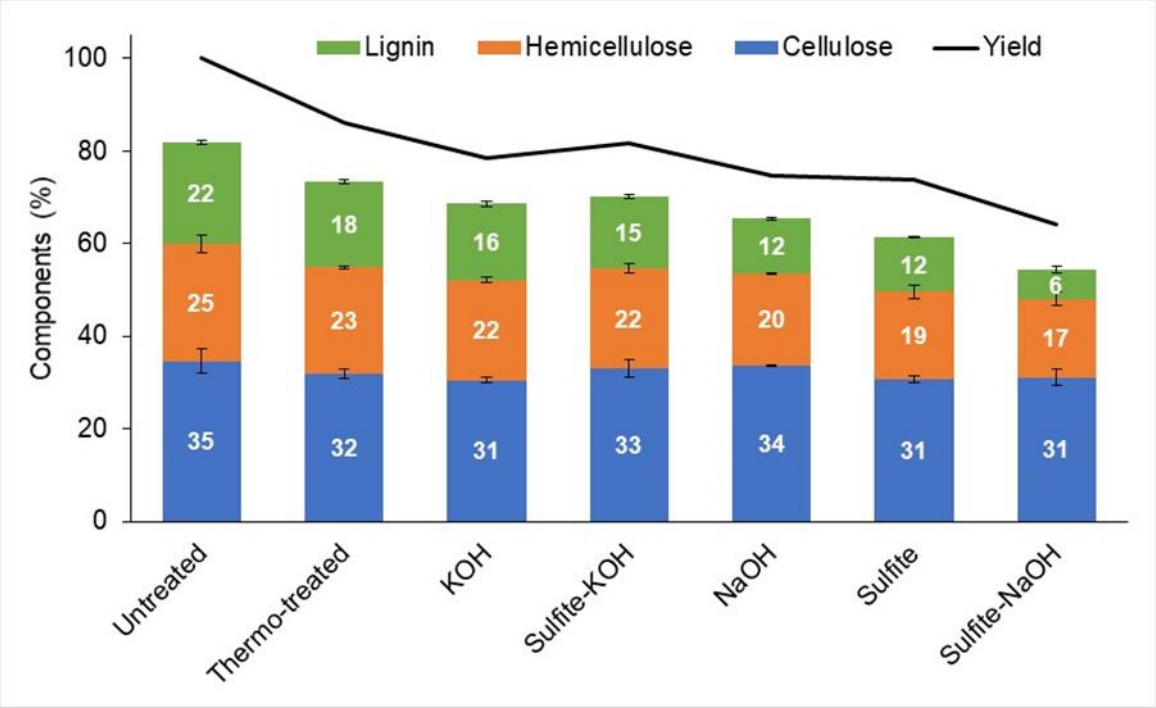

Figure 2.1. Chemical composition and yield of sugarcane bagasse (SB) after different chemical pretreatments. Data presented in percentage (gram of component/100g of original SB, dry basis). Extractives in the untreated sample=7.8 % (g/100 g of original SB, dry basis). SB after pretreatments did not show significant extractive levels.

Table 2.1. Comparison of the efficiency of sugarcane bagasse (SB) components removal for different chemical pretreatments.

Pretreatment conditions					Biomass components (as g/100g of SB)			% of components loss (biomass components as g/100g of Untreated SB)				Ref.
	Temp. (°C)	Time (h)	Reagents per 100g of SB (g)	Cons. (%)	Cellulose (%)	Hemicel. (%)	Lignin (%)	Cellulose (%)	Hemicel. (%)	Lignin (%)	Yield (%)	
Untreated	-		-		34.6 ± 2.5	25.3 ± 1.8	21.9 ± 0.5	- (34.6)[a]	- (25.3)[a]	- (21.9)[a]	-	
Thermo-treated	140	0.5	-		37.0 ± 1.1	26.6 ± 0.4	21.5 ± 0.5	7.9 (31.9)[a]	9.5 (22.9)[a,b]	15.5 (18.5)[b]	86.2	
NaOH	140	0.5	5g		45.2 ± 0.3	26.5 ± 0.1	15.9 ± 0.4	2.7 (33.7)[a]	21.8 (19.8)[b,c,d]	45.8 (11.9)[d]	74.6	
Sulfite-NaOH	140	0.5	5g NaOH+10g Na_2SO_3	10	48.4 ± 2.9	24.0 ± 2.9	9.8 ± 1.0	10.2 (31.1)[a]	33.3 (16.9)[d]	71.3 (6.3)[e]	64.2	This work
KOH	140	0.5	5g		38.8 ± 0.8	27.4 ± 0.7	21.0 ± 0.9	11.9 (30.5)[a]	15.0 (21.6)[a,b,c]	24.7 (16.5)[c]	78.6	
Sulfite-KOH	140	0.5	5g KOH+10g Na_2SO_3		40.2 ± 2.3	26.6 ± 1.3	18.9 ± 0.5	8.0 (31.8)[a]	14.0 (21.8)[a,b,c]	29.4 (15.5)[c]	81.8	
Sulfite-neutral	140	0.5	10g		43.6 ± 3.4	25.5 ± 2.0	15.8 ± 0.1	11.1 (30.8)[a]	25.6 (18.9)[c,d]	46.6 (11.7)[d]	73.9	
Untreated	-	-	-	-	43.7	27.4	24.4	-	-	-	-	
NaOH	120	2	5g	10	47.0	25.9	17.8	1.6	13.5	33.3	91.5	[9,11]
Sulfite-NaOH	120	2	5g NaOH+10g Na_2SO_3	10	54.5	26.9	15.3	7.3	27.1	53.4	74.3	
Untreated	-	-	-		42.6	26.2	22.5	-	-	-	-	
NaOH	130	0.5	22.5g	6.7	58.6	22.1	8.8	28.2	56.0	79.6	52.2	
NaOH	170	0.5	22.5g	6.7	63.1	21.1	7.1	21.9	57.6	83.4	52.7	[38]
NaOH+AQ	130	0.5	22.5g NaOH+2.25g AQ	6.7	60.5	24.1	9.4	9.1	41.1	73.3	64.0	
NaOH+AQ	170	0.5	22.5g NaOH+2.25g AQ	6.7	67.0	22.8	5.2	16.3	53.7	87.5	53.2	
Untreated	-	-	-		38.0	32.0	27.0	-	-	-	-	
US	50	0.75	-	10	46.9	29.3	20.7	1.3	26.8	38.7	80.0	[39]
Ammonia	80	0.5	200g	10	50.4	26.8	19.8	4.5	39.7	47.2	72.0	
US+Ammonia	80	0.75	200g	10	56.1	19.6	18.2	4.5	60.4	56.4	64.7	
Untreated	-	-	-		37.5	24.3	19.3	-	-	-	-	[12]
Sulfite-NaOH	150	0.75	5g NaOH+10g Na_2SO_3	8	55.0	27.5	9.5	1.9	24.3	67.1	66.9	

SB=Sugarcane Bagasse. Extract content of untreated sugarcane bagasse in this work=7.8 % (w/w). AQ=Anthraquinone. US=Ultrasound. Hemicel=Hemicellulose. Cons=Consistency % (w/v).

SB components (cellulose, hemicellulose and lignin) reported in raw data.

The levels of lignin, hemicellulose, cellulose, and extractives in the untreated SB were 21.9%, 25.3%, 34.6%, and 7.8%, respectively (w/w). The sum of the components reached 89.6% (w/w) (Figure 2.1 and Table 2.1). The undetermined components can be attributed to the presence of methyl-glucuronic acid, which is often found in the grass hemicellulose chains, which were not quantified in the study samples [40]. In addition, the formation of sugar oxidation products (such as hydroxymethylfurfural, furfural, formic acid, and levulinic acid) generated in an acidic environment also makes up the content of the undetermined components [41].

The chemical composition presented corroborates with other SBs reported in previous studies (Table 2.1). Still, small variations can be explained by regional crop conditions and plant age, among others [16].

When performing a visual comparison of the SBs after the pretreatments, it was found that the material submitted to the thermo-treatment was darker than the untreated material. This darkening has also been reported in previous studies for hydrothermal and acid pretreatments on other agroindustry byproducts. This effect can be attributed to the formation of products derived from lignin that are formed on the cellulose surface, called pseudo-lignin [8,10]. However, materials pretreated with sulfite-KOH, sulfite-neutral, and sulfite-NaOH were paler than untreated and thermo-treated materials. This bleaching can be attributed to the substantial removal of lignin in these materials after pretreatment [8,9,11]. Pretreatments with NaOH and KOH showed an intermediate color between those verified for untreated and thermo-treated materials.

The pretreatment yields with distilled water (thermo-treatment), NaOH, sulfite-NaOH, KOH, sulfite-KOH, and sulfite-neutral were 86.2%, 74.6%, 64.2%, 78.6%, 81.8%, and 73.9% (dry basis, w/w), respectively (Table 2.1 and Table 2.1). The lowest yield occurred in SB pretreated with sulfite-NaOH; nevertheless, all pretreatments can be considered high-yield processes, that is, there was no significant loss of starting material (untreated SB). The raw levels of lignin, hemicellulose, and cellulose in the SBs after the pretreatments ranged between 9.5-22.2%, 27.7-24.6%, and 33.5-48.4% (dry basis, w/w), respectively (Table 2.1). Nevertheless, for a direct comparison of the pretreated materials with the untreated and thermo-treated materials, it was necessary to perform a mass balance (Figure 2.1). According to the mass balance, the thermo-treated material did not show significant reductions in the contents of hemicellulose and cellulose, but had a 15.5% reduction in lignin content (Figure 2.1). All pretreatments performed in alkaline media resulted in the dissolution of the lignin fraction, with pretreatment with sulfite-NaOH being the most effective (reduction of 71.3%) (Figure 2.1 and Table 2.1). The hemicellulose fraction was also removed in all pretreatments performed in an alkaline medium, with sulfite-neutral and sulfite-NaOH being the most effective (25.6% and 33.3%, respectively). The cellulose fraction was not significantly removed in any of the pretreatments under study (Figure 2.1 and Table 2.1). The high removal of lignin and hemicellulose from SB pretreated with sulfite-NaOH corroborates the lower yield verified in the process (64.2%, Figure 2.1 and Table 2.1). A direct comparison of the untreated and pretreated SB indicated that SB pretreated with sulfite-NaOH presented the greatest

dissolution/degradation of lignin (71.3%) (Table 2.1). Previous studies have performed different pretreatments in alkaline media in SB under conditions similar to those presented in this study (Table 2.1). Mendes et al. [9,11] reported alkaline pretreatments in SB (NaOH and sulfite-NaOH), but carried these out at 120°C for 60 min without mechanical agitation, while the conditions in the present study were 140°C for 30 min and 4 rpm of mechanical agitation (Table 2.1). The authors reported the following levels of removal/degradation of material fractions: 33.2% and 53.3% (lignin), 13.5% and 27.1% (hemicellulose), and 1.6% and 7.3% (cellulose) for SBs pretreated with NaOH and sulfite-NaOH, respectively (Table 2.1). Nakanishi et al. [38] reported alkaline pretreatments in SB (NaOH and NaOH + anthraquinone), performed at 130-170°C for 30 min without mechanical agitation (Table 2.1). The authors reported the following levels of removal/degradation of material fractions: 79.6% and 73.3% (lignin), 56.0% and 41.1% (hemicellulose), and 28.2% and 9.1% (cellulose) for SBs pretreated with NaOH and NaOH + anthraquinone at 130°C, respectively. Ramadoss and Muthukumar [39] reported pretreatments with ammonia in SB performed at 80°C for 30-45 min without mechanical agitation (Table 2.1). The authors reported removal/degradation of lignin, hemicellulose, and cellulose of 47.2-56.4%, 39.7-60.4%, and 4.5%, respectively. Tavares et al. [12] reported pretreatments with sulfite-NaOH in SB performed at 150°C for 45 min without mechanical agitation (Table 2.1). The authors reported removal/degradation of lignin, hemicellulose, and cellulose of 67.1%, 24.3%, and 1.9%, respectively. However, the sulfite-NaOH pretreatment in the present study showed

removal/degradation of lignin and hemicellulose of 71.3% and 33.3%, respectively. This shows more effective removal of lignin than other alkaline pretreatments shown in Table 2.1, with the exception of pretreatment with NaOH + anthraquinone, which promoted a reduction of 73.3-87.5% in lignin content, similar to the pretreatment with sulfite-NaOH in the present study. Nevertheless, these tests were performed with a high load of NaOH (22.5g/100 g of SB, dry basis), while the average NaOH load of the other studies, including the present one, was 5g/100 g of SB (dry base).

ATR-FTIR was also evaluated in SBs (untreated and chemically pretreated) (2e 2.1S and Table 2.S3). Untreated SB showed characteristic lignin bands (2924, 2854, 1602, 1507, 1424, 1240, and 833 cm^{-1}), hemicellulose (1729 cm^{-1}), and cellulose (1367, 1322, 1157, and 897 cm^{-1}) [29,42,43]. In the present study, the spectra were only compared qualitatively to corroborate the chemical composition data. Therefore, it was verified that the characteristic cellulose bands present in the spectrum of untreated SB were also found in the spectra of pretreated SBs, which corroborates the chemical composition data; that is, there was no significant degradation of the cellulose fraction. However, the characteristic bands of hemicellulose and lignin disappeared/decreased in the spectra, mainly for SB pretreated with sulfite-NaOH and sulfite-neutral. The spectrum of thermo-treated SB did not show differences in the characteristic bands of cellulose, hemicellulose, and lignin when compared to untreated SB, which also corroborates the chemical composition data.

The XRD was also evaluated in untreated and chemically pretreated SBs (Figure 2.S2). The untreated SB presented a CrI of 44.3, corroborating the results of previous studies [29,43,44]. There was no appreciable difference in the CrI of the pretreated SBs, with the exception of sulfite-NaOH, which showed a CrI of 51.3, corroborating the substantial removal of lignin (71.3%, Figure 2.1 and Table 2.1), which is an amorphous macromolecule.

Evaluation of enzymatic hydrolysis of sugarcane bagasse in response to different pretreatments

Enzymatic activity of the commercial preparation Cellic CTec 2 was determined and reported in Table 2.S4. The results of total cellulase activity agreed with those reported in previous studies; however, slight differences in results can be explained by the use of different methodologies and substrates [45,46].

Untreated and pretreated SBs were hydrolyzed using this enzyme preparation. The kinetic profile of enzymatic hydrolysis of cellulose and xylan of pretreated SB under different conditions corroborated the results of previous studies, that is, the reaction reaches a maximum rate of product formation in 8-24 h as a function of the enzyme saturation by the substrate (Figure 2.2) [9,16]. It should be noted that the enzymatic hydrolysis process of pretreated SB occurs in a heterogeneous phase (pretreated SB in buffer solution with enzyme), which makes it difficult for the enzymes to penetrate the material, resulting in a slow bioprocess of bioproduct formation. Figure 2.2a shows the cellulose conversions into glucose from pretreated SB under different

conditions. The cellulose conversions into glucose, after 24 h of enzymatic hydrolysis, of the untreated, thermo-treated, KOH, sulfite-KOH, NaOH, sulfite-neutral, and sulfite-NaOH assays were 23.7%, 28.0%, 30.2%, 42.1%, 51.7%, 75.7%, and 82.7%, respectively (Figure 2.2a and Table 2.2).

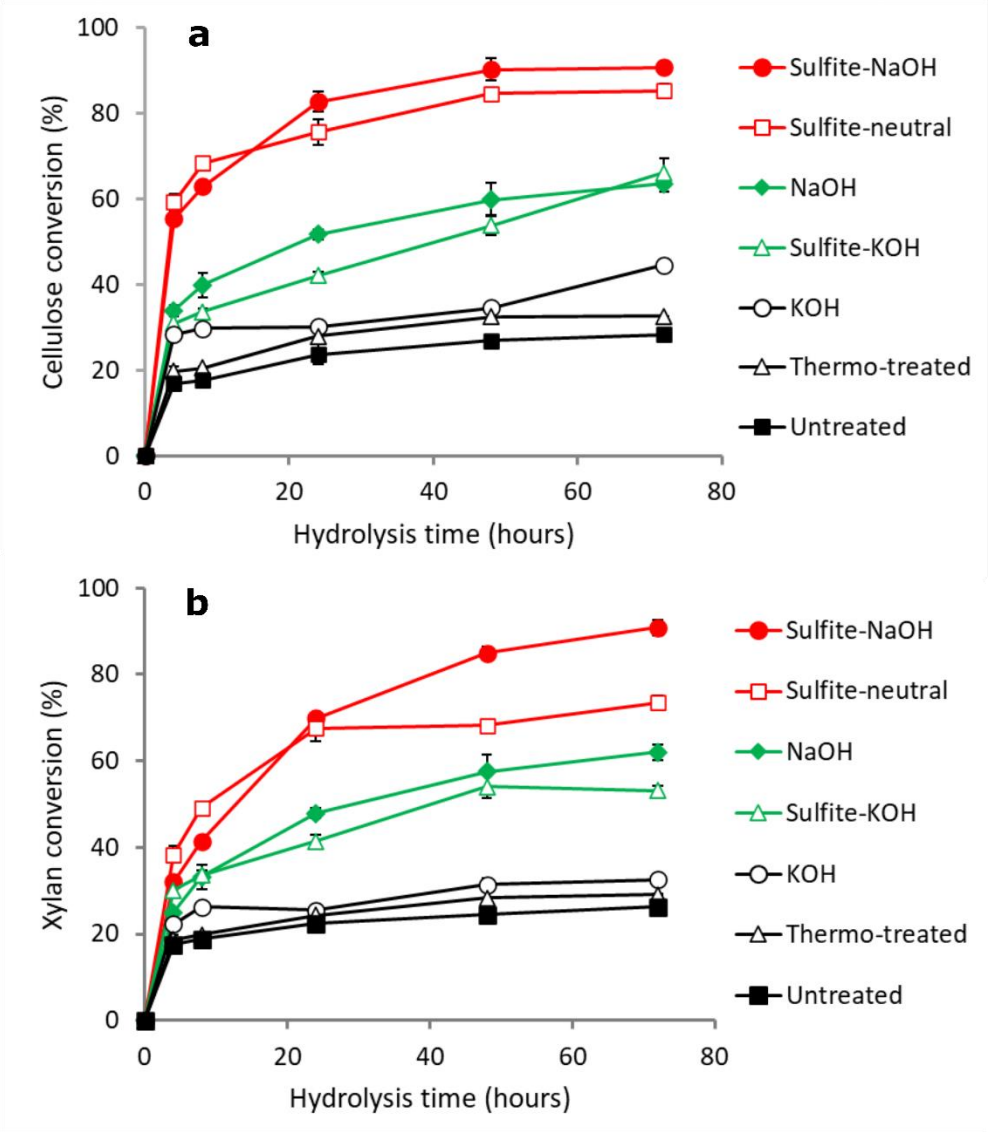

Figure 2.2. Enzymatic hydrolysis of sugarcane bagasse (SB) after different chemical pretreatments. (a) Cellulose conversion into glucose. (b) Xylan conversion into xylose. The error bars that are not visible are less than the own symbol.

Table 2.2. Comparison of the efficiency of sugarcane bagasse (SB) enzymatic hydrolysis over different chemical pretreatments.

	Pretreatment conditions				Enzymatic hydrolysis conditions			Conversion after 24h of enzymatic hydrolysis		Ref.
	Temp. (°C)	Time (h)	Reagents per 100g of SB (g)	Cons. (%)	Enzyme units per gram of SB	Enzymatic preparation	Cons. (%)	Cellulose (%)	Xylan (%)	
Untreated	-		-	-				23.7±2.3	22.4±0.5	
NaOH			5g					51.7±1.1	47.9±1.4	
Sulfite-NaOH			5g NaOH+10g Na_2SO_3					82.7±2.3	69.9±0.7	
Thermo-treated	140	0.5	-	10	13.2 FPU	Cellic CTec 2 (Novozymes)	5	28.0±0.8	24.3±1.1	This work
Sulfite-KOH			5g KOH+10g Na_2SO_3					42.1±1.0	41.4±1.5	
Sulfite-neutral			10g Na_2SO_3					75.7±3.0	67.6±1.9	
KOH			5g					30.2±0.8	25.5±0.9	
Untreated	-	-	-	-		Celluclast + Novozym 188 (Novozymes)		11.0	8.5	
NaOH	120	2	5g	10	8.8 FPU + 13.3 IU		2	27.0	24.0	[9]
Sulfite-NaOH			5g NaOH+10g Na_2SO_3					52.0	39.5	
Untreated	-	-	-					17.0	NR	
Sulfite-NaOH			2g NaOH+4g Na_2SO_3					27.0	NR	
Sulfite-NaOH	120	2	3g NaOH+6g Na_2SO_3	12	20 FPU	Multifect CX (Danisco)	5	45.0	NR	[47]
Sulfite-NaOH			4g NaOH+8g Na_2SO_3					50.0	NR	
Untreated	-	-	-					17.0	NR	
NaOH			45g NaOH					66.0	NR	
NaOH+US	25	0.75	45g NaOH	4	20 FPU	Cellic CTec (Novozymes)	5	85.0	NR	[48]
NaOH+HC			45g NaOH					96.0	NR	
Sulfite-NaOH	150	0.75	5g NaOH+10g Na_2SO_3	8	10 FPU + 10 IU	Celluclast + Novozym 188 (Novozymes)	5	53.5	46.2	[12]

NR=Not reported. SB=Sugarcane Bagasse. US=Ultrasound. HC=Hydrodynamic Cavitation. FPU=Filter Paper Units. IU=International units. Cons=Consistency.

Therefore, it was possible to identify three different groups of pretreated SBs under different conditions, depending on the potential for converting cellulose into glucose. The first group (black) showed low conversions of cellulose to glucose (untreated, thermo-treated, and KOH); the second group (green) showed intermediate cellulose to glucose conversions (sulfite-KOH and NaOH); and the third group (red) showed higher conversion of cellulose into glucose (sulfite-neutral and sulfite-NaOH) (Figure 2.2a and Table 2.2). Figure 2.2b shows the xylan conversions into xylose from pretreated SBs under different conditions. The xylan conversions into xylose, after 24 h of enzymatic hydrolysis, for the untreated, thermo-treated, KOH, sulfite-KOH, NaOH, sulfite-neutral, and sulfite-NaOH assays were 22.4%, 24.3%, 25.5%, 41.4%, 47.9%, 67.6% and 69.9%, respectively (Figure 2.2b and Table 2.2). Three distinct groups of pretreated SBs were highlighted due to the xylan conversion potential. The first group (black) showed low xylan conversions into xylose (untreated, thermo-treated, and KOH); the second group (green) showed intermediate xylan conversions into xylose (sulfite-KOH and NaOH); and the third group (red) showed high xylan conversions into xylose (sulfite-neutral and sulfite-NaOH) (Figure 2.2b and Table 2.2).

To determine the maximum reaction rate of glucose or xylose formation, the first derivative of C with respect to t in Equation (3) (dC/dt) was calculated, which corresponds to the reaction rate at a given instant of time t, whose maximum value occurs for $t = 0$ and is equal to $k \cdot C_{max}$. Table 2.S5 shows the maximum rate of glucose or xylose formation as well as the reaction kinetic

constant (k) and maximum asymptotic concentration of glucose or xylose (C_{max}).

As previously highlighted, three distinct groups of pretreated SBs were identified as a function of the potential for converting cellulose into glucose (Figure 2.2a), which is related to the maximum rate of glucose formation (Table 2.S5). The exception is the SB pretreated with KOH, which showed a maximum rate of glucose significantly different from untreated and thermo-treated SBs. However, pretreatment with KOH was incorporated into the group of untreated and thermo-treated SBs (black group, Figure 2.2a) because, despite the SB pretreated with KOH presenting a maximum rate of glucose formation higher than untreated and thermo-treated SBs, the SBs pretreated with NaOH and sulfite-KOH showed a profile of progressive increase in the cellulose conversion into glucose in 24-72 h of enzymatic hydrolysis, unlike in the case of the SB pretreated with KOH, which resulted in stabilization of the cellulose conversion into glucose in 24-72 h of enzymatic hydrolysis (Figure 2.2a).

The highest maximum rates of xylose formation were achieved in SBs pretreated with sulfite-neutral, sulfite-KOH, KOH, and sulfite-NaOH. Pretreatments with NaOH, thermo-treated, and untreated showed lower values of the maximum rate of xylose compared to other pretreatments, with no significant differences between them (Table 2.S5). However, in the same mode that occurred in the conversion of cellulose to glucose, pretreatment with KOH, despite having a high maximum rate of xylose, showed a profile of xylan

conversion into xylose similar to that of the untreated and thermo-treated SBs after 24-72 h of hydrolysis (Figure 2.2b).

A direct comparison of enzymatic hydrolysis assays in untreated and pretreated SBs, both performed in the present study as well as previous studies, is shown in Table 2.2. The tests reported in the study used the following enzyme preparations: Celuclast + Novozym 188 (Novozymes), with loads between 8.8-20 $FPU.g^{-1}$ and 10-13.3 $IU.g^{-1}$ of substrate, respectively; Multifect CX (Danisco), Cellic CTec (Novozymes), both with a load of 20 $FPU.g^{-1}$. In the present study, we used the enzymatic preparation Cellic CTec 2 (Novozymes) with a load of 13.2 $FPU.g^{-1}$ of substrate. In addition, the pretreatments with sulfite-NaOH reported in previous studies resulted in different levels of lignin compared to the pretreatment with sulfite-NaOH carried out in the present study (Figure 2.1 and Table 2.1). Therefore, there was a significant difference in cellulose conversion to glucose and xylan to xylose after 24 h of enzymatic hydrolysis. In general, pretreatment with sulfite-NaOH carried out in this study showed cellulose and xylan conversions to glucose and xylose, respectively. These were relatively superior to those reported in previous studies, with the exception of pretreatments with NaOH + ultrasound and cavitation, which showed cellulose conversion to glucose of 85% and 96%, respectively, which is similar to what was reported for pretreatment with sulfite-NaOH in the present study (82.7%) (Table 2.2). However, pretreatments with NaOH + ultrasound and NaOH + cavitation used a load of NaOH of 45g/100 g of SB (dry basis), while pretreatment with sulfite-

NaOH performed in this study used a load of NaOH of 5g/100 g + Na_2SO_3 of 10g/100 g of SB (dry basis).

Figure 2.S3 shows the cellulose and xylan conversions as a function of lignin content of pretreated SBs. These experimental data were well-fitted by linear mathematical models, resulting in determination coefficients (R^2) of 0.90 and 0.94, respectively (Figure 2.S3). Consequently, the greater the removal of the lignin fraction, the higher the cellulose and xylan conversions to glucose and xylose, respectively. Previous studies have reported a similar behavior in the conversion of cellulose to glucose as a function of the lignin content for SB of different sugarcane hybrids, in addition to SB previously pretreated with sodium chlorite under different conditions [16,49]. In addition, lignin sulfonation (reaction present in pretreatments with the addition of sodium sulfite) amplifies the potential for enzymatic hydrolysis of cellulose and xylan [11].

The sulfite-NaOH and sulfite-neutral pretreatments stood out for presenting higher cellulose and xylan conversions to glucose and xylose, respectively, in relation to the other pretreatments performed in the present study. However, the sulfite-NaOH pretreatment showed a greater tendency to increase the conversion of cellulose and xylan into glucose and xylose, respectively, after 8 h of hydrolysis, since, in alkaline medium, there is a higher rate of sulfonation and swelling of residual lignin, facilitating enzymatic hydrolysis of cellulose and xylan fractions [11]. The enzymatic hydrolysis tests presented so far have been carried out with a consistency of 5% (5 g SB/100 mL of buffer), which has resulted in a maximum concentration of glucose and xylose of approximately 25 and 12 $g.L^{-1}$, respectively. Pretreatment with sulfite-

NaOH was selected to evaluate studies of increased mass load or consistency and different enzyme loads. Sugar concentrations were monitored to obtain a hydrolysate rich in glucose (concentration 80-100 $g.L^{-1}$) without appreciable cellulose and xylan conversion losses.

Evaluation of increased consistency and enzyme load on the enzymatic hydrolysis of sugarcane bagasse pretreated with sulfite-NaOH

SB pretreated with sulfite-NaOH was subjected to enzymatic hydrolysis assays in Erlenmeyer flasks operated in batch mode under different consistencies (2%, 5%, 10%, 20%, and 30%, w/v). Figure 2.3ac shows the temporal kinetic profiles of the cellulose and xylan conversions to glucose and xylose, respectively.

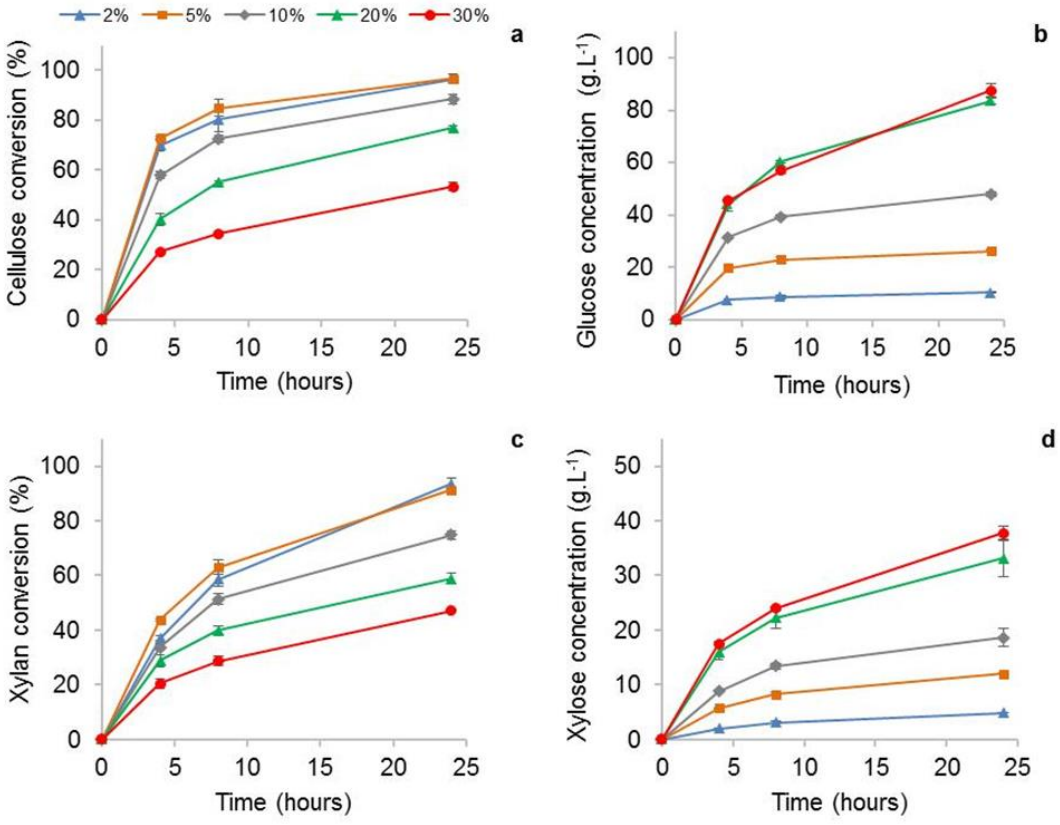

Figure 2.3. Enzymatic hydrolysis of sugarcane bagasse pretreated with sulfite-NaOH under different consistencies or mass loads presented in percentage

(w/v): (a) Cellulose conversion into glucose. (b) Glucose concentration. (c) Xylan conversion into xylose. (d) Xylose concentration.

The cellulose and xylan conversions into glucose and xylose, respectively, from SB pretreated with sulfite-NaOH under 2% and 5% (w/v) consistencies were similar, reaching a maximum cellulose or xylan conversion, after 24 h, of approximately 90% (Figure 2.3ac). The kinetic profiles of enzymatic hydrolysis carried out under consistencies of 20% and 30% (w/v) resulted in lower conversions, reaching, in 24 h, 77% and 53% of cellulose conversion and 58.8% and 47.2% of xylan conversion, respectively (Figure 2.3ac). In contrast, the kinetic profile of enzymatic cellulose hydrolysis performed with consistencies of 10% (w/v), presented an intermediate cellulose and xylan conversion in 24 h (88% and 75%, respectively), suggesting efficiency loss in enzymatic hydrolysis for tests performed with a consistency greater than or equal to 10% (w/v) (Figure 2.3ac). Caspeta et al. [22] reported the enzymatic hydrolysis of agave bagasse cellulose in Erlenmeyer flask tests with high mass loads (high consistency). The enzymatic hydrolysis assays were conducted in fed-batch mode, with initial consistencies of 5-10% (w/v), reloading the flasks with an additional 10 % of biomass after 12 h of hydrolysis, which resulted in final consistencies of 15-20% (w/v), respectively. The enzymatic loads used in the tests were 15 $FPU.g^{-1}$ substrate (total cellulases) and 20 $IU.g^{-1}$ substrate (β-glycosidase) of the enzyme preparations NS50013 and NS50010, respectively (®Novozymes). The hydrolysis of the agave bagasse pretreated with ethanosolv under consistencies of 15-20% (w/v) resulted in a cellulose conversion to glucose of

approximately 37% in 24 h of hydrolysis [22]. However, this result was lower than that of the enzymatic hydrolysis assay of SB pretreated with sulfite-NaOH with a consistency of 20% (77 %) (Figure 2.3a).

The efficiency loss in the enzymatic hydrolysis of the cellulose and xylan fractions due to the high consistencies can be attributed to the mass transfer limitations. Moreover, the higher the consistency, the lower the volume of the buffering solution with enzyme added to the assay [21–23]. Therefore, tests with consistencies of 2-10% (w/v) did not present problems associated with mass transfer, as these were liquefied since the beginning of the experimental test, while tests with consistencies of 20-30% (w/v) presented a solid aspect (high rheology) since the beginning of the experimental test. The difficulty of mass transfer can be exemplified through the visual aspect of enzymatic hydrolysis of SB pretreated with sulfite-NaOH at $t =$ 24 h, under a consistency of 20% and 30% (w/v), when it is possible to verify the more solid aspect of the test with a consistency of 30% (w/v) in contrast to the test with 20%, which is presented in liquefied form (Figure 2.S4).

The efficiency loss of enzymatic hydrolysis can also be attributed to the inhibition of the enzyme by the reaction product (inhibition of cellulases and xylanases by glucose and xylose, respectively), since higher consistencies result in higher concentrations of glucose and xylose in the enzymatic hydrolysate [21–24].

Figure 2.3b shows the glucose concentration as a function of hydrolysis time. Tests with consistencies of 2%, 5%, 10%, 20%, and 30% (w/v) resulted in maximum concentrations of glucose, after 24 h of hydrolysis, of 10, 26, 48,

83.5 and 87.5 g.L^{-1}, respectively. Caspeta et al. [22] reported the formation of glucose in concentrations of 60-80 g.L^{-1} in the enzymatic hydrolysis of agave bagasse pretreated with ethanosolv under consistencies of 15-20% (w/v) in an assay performed in fed-batch mode. These concentrations were lower than those obtained in the present study (Figure 2.3b). Figure 2.3d shows the xylose concentration over time for the hydrolysis of the xylan fraction. The tests performed with consistencies of 2%, 5%, 10%, 20%, and 30% (w/v) resulted in maximum concentrations of xylose, after 24 h of hydrolysis, of 5, 12, 18.5, 33, and 37.5 g.L^{-1}, respectively.

Table 2.3 presents the values of the maximum rate of glucose and xylose formation, in addition to the reaction constant (k) and maximum asymptotic concentration of glucose or xylose (C_{max}) for enzymatic hydrolysis under different consistencies.

Table 2.3. Kinetic parameters of enzymatic hydrolysis of sugarcane bagasse pretreated with sodium sulfite and sodium hydroxide under different consistencies (w/v).

Bioproduct	Consistency (%, w/v)	k (h^{-1})	C_{max} (g.L^{-1})	Maximum rate of product formation (g.L^{-1}.h^{-1})	R^2
Glucose	30	0.15 ± 0.01	88.70 ± 3.36	13.41 ± 0.74^{a}	0.9858
	20	0.17 ± 0.00	84.26 ± 0.65	14.42 ± 0.71^{a}	0.9965
	10	0.26 ± 0.00	47.37 ± 0.71	12.37 ± 0.13	0.9975
	5	0.34 ± 0.01	25.73 ± 0.39	8.75 ± 0.38	0.9955
	2	0.33 ± 0.02	10.04 ± 0.34	3.26 ± 0.19	0.9906
Xylose	30	0.13 ± 0.00	39.12 ± 1.42	5.12 ± 0.01^{a}	0.9939
	20	0.14 ± 0.01	33.97 ± 3.59	4.90 ± 0.38^{a}	0.9946
	10	0.16 ± 0.02	19.11 ± 1.93	2.95 ± 0.18	0.9999
	5	0.15 ± 0.01	12.26 ± 0.13	1.81 ± 0.08	0.9975
	2	0.11 ± 0.01	5.26 ± 0.09	0.59 ± 0.05	0.9988

Data are in format: mean ± standard deviation. The values with the same superscripts do not differ among themselves at a significance level of 0.05 (Tukey test). Enzyme load of 13.2 FPU.g^{-1}. k = reaction rate constant (h^{-1}). C_{max} = asymptotic maximum glucose or xylose concentration (g.L^{-1}).

The kinetic profiles of enzymatic hydrolysis, as shown in Figure 2.3, suggest loss of efficiency in the hydrolysis of experimental tests conducted

with consistencies above 10% (w/v). It was found that the tests conducted with consistencies of 20% and 30% (w/v) did not show significant differences in the maximum rates of glucose and xylose formation. On the other hand, the tests performed with consistencies of 2%, 5%, and 10% (w/v) showed significantly different maximum rates of glucose and xylose formation, as well as being significantly different for the tests with consistencies of 20% and 30% (w/v) (Table 2.3). In this way, analysis of the maximum rates of glucose and xylose formation estimated for the tests performed under different consistencies confirmed the loss of conversion efficiency of cellulose and xylose into glucose and xylose, respectively, in the tests performed with consistencies of 20% and 30% (w/v) (Figure 2.3). This loss of efficiency can be attributed to problems associated with mass transfer and/or inhibition of enzymes by the product, since the maximum rates of glucose and xylose formation for the tests performed with consistencies of 20% and 30% (w/v) were statistically equal, corroborating the aforementioned problems. Since, product inhibition and mass transfer problems in the test with 30% resulted in substantial loss of cellulose and xylan conversions compared to test with 20% consistency (Figure 2.3 and Table 2.3), subsequent assays continued to be performed with a consistency of 20%

Hydrolysis of SB pretreated with sulfite-NaOH was also evaluated under different enzymatic loads (3.3, 13.2, and 30.0 $FPU.g^{-1}$) with consistency set at 20% (w/v). Figure 2.4 shows the temporal kinetic profiles of the cellulose and xylan conversions to glucose and xylose.

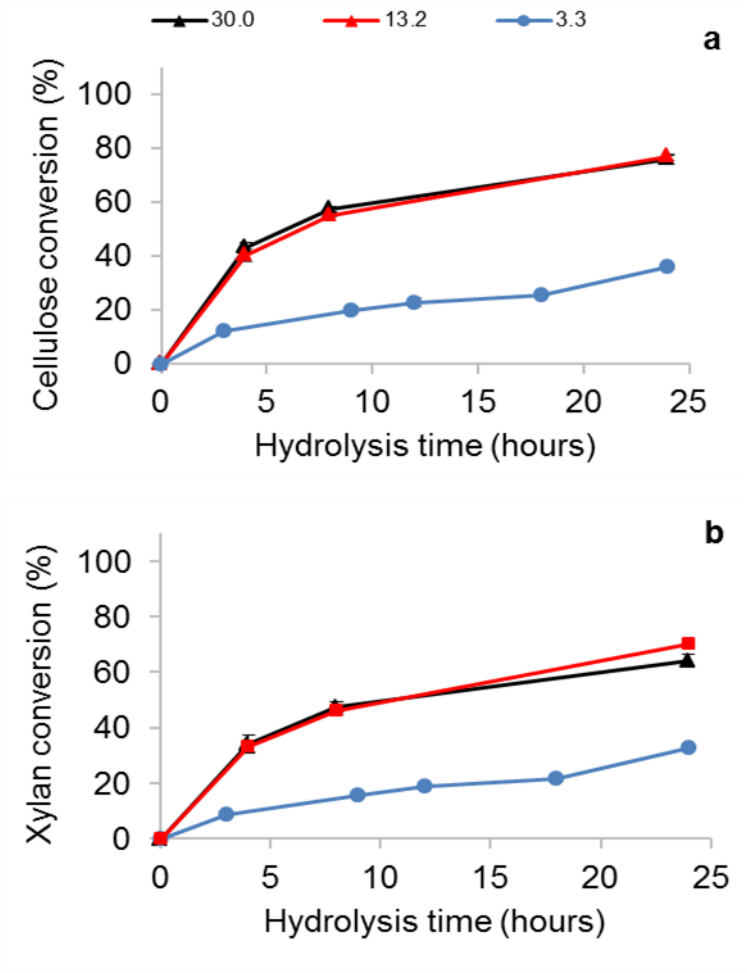

Figure 2.4. Enzymatic hydrolysis of sugarcane bagasse pretreated with sulfite-NaOH under consistency of 20 % (w/v) and different enzymatic loads (total cellulases and β-glucosidase) of enzymatic preparation Cellic CTec 2 (Novozymes): (a) Cellulose conversion into glucose. (b) Xylan conversion into xylose

The cellulose and xylan conversions into glucose and xylose of SB pretreated with sulfite-NaOH under the enzymatic load of 3.3 FPU.g^{-1}, after 24 h, were approximately 36% and 33%, respectively (Figure 2.4). The maximum rates of glucose and xylose formation for the enzymatic load of 3.3 FPU.g^{-1} were 4.61 and 1.54 g.L^{-1}.h^{-1}, respectively. However, assays with enzymatic loads of 13.2 and 30.0 FPU.g^{-1} showed very similar cellulose and xylan conversions, reaching values of approximately 77% and 67%, after 24 h,

respectively (Figure 2.4). The maximum rates of glucose formation for the tests with 13.2 and 30.0 FPU.g^{-1} were 13.4 and 16.6 g.L^{-1}.h^{-1}, respectively, while the maximum rates of xylose formation for tests with 13.2 and 30.0 FPU.g^{-1} were 4.9 and 6.2 g.L^{-1}.h^{-1}, respectively. The values of the maximum rates of glucose and xylose formation for the tests under different consistencies were significantly different, but very similar for the tests with enzymatic loads of 13.3 and 30.0 FPU.g^{-1}, although there was a significant difference in the values of the maximum rate of glucose and xylose formation.

The assay with a consistency of 20% (w/v) and enzyme load of 13.2 FPU.g^{-1} resulted in average concentrations of glucose and xylose, in 24 h of enzymatic hydrolysis, of 80 and 33 g.L^{-1}, respectively. On the other hand, this assay resulted in losses of cellulose and xylan conversions into glucose and xylose of approximately 28% and 37% in relation to consistencies of 2% and 5% (Figure 2.3), respectively. Therefore, increasing the consistency in the enzymatic hydrolysis of SB has the advantage of avoiding or reducing the time of the concentration step of the enzymatic hydrolysate, in addition to decreasing the final reaction volume. These combined effects result in an increase in the productivity of the bioproduct production processes, such as 2G ethanol. In this way, the enzymatic load of 13.2 FPU.g^{-1} and consistency of 20% (w/v) were established to continue assays of enzymatic hydrolysis of SB pretreated with sulfite-NaOH in a bench-scale bioreactor, equipped with mechanical agitation and temperature control to minimize conversion losses due to the increased consistency.

Evaluation of enzymatic hydrolysis of sugarcane bagasse pretreated with sulfite-NaOH in a bioreactor subject to high mass load

SB pretreated with sulfite-NaOH was subjected to enzymatic hydrolysis assays in a bench-top stirred tank bioreactor with temperature control and mechanical agitation compared to a simultaneous assay performed in Erlenmeyer flasks, both operated in batch mode for 72 h under a consistency of 20% (w/v). The details of the bioreactor and impeller are shown in Figure 2.S5.

The visual aspect of SB pretreated with sulfite-NaOH enzymatically hydrolyzed in an Erlenmeyer flask and bioreactor is shown in Figure 2.5 and Video 1 and 2.

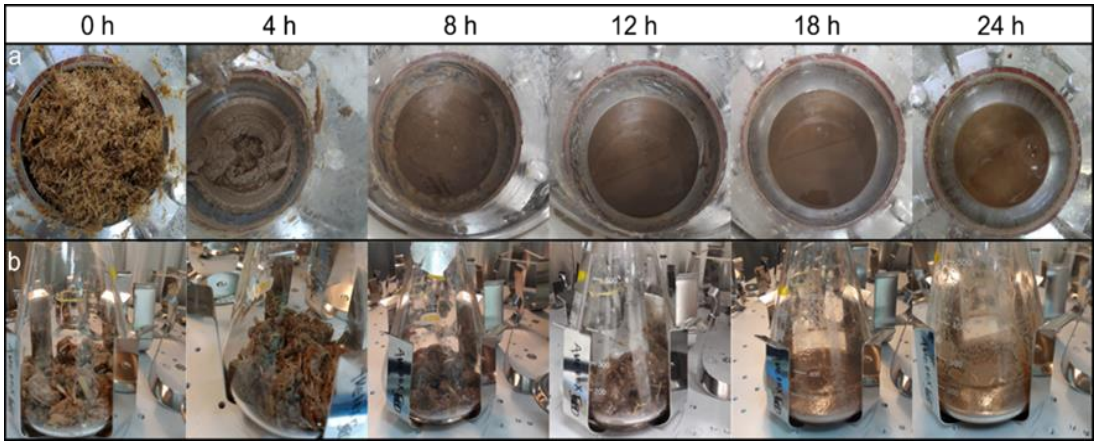

Figure 2.5. Visual aspect of the enzymatic hydrolysis assays of sugarcane bagasse pretreated with sulfite-NaOH under consistency of 20 % (w/v): (a) Hydrolysis performed in a bioreactor. (b) Enzymatic hydrolysis performed in Erlenmeyer flask.

It was found that the visual aspect changed more quickly in the enzymatic hydrolysis performed in the stirred tank bioreactor compared to in the Erlenmeyer flask. After 8 h of enzymatic hydrolysis in the bioreactor, it was already possible to verify the liquefaction of the SB, whereas in the Erlenmeyer

flask this aspect was only verified after 18 h of hydrolysis. Therefore, considering the visual aspect, greater efficiency in the hydrolysis of the SB in the bioreactor is evident when compared to that in the Erlenmeyer flask (Figure 2.5, Video 1 and 2).

Figure 2.6 shows the temporal kinetic profiles of the cellulose and xylan conversions into glucose and xylose for the enzymatic hydrolysis of SB pretreated with sulfite-NaOH in the bioreactor and Erlenmeyer flask.

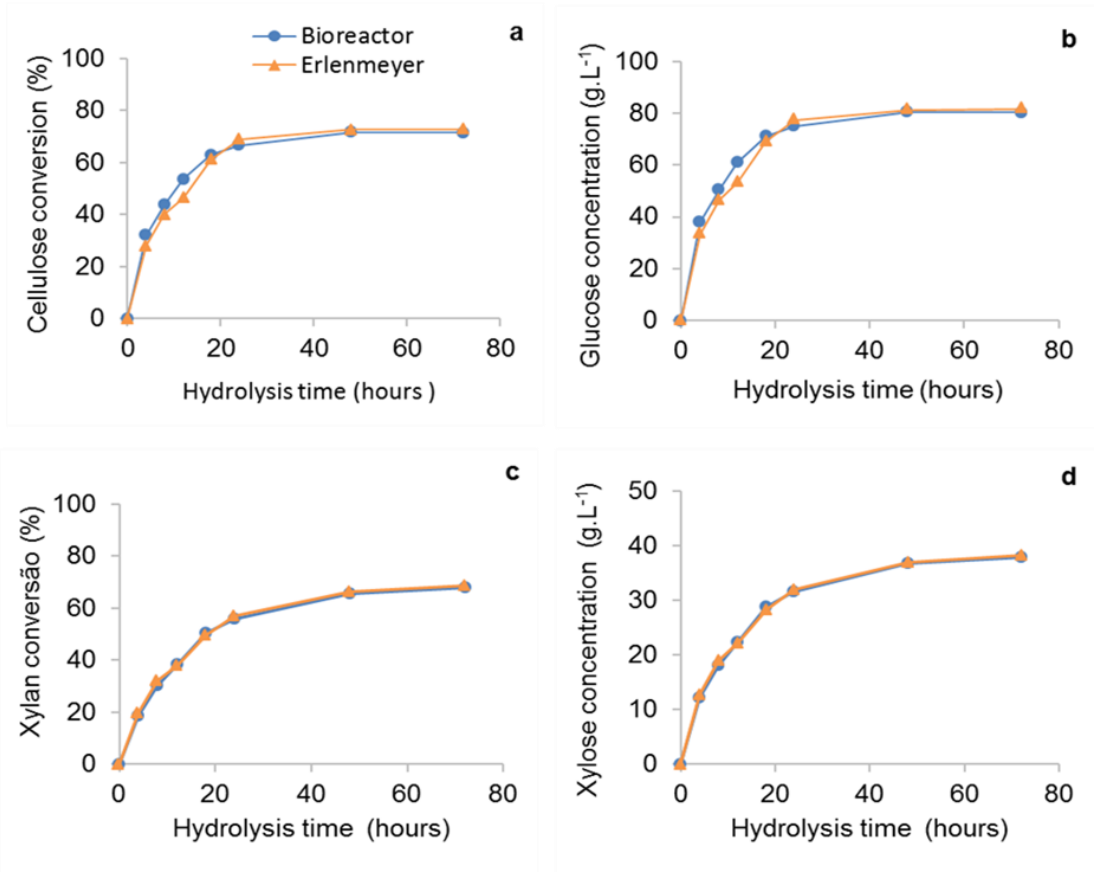

Figure 2.6. Enzymatic hydrolysis assays of sugarcane bagasse pretreated with sulfite-NaOH under consistency of 20 % (w/v): (a) Cellulose conversion into glucose. (b) Glucose concentration. (c) Xylan conversion into xylose. (d) Xylose concentration.

The cellulose and xylan conversions into glucose and xylose from SB pretreated with sulfite-NaOH, under a consistency of 20% (w/v) performed in a bioreactor and Erlenmeyer flask were similar, reaching a maximum cellulose and xylan conversion in 24 h of approximately 70% and 60%, respectively (Figure 2.6ac). However, there was a slight improvement in the efficiency of enzymatic hydrolysis of the cellulose fraction in the period of 4-18 h in the bioreactor assay when compared to the Erlenmeyer flask, which corroborates the visual aspect of the SB (Figure 2.5, Video 1 and 2). The maximum concentrations of glucose and xylose were also reached in 24 h of hydrolysis, resulting in 80 and 33 $g.L^{-1}$, respectively (Figure 2.7bd). The maximum rates of glucose and xylose formation estimated in the bioreactor were 10.6 and 3.0 $g.L^{-1}.h^{-1}$, respectively, while in the Erlenmeyer flask were 8.5 and 3.0 $g.L^{-1}.h^{-1}$, corroborating the higher conversion efficiency of the cellulose fraction (Figure 2.6a) and the visual aspect of SB (Figure 2.5, Video 1 and 2).

Caspeta et al. [22] reported the enzymatic hydrolysis of pretreated agave bagasse with ethanosolv under consistencies of 15-20% (w/v) in a bioreactor with peg-mixer. The authors reported an improvement in the enzymatic hydrolysis efficiency of approximately 30% compared to the process conducted in Erlenmeyer flasks. These results were slightly superior to those obtained in the present study. However, the experimental assay was operated in fed-batch mode, which can reduce the inhibitory effects on the enzyme by the product. In addition, there are also differences in the type of impeller used in each bioreactor, which can affect the mass transfer rates.

In general, enzymatic hydrolysis of SB pretreated with sulfite-NaOH at a high consistency in bioreactors showed a slight improvement compared to hydrolysis in Erlenmeyer flasks (both carried out in batch mode), indicating that problems of mass transfer and/or inhibition can be avoided using impellers designed for this purpose and the fed-batch mode to operate the bioreactor. Nevertheless, studies with alternative designs of impellers and tests conducted in fed-batch mode should be carried out to improve the enzymatic hydrolysis of SB under high consistency.

CONCLUSION

The pretreatment of SB with sulfite-NaOH was the most efficient in removing lignin, keeping the cellulose intact. In addition, the recovered pulp (solid fraction rich in cellulose and xylan) showed an excellent response in the enzymatic hydrolysis of the polysaccharide fractions, presenting conversions of approximately 90%.

The increase in consistency in the enzymatic hydrolysis of SB pretreated with sulfite-NaOH resulted in the loss of hydrolysis efficiency, mainly for consistencies ≥ 10%, which can be attributed to problems of mass transfer and/or inhibition of the enzyme by the product. However, at a consistency of 20%, the enzymatic hydrolysis of the cellulose and xylan fractions reached 70% and 60% conversions, respectively, resulting in an enzymatic hydrolysate with glucose and xylose concentrations of 80 and 33 $g.L^{-1}$, respectively.

The SB enzymatic hydrolysis assay performed in a stirred tank bioreactor showed better efficiency, mainly in SB liquefaction, resulting in a higher

maximum rate of glucose formation compared to the assay performed in Erlenmeyer flasks. The increase in the concentration of fermentable sugars in the enzymatic hydrolysate has the advantage of avoiding or reducing the time of a concentration step prior to the use of the hydrolysate, resulting in lower energy consumption. In addition, higher concentrations of fermentable sugars result in higher productivity of bioproducts formulated from sugar hydrolysate, such as cellulosic ethanol (2G ethanol).

Accordingly, studies regarding the design of bioreactors and mechanical impellers, in addition to the setup of the process (batch or fed-batch), are extremely relevant for the optimization of the SB enzymatic hydrolysis bioprocess under high consistency.

DECLARATIONS SECTION

List of abbreviations

(ATR-FTIR) Attenuated Total Reflection-Fourier Transform Infrared; (*CrI*) Crystallinity Index; (COS) Cello-oligosaccharides; (FPU) Filter Paper Units; (IU) International units; (SB) Sugarcane Bagasse; (IU) International Units; (XOS) Xylooligosaccharides; (XRD) X-Ray Diffraction; (CONAB) National Company of Supplying; (HPLC) High-performance liquid chromatography system; (DNS) 3,5-dinitrosalicylic acid reagent;.

Ethical Approval and Consent to participate

Not applicable.

Consent for publication

All authors read and approved the final manuscript.

Availability of supporting data

We are providing a document with supplementary information.

Conflicts of interest

There are no conflicts to declare.

Funding

São Paulo State Research Support Foundation (FAPESP, contract number 2018/06241-3), and Scientific Development Support Program of the School of Pharmaceutical Sciences (PADC) (contract number 2016/09-I) funding this work. Coordination of Improvement of Higher Education Personnel (CAPES) funding the doctoral scholarship of Fernando Roberto Paz-Cedeno and Eddyn Gabriel Solorzano-Chavez student.

Authors' contributions

FRPC, LH, EGSC, MS, FPP, IUMR performed pretreatments, chemical characterization, analyses of samples, data interpretation. FM, SCO, EGSC, IUMR and RM participated in the design of the experiments, data interpretation and mathematical modeling. FM, FRPC, SCO, LH, EGSC, MS, FPP, IUMR participated in the reviewed the manuscript. All authors read and approved the final manuscript.

Acknowledgements

FAPESP (contract number 2018/06241-3), and Scientific Development Support Program of the School of Pharmaceutical Sciences (PADC) (contract number 2016/09-I) funding this work. Coordination of Improvement of Higher Education Personnel (CAPES) funding the doctoral scholarship of Fernando Roberto Paz-Cedeno, Lucas Ragnini Henares and Eddyn Gabriel Solorzano-Chavez student.

REFERENCES

[1] M. Millinger, K. Meisel, D. Thrän, Greenhouse gas abatement optimal deployment of biofuels from crops in Germany, Transp. Res. Part D Transp. Environ. 69 (2019) 265–275. doi:https://doi.org/10.1016/j.trd.2019.02.005.

[2] M. Daraei, E. Thorin, A. Avelin, E. Dotzauer, Potential biofuel production in a fossil fuel free transportation system: A scenario for the County of Västmanland in Sweden, Energy Procedia. 158 (2019) 1330–1336. doi:https://doi.org/10.1016/j.egypro.2019.01.327.

[3] J. Mączyńska, M. Krzywonos, A. Kupczyk, K. Tucki, M. Sikora, H. Pińkowska, A. Bączyk, I. Wielewska, Production and use of biofuels for transport in Poland and Brazil – The case of bioethanol, Fuel. 241 (2019) 989–996. doi:https://doi.org/10.1016/j.fuel.2018.12.116.

[4] L.L. Benites-Lazaro, N.A. Mello-Théry, M. Lahsen, Business storytelling about energy and climate change: The case of Brazil's ethanol industry, Energy Res. Soc. Sci. 31 (2017) 77–85.

doi:https://doi.org/10.1016/j.erss.2017.06.008.

[5] Empresa de Pesquisa Energetica EPE, Brazilian Energy Balance 2019, 2019. https://www.epe.gov.br/sites-pt/publicacoes-dados-abertos/publicacoes/PublicacoesArquivos/publicacao-377/topico-494/BEN 2019 Completo WEB.pdf.

[6] CONAB, Acompanhamento da Safra Brasileira de Cana-de-açucar Safra 2019/20, Brasilia, 2020. doi:2318-7921.

[7] L. Canilha, A.K. Chandel, T. Suzane dos Santos Milessi, F.A.F. Antunes, W. Luiz da Costa Freitas, M. das Graças Almeida Felipe, S.S. da Silva, Bioconversion of Sugarcane Biomass into Ethanol: An Overview about Composition, Pretreatment Methods, Detoxification of Hydrolysates, Enzymatic Saccharification, and Ethanol Fermentation, J. Biomed. Biotechnol. 2012 (2012) 989572. doi:10.1155/2012/989572.

[8] M. Ek, G. Gellerstedt, G. Henriksson, Wood Chemistry and Wood Biotechnology, De Gruyter, Berlin, Boston, 2016. doi:https://doi.org/10.1515/9783110213409.

[9] F.M. Mendes, G. Siqueira, W. Carvalho, A. Ferraz, A.M.F. Milagres, Enzymatic hydrolysis of chemithermomechanically pretreated sugarcane bagasse and samples with reduced initial lignin content, Biotechnol. Prog. 27 (2011) 395–401. doi:10.1002/btpr.553.

[10] F.A. Santos, J.H. De Queiróz, J.L. Colodette, S.A. Fernandes, V.M. Guimaraes, S.T. Rezende, Potential of sugarcane straw for ethanol production , Potencial Da Palha Cana-de-Açúcar Para Produção Etanol. 35 (2012) 1004–1010. doi:10.1590/S0100-40422012000500025.

[11] F.M. Mendes, D.F. Laurito, M. Bazzeggio, A. Ferraz, A.M.F. Milagres, Enzymatic digestion of alkaline-sulfite pretreated sugar cane bagasse and its correlation with the chemical and structural changes occurring during the pretreatment step, Biotechnol. Prog. 29 (2013) 890–895. doi:10.1002/btpr.1746.

[12] J. Tavares, R.M. Łukasik, T. De Paiva, F. Da Silva, Hydrothermal alkaline sulfite pretreatment in the delivery of fermentable sugars from sugarcane bagasse, New J. Chem. 42 (2018) 4474–4484. doi:10.1039/c7nj04975g.

[13] L.F. Martins, D. Kolling, M. Camassola, A.J.P. Dillon, L.P. Ramos, Comparison of Penicillium echinulatum and Trichoderma reesei cellulases in relation to their activity against various cellulosic substrates, Bioresour. Technol. 99 (2008) 1417–1424. doi:10.1016/j.biortech.2007.01.060.

[14] M. Brienzo, V. Arantes, A.M.F. Milagres, Enzymology of the thermophilic ascomycetous fungus Thermoascus aurantiacus, Fungal Biol. Rev. 22 (2008) 120–130. doi:10.1016/j.fbr.2009.04.001.

[15] L. Ge, P. Wang, H. Mou, Study on saccharification techniques of seaweed wastes for the transformation of ethanol, Renew. Energy. 36 (2011) 84–89. doi:10.1016/j.renene.2010.06.001.

[16] F. Masarin, D.B. Gurpilhares, D.C. Baffa, M.H. Barbosa, W. Carvalho, A. Ferraz, A.M. Milagres, Chemical composition and enzymatic digestibility of sugarcane clones selected for varied lignin content, Biotechnol. Biofuels. 4 (2011) 55. doi:10.1186/1754-6834-4-55.

[17] K.K. Wong, L.U. Tan, J.N. Saddler, Multiplicity of beta-1,4-xylanase in microorganisms: functions and applications., Microbiol. Rev. 52 (1988) 305–317.

[18] A. Knob, E.C. Carmona, Purification and characterization of two extracellular xylanases from Penicillium sclerotiorum: a novel acidophilic xylanase., Appl. Biochem. Biotechnol. 162 (2010) 429–443. doi:10.1007/s12010-009-8731-8.

[19] L.F. dos Santos, P.L. Ishii, Xilanases: principais metodologias e parâmetros cinéticos, J. Biotechnol. Biodivers. 2 (2011) 7–15. doi:10.20873/jbb.uft.cemaf.v2n2.santos.

[20] T.D.T. Mafei, F.S.P.P. Neto, G. Peixoto, Á. de Baptista Neto, R. Monti, F. Masarin, Extraction and Characterization of Hemicellulose from Eucalyptus By-product: Assessment of Enzymatic Hydrolysis to Produce Xylooligosaccharides, Appl. Biochem. Biotechnol. 190 (2020) 197–217. doi:10.1007/s12010-019-03076-0.

[21] Z. Xiao, X. Zhang, D.J. Gregg, J.N. Saddler, Effects of Sugar Inhibition on Cellulases and β-Glucosidase During Enzymatic Hydrolysis of Softwood Substrates BT - Proceedings of the Twenty-Fifth Symposium on Biotechnology for Fuels and Chemicals Held May 4–7, 2003, in Breckenridge, CO, in: M. Finkelstein, J.D. McMillan, B.H. Davison, B. Evans (Eds.), Humana Press, Totowa, NJ, 2004: pp. 1115–1126.

[22] L. Caspeta, M.A. Caro-Bermúdez, T. Ponce-Noyola, A. Martinez, Enzymatic hydrolysis at high-solids loadings for the conversion of agave bagasse to fuel ethanol, Appl. Energy. 113 (2014) 277–286.

doi:https://doi.org/10.1016/j.apenergy.2013.07.036.

[23] W. Wang, X. Zhuang, Z. Yuan, Q. Yu, W. Qi, Q. Wang, X. Tan, High consistency enzymatic saccharification of sweet sorghum bagasse pretreated with liquid hot water., Bioresour. Technol. 108 (2012) 252–257. doi:10.1016/j.biortech.2011.12.092.

[24] R. Zhai, J. Hu, J.N. Saddler, The inhibition of hemicellulosic sugars on cellulose hydrolysis are highly dependant on the cellulase productive binding, processivity, and substrate surface charges, Bioresour. Technol. 258 (2018) 79–87. doi:https://doi.org/10.1016/j.biortech.2017.12.006.

[25] F. Masarin, F.R.P. Cedeno, E.G.S. Chavez, L.E. de Oliveira, V.C. Gelli, R. Monti, Chemical analysis and biorefinery of red algae Kappaphycus alvarezii for efficient production of glucose from residue of carrageenan extraction process, Biotechnol. Biofuels. 9 (2016) 122. doi:10.1186/s13068-016-0535-9.

[26] S. Park, J.O. Baker, M.E. Himmel, P.A. Parilla, D.K. Johnson, Cellulose crystallinity index: measurement techniques and their impact on interpreting cellulase performance, Biotechnol. Biofuels. 3 (2010) 10. doi:10.1186/1754-6834-3-10.

[27] N. Terinte, R. Ibbett, K. Schuster, Overview on native cellulose and microcrystalline cellulose I structure studied by X-ray diffraction (WAXD): Comparison between measurement techniques, Lenzinger Berichte. 89 (2011).

[28] M.-J. Chen, X.-Q. Zhang, A. Matharu, E. Melo, R.-M. Li, C.-F. Liu, Q.-S.

Shi, Monitoring the Crystalline Structure of Sugar Cane Bagasse in Aqueous Ionic Liquids, ACS Sustain. Chem. Eng. 5 (2017) 7278–7283. doi:10.1021/acssuschemeng.7b01526.

[29] I.U.M. Roldan, A.T. Mitsuhara, J.P.M. Desajacomo, L.E. De Oliveira, V.C. Gelli, R. Monti, L.V.S. Sacramento, F. Masarin, Chemical, structural and ultrastructural analysis of waste from the carrageenan and sugar-bioethanol processes for future bioenergy generation., Biomass and Bioenergy. No press (2017).

[30] T.K. Ghose, Measurement of cellulase activities, Pure Appl. Chem. 59 (1987) 257–268. doi:10.1351/pac198759020257.

[31] M. Tanaka, M. Taniguchi, R. Matsuno, T. Kamikubo, Purification and Properties of Cellulases from Eupencillium javanicum : Studies on the Re-utilization of Cellulosic Resources(VII), J. Ferment. Technol. 59 (1981) 177–183. http://ci.nii.ac.jp/naid/110002672575/en/ (accessed July 26, 2016).

[32] M.J. Bailey, P. Biely, K. Poutanen, Interlaboratory testing of methods for assay of xylanase activity, J. Biotechnol. 23 (1992) 257–270. doi:10.1016/0168-1656(92)90074-J.

[33] L.U.L. Tan, P. Mayers, J.N. Saddler, Purification and characterization of a thermostable xylanase from a thermophilic fungus Thermoascus aurantiacus, Can. J. Microbiol. (1987) 689–691. doi:10.1139/m87-120.

[34] S.C. Oliveira, F.R. Paz-Cedeno, F. Masarin, Kinetic modeling of monomeric sugars formation during the enzymatic hydrolysis of the residue generated in the carrageenan production from algal biomass, in:

XXI SINAFERM, Aracaju, 2017. https://proceedings.galoa.com.br/sinaferm/sinaferm-2017/trabalhos/kinetic-modeling-of-monomeric-sugars-formation-during-the-enzymatic-hydrolysis-of-the-residue?lang=en.

[35] S.C. Oliveira, F.R. Paz-Cedeno, F. Masarin, Mathematical modeling of glucose accumulation during enzymatic hydrolysis of carrageenan waste, in: A. Silva Santos (Ed.), Avanços Científicos e Tecnológicos Em Bioprocessos, Atena Editora, 2018: pp. 97–103. doi:10.22533/at.ed.475180110.

[36] F.R. Paz-Cedeno, E.G. Solórzano-Chávez, L.E. de Oliveira, V.C. Gelli, R. Monti, S.C. de Oliveira, F. Masarin, Sequential Enzymatic and Mild-Acid Hydrolysis of By-Product of Carrageenan Process from Kappaphycus alvarezii, BioEnergy Res. 12 (2019) 419–432. doi:10.1007/s12155-019-09968-7.

[37] E.G. Solorzano-Chavez, F.R. Paz-Cedeno, L. Ezequiel de Oliveira, V.C. Gelli, R. Monti, S. Conceição de Oliveira, F. Masarin, Evaluation of the Kappaphycus alvarezii growth under different environmental conditions and efficiency of the enzymatic hydrolysis of the residue generated in the carrageenan processing, Biomass and Bioenergy. 127 (2019). doi:10.1016/j.biombioe.2019.105254.

[38] S.C. Nakanishi, V.M. Nascimento, S.C. Rabelo, I.L.M. Sampaio, T.L. Junqueira, G.J.M. Rocha, Industrial Crops & Products Comparative material balances and preliminary technical analysis of the pilot scale sugarcane bagasse alkaline pretreatment to 2G ethanol production, Ind.

Crop. Prod. 120 (2018) 187–197. doi:10.1016/j.indcrop.2018.04.064.

[39] G. Ramadoss, K. Muthukumar, Ultrasound assisted ammonia pretreatment of sugarcane bagasse for fermentable sugar production, Biochem. Eng. J. 83 (2014) 33–41. doi:10.1016/j.bej.2013.11.013.

[40] J.B. Sluiter, R.O. Ruiz, C.J. Scarlata, A.D. Sluiter, D.W. Templeton, Compositional analysis of lignocellulosic feedstocks. 1. Review and description of methods, J. Agric. Food Chem. 58 (2010) 9043–9053. doi:10.1021/jf1008023.

[41] A. Sluiter, R. Ruiz, C. Scarlata, J. Sluiter, D. Templeton, Determination of Extractives in Biomass: Laboratory Analytical Procedure (LAP), 2008. http://www.nrel.gov/biomass/pdfs/42619.pdf.

[42] M.M. de S. Moretti, D.A. Bocchini-Martins, C. da C.C. Nunes, M.A. Villena, O.M. Perrone, R. da Silva, M. Boscolo, E. Gomes, Pretreatment of sugarcane bagasse with microwaves irradiation and its effects on the structure and on enzymatic hydrolysis, Appl. Energy. 122 (2014) 189–195. doi:https://doi.org/10.1016/j.apenergy.2014.02.020.

[43] A. Mandal, D. Chakrabarty, Isolation of nanocellulose from waste sugarcane bagasse (SCB) and its characterization, Carbohydr. Polym. 86 (2011) 1291–1299. doi:https://doi.org/10.1016/j.carbpol.2011.06.030.

[44] S. Nie, C. Zhang, Q. Zhang, K. Zhang, Y. Zhang, P. Tao, S. Wang, Enzymatic and cold alkaline pretreatments of sugarcane bagasse pulp to produce cellulose nanofibrils using a mechanical method, Ind. Crops Prod. 124 (2018) 435–441.

doi:https://doi.org/10.1016/j.indcrop.2018.08.033.

[45] J. Alftrén, T.J. Hobley, Immobilization of cellulase mixtures on magnetic particles for hydrolysis of lignocellulose and ease of recycling, Biomass and Bioenergy. 65 (2014) 72–78. doi:10.1016/j.biombioe.2014.03.009.

[46] X.S. Qu, B. Bin Hu, M.J. Zhu, Enhanced saccharification of cellulose and sugarcane bagasse by: Clostridium thermocellum cultures with Triton X-100 and β-glucosidase/Cellic®CTec2 supplementation, RSC Adv. 7 (2017) 21360–21365. doi:10.1039/c7ra02477k.

[47] J.F. Mesquita, A. Ferraz, A. Aguiar, Alkaline-sulfite pretreatment and use of surfactants during enzymatic hydrolysis to enhance ethanol production from sugarcane bagasse, Bioprocess Biosyst. Eng. 39 (2016) 441–448. doi:10.1007/s00449-015-1527-z.

[48] R. Terán Hilares, J.C. dos Santos, M.A. Ahmed, S.H. Jeon, S.S. da Silva, J.I. Han, Hydrodynamic cavitation-assisted alkaline pretreatment as a new approach for sugarcane bagasse biorefineries, Bioresour. Technol. 214 (2016) 609–614. doi:10.1016/j.biortech.2016.05.004.

[49] G. Siqueira, A.M.F. Milagres, W. Carvalho, G. Koch, A. Ferraz, Topochemical distribution of lignin and hydroxycinnamic acids in sugar-cane cell walls and its correlation with the enzymatic hydrolysis of polysaccharides, Biotechnol. Biofuels. 4 (2011) 7. doi:10.1186/1754-6834-4-7.

ANNEX. Electronic Supplementary Information

Evaluation of the effects of different chemical pretreatments in sugarcane bagasse on the response of enzymatic hydrolysis in batch systems subject to high mass loads

Fernando Roberto Paz-Cedeno, Lucas Ragnini Henares, Eddyn Gabriel Solorzano-Chavez, Mateus Scontri, Flávio Pereira Picheli, Ismael Ulises Miranda Roldán, Rubens Monti, Samuel Conceição de Oliveira and Fernando Masarin*

São Paulo State University (UNESP), School of Pharmaceutical Sciences (FCF), Department of Bioprocess Engineering and Biotechnology. Araraquara-SP, Brazil. 14800-903.

(*) corresponding author

Email addresses:
FRPC: fernando.paz@unesp.br
LH: lucas_henares@hotmail.com
EGSC: eddynsch04@hotmail.com
MS: mateus.scontri@unesp.br
FPP: flavio.picheli@unesp.br
IUMR: imiranda_3@hotmail.com
RM: rubens.monti@unesp.br
SCO: samuel.oliveira@unesp.br
*FM: fernando.masarin@unesp.br

Table 2.S1. Volume and concentration of the respective solutions of alkali and sodium sulfite used in each chemical pretreatment in sugarcane bagasse (SB).

Pretreatment	Reaction medium
Untreated	-
Thermo-treated	500mL H_2O
KOH	250mL H_2O + 250mL KOH 1%
Sulfite-KOH	250mL KOH 1% + 250mL Na_2SO_3 2%
NaOH	250mL H_2O + 250mL NaOH 1%
Sulfite-NaOH	250mL NaOH 1% + 250mL Na_2SO_3 2%
Sulfite-neutral	250mL H_2O + 250mL Na_2SO_3 2%

All pretreatments were performed using 50 g of SB at 140°C and 4 rpm for 30 min. The concentrations of the solutions are reported in percentage (w/v).

Table 2.S2. Enzyme load of enzymatic preparation (Cellic CTec 2) based on activity of total cellulases and the activity equivalent of other enzymes important for the process of hydrolysis of sugarcane bagasse (SB). Activity expressed per gram of sugarcane bagasse (SB) (dry basis).

	Enzymatic loading equivalent for enzyme group activities ($IU.g^{-1}$)				
***Cellulases ($FPU.g^{-1}$)**	**EG**	**CBH**	**BG**	**XL**	**BX**
3.3	45.7	0.8	435.0	352	2.2
12.4	173.1	2.8	1640.0	1331	8.4
13.2	183.8	3.0	1740.0	1413	8.9
26.6	370.3	6.1	3500.0	2849	18.0

**Cellulases=Total cellulases load in hydrolysis. EG=Endocellulase or Endoglucanase. CBH=Exoglucanase or Cellobihydrolase. BG=β-glucosidase. XL=Xylanases. BX=β-xylosidase.*

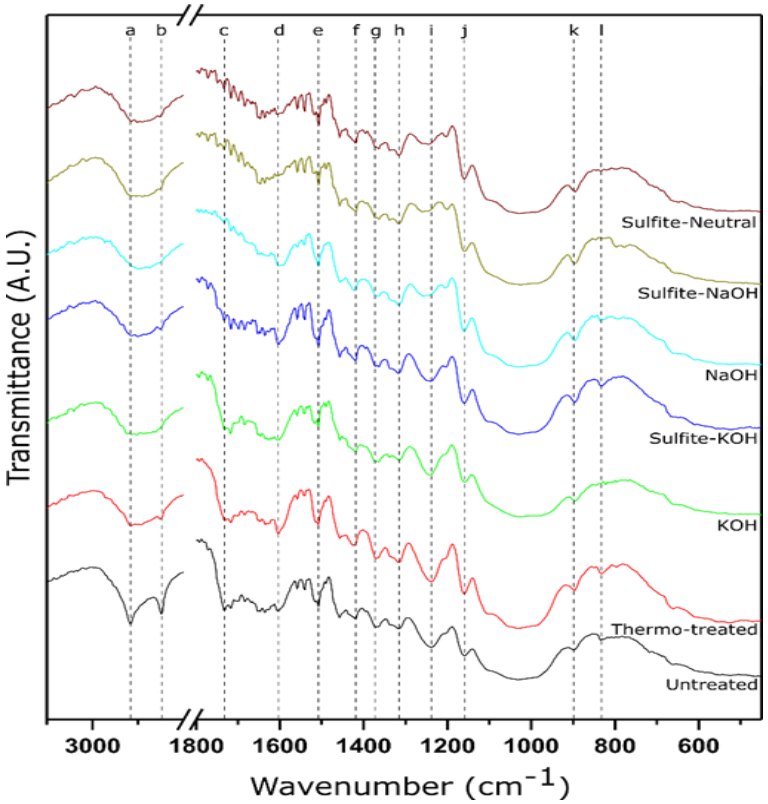

Figure 2.S1. Total attenuated reflection in the infrared with Fourier transform (ATR-FTIR) spectrum of sugarcane bagasse (SB) after different chemical pretreatments.

Table 2.S3. Characteristic bands from sugarcane bagasse (SB) in the medium infrared spectrum.

Wavenumber (cm^{-1})	Absorption band identification	Letters identifying the bands in Figure 2.1S
2924, 2854	Symmetric and asymmetric C-H (CH_2 and CH_3) stretching of alkanes, alcohols and aromatic ring	a, b
1729	Stretch C=O Hemicellulose Aldehyde/Ketone	c
1602, 1507	Lignin aromatic ring vibration C=C	d, e
1424	Aromatic skeleton combined with C-H in the plane of deformation and elongation	f
1367	Symmetrical angular deformation in the C-H plane of cellulose	g
1322	Vibration of asymmetric angular deformation (or balance) CH_2 of cellulose	h
1240	C-H in-plane deformation of lignin	i
1157	Asymmetric stretching of the C-O-C oxygen in cellulose	j
897	Glucose ring stretch, glycosidic C_1-H deformation of cellulose	k
833	Aromatic C-H out-of-plane deformation (only in GS and H lignin types)	l

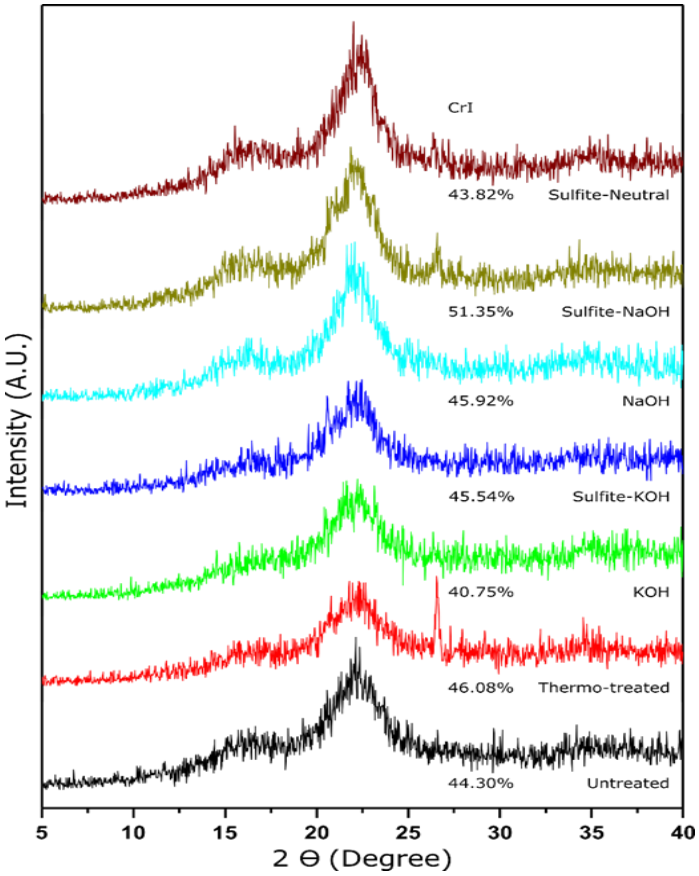

Figure 2.S2. X-ray diffraction (XRD) of sugarcane bagasse (SB) after different chemical pretreatments.

Table 2.S4. Total protein content, enzymatic activities and specific enzymatic activities of commercial enzyme preparation (Cellic CTec 2). Activity expressed per volume or gram of protein (dry basis), respectively.

		Enzymatic activities (IU.mL^{-1})				
Protein (mg.mL^{-1})	***Cellulases (FPU.mL^{-1})**	**EG**	**CBH**	**BG**	**XL**	**BX**
89.2	116.0	1632.4	26.8	15458.4	12559.4	80.3
		Specific enzymatic activities (IU.g^{-1})				
	***Cellulases (FPU.g^{-1})**	**EG**	**CBH**	**BG**	**XL**	**BX**
-	1.3	18.3	0.3	173.3	140.8	0.9

**Cellulases=Total cellulases. EG=Endocellulase or Endoglucanase. CBH=Exoglucanase or Cellobihydrolase. BG=β-glucosidase. XL=Xylanases. BX=β-xylosidase.*

Table 2.S5. Kinetic parameters of enzymatic hydrolysis of sugarcane bagasse (SBs) on different chemical pretreatments.

Bioproduct	Pretreatment	k (h^{-1})	C_{max} (gL^{-1})	Maximum rate of product formation ($gL^{-1}h^{-1}$)	R^2
Glucose	Sulfite-NaOH	0.26 ± 0.02	21.92 ± 0.60	5.64 ± 0.30[a]	0.9815
	Sulfite-Neutral	0.40 ± 0.05	16.57 ± 0.39	6.54 ± 0.72[a]	0.9973
	NaOH	0.26 ± 0.01	11.99 ± 0.35	3.07 ± 0.07[b]	0.9840
	Sulfite-KOH	0.34 ± 0.02	8.44 ± 0.08	2.84 ± 0.19[b]	0.9820
	KOH	0.35 ± 0.01	8.09 ± 0.00	2.82 ± 0.11[b]	0.9999
	Thermo-treated	0.30 ± 0.01	5.26 ± 0.06	1.60 ± 0.09[c]	0.9662
	Untreated	0.34 ± 0.10	4.26 ± 0.30	1.42 ± 0.31[c]	0.9727
Xylose	Sulfite-NaOH	0.13 ± 0.01	9.64 ± 0.17	1.25 ± 0.03[b]	0.9851
	Sulfite-Neutral	0.19 ± 0.01	7.92 ± 0.21	1.48 ± 0.06[a]	0.9920
	NaOH	0.16 ± 0.00	6.07 ± 0.16	0.98 ± 0.02[c]	0.9920
	Sulfite-KOH	0.31 ± 0.01	4.61 ± 0.11	1.43 ± 0.06[a]	0.9858
	KOH	0.33 ± 0.03	3.99 ± 0.05	1.31 ± 0.10[a,b]	0.9980
	Thermo-treated	0.36 ± 0.02	2.66 ± 0.06	0.95 ± 0.07[c]	0.9817
	Untreated	0.38 ± 0.04	2.19 ± 0.03	0.84 ± 0.08[c]	0.9861

Data are in format: mean ± standard deviation. The values with the same superscripts do not differ among themselves at a significance level of 0.05 (Tukey test). Enzymatic load of 13.2 FPU.g^{-1}. Consistency = 5 (%, w/v). k = reaction rate constant (h^{-1}). C_{max} = asymptotic maximum glucose or xylose concentration ($g.L^{-1}$).

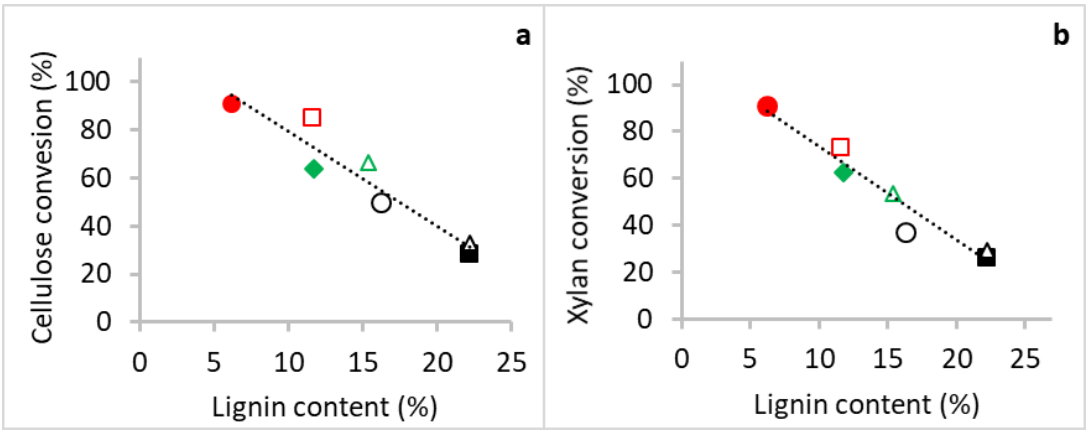

Figure 2.S3. Cellulose and xylan conversions to glucose (a) and xylose (b) as a function of lignin content of sugarcane bagasse (SB) submitted to different pretreatments. Untreated (filled black square), thermo-treated (empty black triangle), KOH (empty blue circle), sulfite-KOH (empty green triangle), NaOH (filled green diamond), sulfite-neutral, (empty red square) and sulfite-NaOH (full red circle).

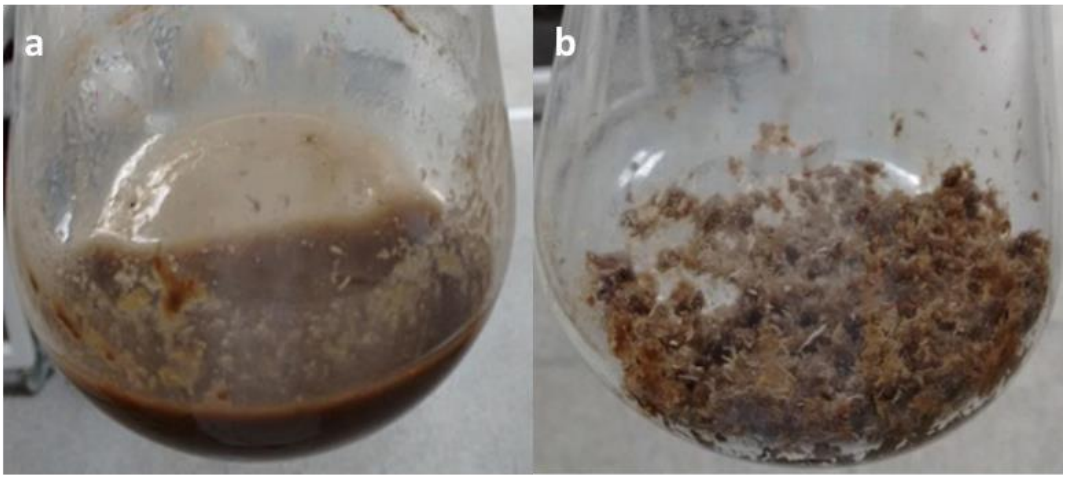

Figure 2.S4. Visual aspect of sugarcane bagasse pretreated with sulfite-NaOH after 24h of enzymatic hydrolysis: (a) Consistency of 20 % (w/v). (b) Consistency of 30 % (w/v).

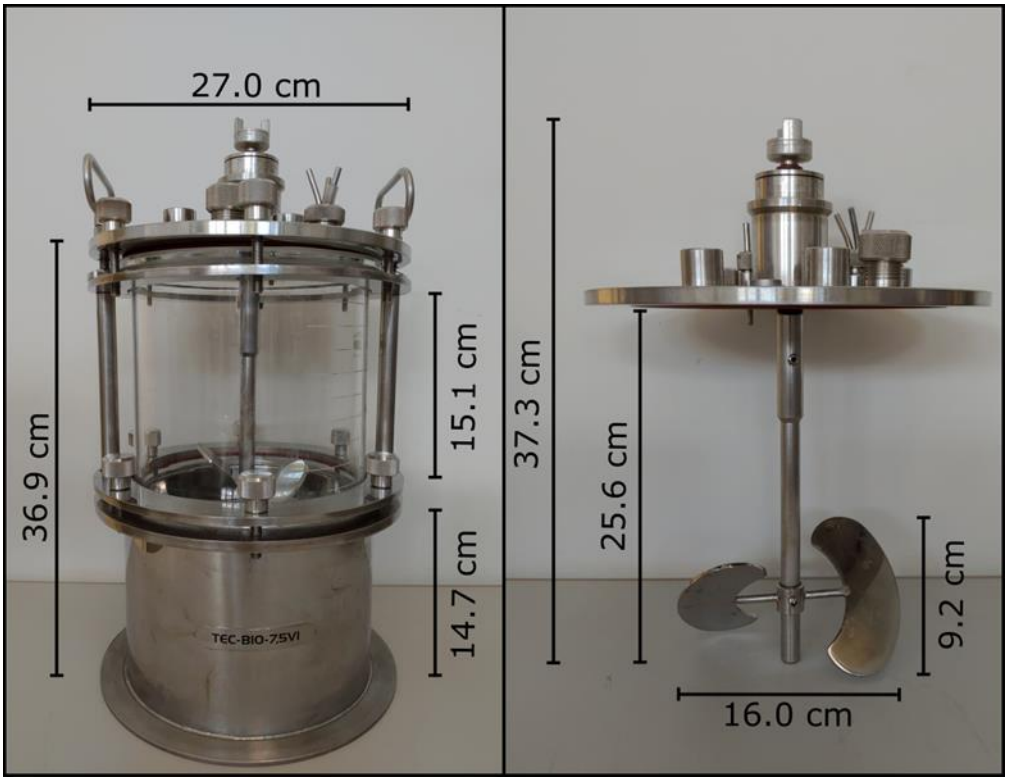

Figure 2.S5. Bioreactor and impeller used in the assays of enzymatic hydrolysis of sugarcane bagasse (SB).

ELSEVIER

Publishing Agreement

Elsevier Ltd
Evaluation of the effects of different chemical pretreatments in sugarcane bagasse on the response of enzymatic hydrolysis in batch systems subject to high mass loads

Corresponding author
Dr. Fernando Masarin
E-mail address
fernando.masarin@unesp.br
Journal
Renewable Energy
Our reference
RENE14382
PII
S0960-1481(20)31658-X
DOI
10.1016/j.renene.2020.10.092

Your Status

- I am one author signing on behalf of all co-authors of the manuscript

Assignment of Copyright

I hereby assign to Elsevier Ltd the copyright in the manuscript identified above (where Crown Copyright is asserted, authors agree to grant an exclusive publishing and distribution license) and any tables, illustrations or other material submitted for publication as part of the manuscript (the "Article"). This assignment of rights means that I have granted to Elsevier Ltd, the exclusive right to publish and reproduce the Article, or any part of the Article, in print, electronic and all other media (whether now known or later developed), in any form, in all languages, throughout the world, for the full term of copyright, and the right to license others to do the same, effective when the Article is accepted for publication. This includes the right to enforce the rights granted hereunder against third parties.

Supplemental Materials

"Supplemental Materials" shall mean materials published as a supplemental part of the Article, including but not limited to graphical, illustrative, video and audio material.

With respect to any Supplemental Materials that I submit, Elsevier Ltd shall have a perpetual worldwide, non-exclusive right and license to publish, extract, reformat, adapt, build upon, index, redistribute, link to and otherwise use all or any part of the Supplemental Materials in all forms and media (whether now known or later developed), and to permit others to do so.

Research Data

"Research Data" shall mean the result of observations or experimentation that validate research findings and that are published separate to the Article, which can include but are not limited to raw data, processed data, software, algorithms, protocols, and methods.

With respect to any Research Data that I wish to make accessible on a site or through a service of Elsevier Ltd, Elsevier Ltd shall have a perpetual worldwide, non-exclusive right and license to publish, extract,

reformat, adapt, build upon, index, redistribute, link to and otherwise use all or any part of the Research Data in all forms and media (whether now known or later developed) and to permit others to do so. Where I have selected a specific end user license under which the Research Data is to be made available on a site or through a service, the publisher shall apply that end user license to the Research Data on that site or service.

Reversion of rights

Articles may sometimes be accepted for publication but later rejected in the publication process, even in some cases after public posting in "Articles in Press" form, in which case all rights will revert to the author (see https://www.elsevier.com/about/our-business/policies/article-withdrawal).

Revisions and Addenda

I understand that no revisions, additional terms or addenda to this Journal Publishing Agreement can be accepted without Elsevier Ltd's express written consent. I understand that this Journal Publishing Agreement supersedes any previous agreements I have entered into with Elsevier Ltd in relation to the Article from the date hereof.

Author Rights for Scholarly Purposes

I understand that I retain or am hereby granted (without the need to obtain further permission) the Author Rights (see description below), and that no rights in patents, trademarks or other intellectual property rights are transferred to Elsevier Ltd.
The Author Rights include the right to use the Preprint , Accepted Manuscript and the Published Journal Article for Personal Use and Internal Institutional Use . They also include the right to use these different versions of the Article for Scholarly Sharing purposes, which include sharing:

- the Preprint on any website or repository at any time;
- the Accepted Manuscript on certain websites and usually after an embargo period;
- the Published Journal Article only privately on certain websites, unless otherwise agreed by Elsevier Ltd.

In the case of the Accepted Manuscript and the Published Journal Article the Author Rights exclude Commercial Use (unless expressly agreed in writing by Elsevier Ltd), other than use by the author in a subsequent compilation of the author's works or to extend the Article to book length form or re-use by the author of portions or excerpts in other works (with full acknowledgment of the original publication of the Article).

Author Representations / Ethics and Disclosure / Sanctions

I affirm the Author Representations noted below, and confirm that I have reviewed and complied with the relevant Instructions to Authors, Ethics in Publishing policy, Declarations of Interest disclosure and information for authors from countries affected by sanctions (Iran, Cuba, Sudan, Burma, Syria, or Crimea). Please note that some journals may require that all co-authors sign and submit Declarations of Interest disclosure forms. I am also aware of the publisher's policies with respect to retractions and withdrawal (https://www.elsevier.com/about/our-business/policies/article-withdrawal).

For further information see the publishing ethics page at https://www.elsevier.com/about/our-business/policies/publishing-ethics and the journal home page. For further information on sanctions, see https://www.elsevier.com/about/our-business/policies/trade-sanctions

Author representations

- The Article I have submitted to the journal for review is original, has been written by the stated authors and has not been previously published.
- The Article was not submitted for review to another journal while under review by this journal and will not be submitted to any other journal.

- The Article and the Supplemental Materials do not infringe any copyright, violate any other intellectual property, privacy or other rights of any person or entity, or contain any libellous or other unlawful matter.
- I have obtained written permission from copyright owners for any excerpts from copyrighted works that are included and have credited the sources in the Article or the Supplemental Materials.
- Except as expressly set out in this Journal Publishing Agreement, the Article is not subject to any prior rights or licenses and, if my or any of my co-authors' institution has a policy that might restrict my ability to grant the rights required by this Journal Publishing Agreement (taking into account the Author Rights permitted hereunder, including Internal Institutional Use), a written waiver of that policy has been obtained.
- If I and/or any of my co-authors reside in Iran, Cuba, Sudan, Burma, Syria, or Crimea, the Article has been prepared in a personal, academic or research capacity and not as an official representative or otherwise on behalf of the relevant government or institution.
- If I am using any personal details or images of patients, research subjects or other individuals, I have obtained all consents required by applicable law and complied with the publisher's policies relating to the use of such images or personal information. See https://www.elsevier.com/about/our-business/policies/patient-consent for further information.
- Any software contained in the Supplemental Materials is free from viruses, contaminants or worms.
- If the Article or any of the Supplemental Materials were prepared jointly with other authors, I have informed the co-author(s) of the terms of this Journal Publishing Agreement and that I am signing on their behalf as their agent, and I am authorized to do so.

Governing Law and Jurisdiction

This Agreement will be governed by and construed in accordance with the laws of the country or state of Elsevier Ltd ("the Governing State"), without regard to conflict of law principles, and the parties irrevocably consent to the exclusive jurisdiction of the courts of the Governing State.

For information on the publisher's copyright and access policies, please see http://www.elsevier.com/copyright.
For more information about the definitions relating to this agreement click here.

☑ **I have read and agree to the terms of the Journal Publishing Agreement.**
30 October 2020
T-copyright-v22/2017

3. CHAPTER 2

Magnetic graphene oxide as a platform for the immobilization of cellulases and xylanases: ultrastructural characterization and assessment of lignocellulosic biomass hydrolysis

Article published in September 2020 in Renewable Energy

DOI: 10.1016/j.renene.2020.09.059

Magnetic graphene oxide as a platform for the immobilization of cellulases and xylanases: ultrastructural characterization and assessment of lignocellulosic biomass hydrolysis

Fernando Roberto Paz-Cedeno,[*a] Jose Miguel Carceller,[b] Sara Iborra,[b] Ricardo Keitel Donato,[c] Anna Paula Godoy,[d] Ariela Veloso de Paula,[a] Rubens Monti,[a] Avelino Corma[*b] and Fernando Masarin[a]

[a]São Paulo State University (UNESP), School of Pharmaceutical Science (FCF), Department of Bioprocess Engineering and Biotechnology. Araraquara-SP, Brazil. 14800-903

[b]Universitat Politècnica de València (UPV), Institute of Chemical Technology (ITQ), Valencia, Spain. 46022

[c]Institute of Macromolecular Chemistry, Czech Academy of Sciences, Prague, Czech Republic.162 06

[d]Graphene and Nanomaterials Research Center, Mackenzie Presbyterian University, São Paulo, Brazil. 01302-907

(*) Corresponding author

Email addresses:

FRPC: fernando.paz@unesp.br
JMC: jocarca8@upvnet.upv.es
SI: siborra@itq.upv.es
RKD: donato@imc.cas.cz
APG: apaulasgodoy@gmail.com
AVP: ariela.veloso@unesp.br
RM: rubens.monti@unesp.br
AC: acorma@itq.upv.es
FM: fernando.masarin@unesp.br

ABSTRACT

For producing second-generation ethanol (cellulosic ethanol) and other value-added bioproducts, magnetic graphene oxide (GO-MNP) was synthesized in this work and used as the immobilization support for an industrial cellulase and xylanase-containing preparation. GO-MNP characterization by TEM, SEM and ATR-FTIR spectroscopy showed that the magnetic nanoparticles are homogeneously distributed onto the GO sheets surface. The enzymatic preparation was immobilized by means of carbodiimide cross-linking chemistry using 1-ethyl-3-(3-dimethylaminopropyl) carbodiimide and *N*-hydroxysuccinimide (NHS). The supported final biocatalyst (GO-MNP-Enz) showed high activity for the hydrolysis of pretreated sugarcane bagasse (PSB) and presented relative endoglucanase, xylanase, β-glucosidase, and β-xylosidase activities of 70%, 66%, 88%, and 70%, respectively, after 10 cycles of hydrolysis of their respective substrates. The biocatalyst also maintained approximately 50% and 80% of its efficiency for cellulose and xylan hydrolysis, respectively, being the TOF ($g.g^{-1}.h^{-1}$) the highest observed when compared with previous results observed in literature. These findings suggest that GO-MNP-Enz may be a prospective candidate for industrial applications such as second-generation ethanol production.

KEYWORDS: Enzyme immobilization, graphene oxide, magnetic nanoparticles, biocatalyst, sugarcane bagasse hydrolysis, monomeric fermentable sugars.

HIGHLIGHTS

- Enzymes immobilized onto graphene oxide-magnetite form a stable biocatalyst.
- The ultrastructural characterization of the magnetic biocatalyst is presented.
- The biocatalyst has all enzymatic activities to hydrolyze lignocellulosic biomass.
- A high turnover frequency is reached after several hydrolysis cycles.
- Magnetic separation allows easy recycling of the biocatalyst.

INTRODUCTION

Brazil is the largest exporter and second-largest producer (after the USA) of ethanol in the world, having produced approximately 33 billion liters in 2019 [1,2]. First-generation ethanol is mainly obtained from sugarcane and corn, while second-generation ethanol is derived from lignocellulosic biomass found in plants. An important step in the production of second-generation ethanol is the biocatalytic process that uses cellulases and xylanases to hydrolyze lignocellulosic material into fermentable sugars. Biocatalytic processes have been applied in several sectors of the biotechnology due to their high specificity and conservation of the environment. However, the use of enzymes in industrial applications may be limited depending on their cost, which is a bottleneck in the production process of second-generation ethanol. In addition, maintaining the structural stability of some enzymes during any biochemical reaction is a major challenge [3].

The immobilization of enzymes onto solid supports offers many advantages, including reuse of the enzyme, relatively easy separation of the product, and increased enzyme stability [4]. Typically, the supports used for enzyme immobilization are agarose, sepharose, silica gel, chitosan, silica-based carriers, polysaccharide derivatives, synthetic polymers, and zeolites [5–12]. Since the support's surface area is a major characteristic for effective enzyme immobilization, two-dimensional (2D) materials, which include graphene and graphene oxide (GO), are exceptionally interesting for this application [13]. GO is an especially versatile chemical platform due to the vast availability of functional groups on its immense surface area (as high as 736.6 $m^2.g^{-1}$ in aqueous solutions) [14], making it an excellent support material for immobilizing enzymes [15,16]. The magnetization of the supports prior to use has shown great potential for recyclable applications [17–19]. A key advantage of using magnetic support for enzyme immobilization is the possibility to recover the supported biocatalyst using an external magnet, which is more viable in comparison to other recovery methods, such as filtration and centrifugation [20]. Recently several published works have developed such types of magnetic composite supports for the immobilization of enzymes [21,22].

Cellulases and xylanases immobilization in solid supports had been studied in the past [23–28]. However, in spite of various immobilization techniques and supports reported in the literature, there is still a demand for more efficient methods and easier recycling of the biocatalyst. This paper aims

to add to the literature on the hydrolysis of lignocellulosic biomass using immobilized enzymes.

Considering the aforementioned, in this study GO-magnetic nanoparticles (GO-MNP) was synthesized and used as the immobilization support for a commercial enzymatic preparation containing cellulase and xylanase activities. Considering the nature of the support GO rich in acids groups, the covalent immobilization was carried out by activating the acid groups on the GO-MNP surface using 1-ethyl-3-(3-dimethylaminopropyl) carbodiimide (EDC) and then reacting with *N*-hydroxysuccinimide (NHS), providing a reactive site for enzyme immobilization (see Figure 3.1) [21,29–31]. The support and biocatalyst were ultrastructurally characterized and assessed for reuse using both specific substrates and an actual lignocellulosic material (sugarcane bagasse).

EXPERIMENTAL METHODS

Synthesis of GO and GO-MNP

GO was prepared using a modified version of Hummers' method [32]. Accordingly, graphite powder (99.99%; < 150 µm; Sigma-Aldrich, St. Louis, MO, USA) was mixed with H_2SO_4 (95-97% v/v) and oxidized to graphite oxide using $KMnO_4$. An aqueous suspension of graphite oxide (1 $mg.mL^{-1}$) was exposed to sonication for 2 h to exfoliate into GO. GO-MNP was obtained by co-precipitation of iron salts [17]. Briefly, $FeCl_3 \cdot 6H_2O$ and $FeCl_2 \cdot 4H_2O$ (molar ratio 2:1) were added to an acetic acid solution (3% v/v) under vigorous stirring, and a GO dispersion (5 $mg.mL^{-1}$) was added. Then, the temperature was

raised to 80 °C, and pH was increased by adding ammonia (25% v/v). Finally, the reaction was stopped, and the solid was collected using an external magnet and washed with ultrapure water and methanol. The solid was dried and stored. Before use, the material was exposed to sonication for 2 h in an aqueous suspension to exfoliate into GO-MNP.

Immobilization of cellulases and xylanases from enzymatic preparation on GO-MNP

The GO-MNP was functionalized to allow for the covalent immobilization of enzymes. For this purpose, 20 mL of a GO-MNP dispersion (0.5 $mg.mL^{-1}$) in acetate buffer (0.05 M; pH 4.8) was sonicated for 2 h. Next, 20 mg of NHS and 24 mg of EDC were added, and the mixture was stirred for 3 h. The solid was collected using an external magnet and washed with the same buffer. Subsequently, the solid was resuspended in acetate buffer (pH 4.8), and a volume (3-120 µL) of enzyme preparation Cellic CTec 2 (Novozymes, Denmark) was added. The suspension was placed on a rolling agitator at 120 rpm for 12 h. Finally, the biocatalyst was collected using an external magnet, washed with acetate buffer (pH 4.8), and resuspended in the same buffer. This biocatalyst was denoted as GO-MNP-Enz.

Ultrastructural characterization

Scanning electron microscopy (SEM) images and energy-dispersive X-ray (EDX) spectra were taken using an AURIGA Focused Ion Beam Scanning Electron Microscope (Zeiss, Germany). For this purpose, the samples were

thoroughly dried in a vacuum oven and placed on a conductive carbon adhesive tape. Transmission electron microscopy (TEM) images and EDX spectra were recorded on a JEM-2100F Transmission Electron Microscope (JEOL, Japan). The samples were dispersed (≈ 0.04 $mg.mL^{-1}$) in ultrapure water (18.2 MΩ cm) and transferred to nickel square mesh grids. EDX spectra analysis provided elemental identification and quantitative compositional information. Atomic force microscopy (AFM) images were recorded on a MultiMode 8 Atomic Force Microscope under tapping mode (Bruker, USA). The samples were prepared by dispersing GO-MNP-Enz in aqueous solution (≈ 0.04 $mg.mL^{-1}$), placing it over a mica surface, and allowing the solvent to evaporate. Raman spectroscopy measurements were recorded using an alpha 300 R confocal microscope spectrometer (WITec, Germany) using 50× objective lens and grading of 600 $g.mm^{-1}$. A 532 nm excitation laser was employed to characterize the GO. A silicon oxide substrate was used to calibrate the spectrometer. The specific surface area of the GO and GO-MNP were calculated by the Brunauer-Emmet-Teller method (BET) by means of nitrogen adsorption at -196°C using an ASAP 2420 (V2.09 J). Lastly, the dried samples were subjected to infrared analysis using attenuated total reflection with a Fourier transform infrared (ATR-FTIR) spectrometer (Platinum-ATR Alpha; Bruker) with a single reflection diamond module.

Enzymatic activity assays

Total cellulase activity was determined according the methodology described by Ghose[33] with some modifications. Briefly, a filter paper strip

(1.0 × 6.0 cm; ≈ 50 mg; Whatman No. 1) was used as the substrate in 1.2 mL of acetate buffer (pH 4.8) and 0.3 mL of enzymatic preparation Enz or biocatalyst suspension for free- or immobilized-enzymes, respectively. Endocellulase activity was measured using the methodology described by Tanaka *et al.* [34]. Accordingly, 0.9 mL of 0.44% (w/v) sodium carboxymethylcellulose (CMC) (≥ 95%; Carbosynth, USA) solution was placed in a tube, and 0.1 mL of Enz or immobilized biocatalyst suspension was added. For xylanase activity determination, we followed the methodology described by Bailey *et al* [35]. Thus, 0.9 mL of 1% (w/v) xylan (≥ 90%; Sigma-Aldrich) solution was added to 0.1 mL of Enz or immobilized biocatalyst suspension. The reactions of total cellulase, endoglucanases and xylanase activities were stopped by adding a volume of 3,5-Dinitrosalicylic acid (DNS), boiled for 5 min, and cooled before their respective absorbances were read at 540 nm.

β-glucosidase and β-xylosidase activities were measured according to Tan *et al* [36]. Following this method, 0.8 mL of 0.1% (w/v) 4-Nitrophenyl β-D-glucopyranoside (≥ 98%; Sigma-Aldrich) or 4-Nitrophenyl β-D-xylopyranoside (≥ 98%; Sigma-Aldrich) solution was added to 0.2 mL of Enz or immobilized biocatalyst suspension, respectively. The reactions were stopped by adding 2 mL of $NaHCO_3$, and the respective absorbances were read at 410 nm.

Yield, efficiency, and recovery activities of the enzyme immobilization were determined according to Equations 1, 2, and 3, respectively [37].

$$Yield = \left(\frac{A_i - A_f}{A_i}\right) * 100\% \qquad \text{(Equation 1)}$$

$$Efficiency = \left(\frac{A_b}{A_i - A_f}\right) * 100\% \qquad \text{(Equation 2)}$$

$$Activity\ recovery = \left(\frac{A_b}{A_i}\right) * 100\% \qquad \text{(Equation 3)}$$

where A_i: total activity on the supernatant before immobilization, A_f: total activity on the supernatant after immobilization, and A_b: total activity on the biocatalyst.

Reuse of immobilized enzymes

To determine the reusability of the immobilized enzymes, GO-MNP-Enz was subjected to catalytic activity assays according to the previously described methods (endoglucanase, xylanase, β-glucosidase, and β-xylosidase). After the activity assay, GO-MNP-Enz was collected with an external magnet, washed with acetate buffer, and then reused into a new activity assay. The turnover frequency (TOF), defined as g of product obtained per g of biocatalyst per h, was calculated for the enzymatic hydrolysis of the respective substrates.

Hydrolysis of pretreated sugarcane bagasse (PSB)

One hundred grams of original sugarcane bagasse (dry basis) and 1 L of a Na_2SO_3 2% (w/v) and NaOH 1% (w/v) solution were added into a 1.5 L reactor (AU/E-20; Regmed, Brazil), culminating in a 1:10 ratio between the bagasse mass (dry basis) and solution volume. The reactor was closed and set to 140 °C and 4 rpm of horizontal rotation for 30 min [38]. Subsequently, the PSB was washed several times with distilled water and dried at 40 °C for 48 h. For the PSB hydrolysis using GO-MNP-Enz, 10 mg of PSB (dry basis) was added to 10 mL of acetate buffer (pH 4.8) in an Erlenmeyer flask. Then,

150 mg of GO-MNP-Enz (44 FPU.g^{-1}) was added, and the reaction was carried out in a thermal bath at 30 °C and 120 rpm of shaking. After 24 h of hydrolysis, the GO-MNP-Enz was recovered using an external magnet, washed several times with acetate buffer (pH 4.8), and reused in a new hydrolysis cycle. The supernatant was recovered and used to determine sugars. This analysis was performed by high performance liquid chromatography (HPLC; C-R7A; Shimadzu, Japan) equipped with a HPX87H column (Bio-Rad, USA) at 60 °C in the isocratic mode using 0.005 M H_2SO_4 as a mobile phase at a flow rate of 0.6 mL.min^{-1} and detected using a RID-20A Refractive Index Detector (Shimadzu) at 60 °C [39–41]. The cellulose and xylan conversions were determined by Equations 4 and 5, respectively.

$$Cellulose\ conversion\ (\%) = \left(\frac{M_g * 0.9}{F_C * M_B}\right) * 100\% \quad \text{(Equation 4)}$$

$$Xylan\ conversion\ (\%) = \left(\frac{M_x * 0.88}{F_X * M_B}\right) * 100\% \quad \text{(Equation 5)}$$

where M_g: mass of glucose (mg) after a hydrolysis cycle, 0.9: conversion factor of glucose to cellulose, F_C: cellulose fraction in the dry PSB (g.g^{-1}), M_B: mass of PSB at the start of the reaction (mg), M_x: xylose concentration (mg) after a hydrolysis cycle, 0.88: conversion factor of xylose to xylan, and F_X: xylan fraction in the dry PSB (g.g^{-1}).

RESULTS AND DISCUSSION

Synthesis and characterization of the biocatalyst (GO-MNP-Enz)

Firstly, GO was obtained from graphite powder, and magnetic nanoparticles were attached onto the surface by coprecipitation of Fe^{2+} and Fe^{3+}. Then, the support was functionalized to allow for enzyme immobilization.

Figure 3.1a shows a general scheme of the synthesis and functionalization of the support, and Figure 3.1 and c displays the magnetic behavior of GO-MNP-Enz.

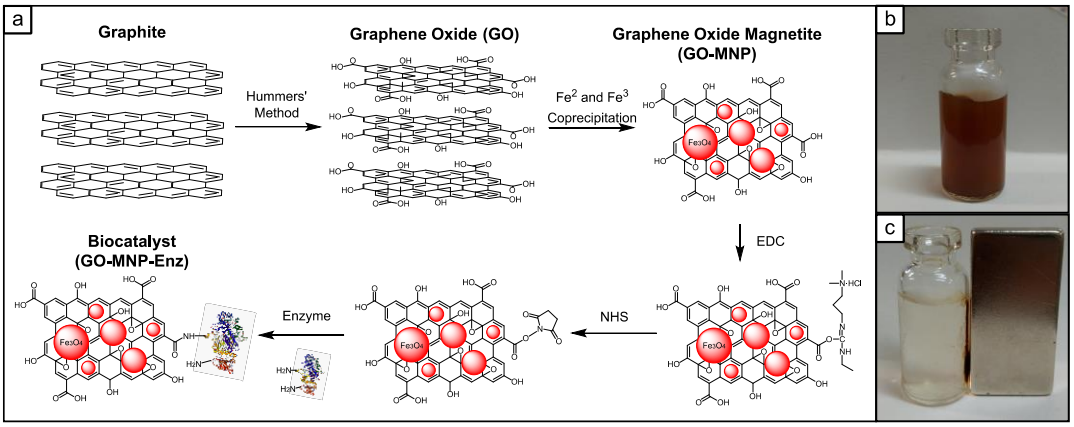

Figure 3.1. (a) Scheme of graphene oxide magnetite (GO-MNP) synthesis, functionalization and enzyme immobilization. Biocatalyst (GO-MNP-Enz) before **(b)** and after **(c)** apply an external magnetic field.

The ATR-FTIR spectra of GO, GO-MNP, GO-MNP-Enz, and Enz are depicted in Figure 3.2. The band at 570 cm^{-1}, present in the GO-MNP and GO-MNP-Enz systems, has been attributed to the elongation of the Fe-O bond within the crystalline network of Fe_3O_4 [42–45]. Thus, the presence of this band in GO-MNP indicates its successful magnetization, hence the absence of this band in GO. The band at 1040 cm^{-1} in the GO-MNP-Enz and Enz spectra has been attributed to C-N bond vibration [46,47]. The band observed at approximately 1540 cm^{-1} has been associated with C-N stretching and N-H bending vibrations in the -CONH groups [47]. The absence of these bands (1040 and 1540 cm^{-1}) in the GO-MNP spectrum showed that the enzymes were successfully immobilized on the support. The bands at 1640 and 3280 cm^{-1} correspond to deformation and stretching vibrations, respectively, of the O-H type connection in strongly intercalated water [48]. Additionally, Raman

spectra (Figure 3.S1) were collected to evaluate the produced GO. According to the average multiple curve of GO (Figure 3.S1), the D, G, and 2D bands are positioned at 1345, 1591 and 2669 cm^{-1}, respectively. The prominent D band with an intensity comparable to the G band indicates an important structural disorder because of the presence of oxygenated groups from GO. The G band is wider than the related to graphite powder, reinforcing structural changes with the insertion of defects [49]. The weak and broad 2D band is another indication of disorder. Near 2950 cm^{-1}, a defect-activated band denoted as D+G was also visible [50]. The I_D/I_G ratio was found to be 1.22, a value that represents a high quantity of defects in the formed GO.

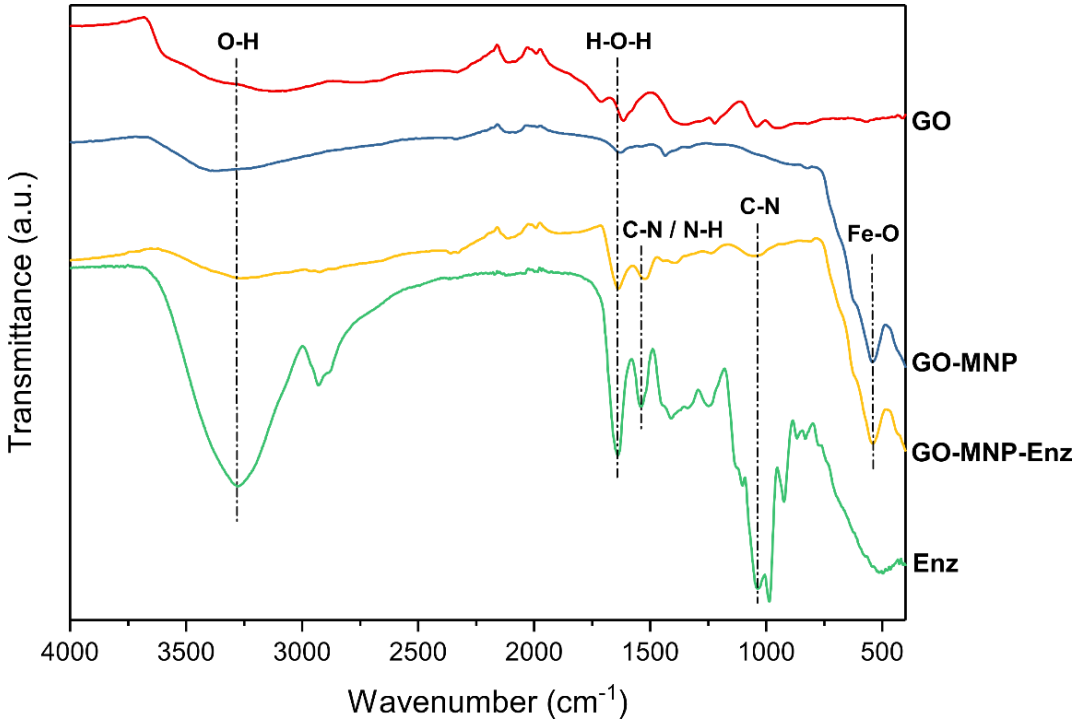

Figure 3.2. Total attenuated reflection in the infrared with Fourier transform (ATR-FTIR) spectrum of graphene oxide (GO), graphene oxide with magnetic nanoparticles (GO-MNP), biocatalyst (GO-MNP-Enz) and commercial enzymatic cocktail (Enz).

The SEM images show the morphology of the material before ultrasonic exfoliation, where the surface morphological aspect of the graphite oxide has the shape of overlapping sheets (Figure 3.3a) as noted by previous reports in the literature [48,51]. It is possible to see the magnetic nanoparticles on the surface of graphite oxide generating graphite oxide-magnetite (Figure 3.3b). The elemental EDX analysis demonstrates that the graphite oxide-magnetite is formed by atoms of C, Fe, and O (Figure 3.3d) while the graphite oxide does not contain Fe in its structure (Figures 3.S2a and b), confirming that the iron nanoparticles have adhered to the GO-MNP surface.

Graphite oxide and graphite oxide-magnetite were further exfoliated to form GO and GO-MNP, respectively, and were characterized by TEM-EDX analysis. TEM images of GO (Figure 3.3c) showed that monolayer and few-layer GO was obtained after exfoliation, also confirming that the magnetic nanoparticles remained onto the GO sheets' surface and were homogeneously distributed (Figure 3.3d). The EDX spectra showed that GO (Figure 3.S2c) is composed exclusively of C and O while GO-MNP (Figure 3.S2d) presents C, Fe, and O in its composition, paralleling the SEM-EDX results (Figures 3.3S2a and 3.S2b). The presence of nickel in the EDX spectrum is attributed to the interference of the grid that is used as a support for the sample. Moreover, by analyzing the AFM height profile of GO-MNP-Enz (Figure 3.3f), it is possible to verify that the enzymes are immobilized on a single layer of GO since the height of the support is approximately 1 nm. BET analysis was performed to investigate the specific surface area of the materials. The surface area of the graphite oxide was 12 $m^2.g^{-1}$. This low value is probably due to the fact that

nitrogen molecules cannot penetrate the interlaminar space of the dry graphite oxide. After the magnetization, the surface area was larger (103 $m^2.g^{-1}$), probably because the magnetite particles in the structure allowed a separation between layers of graphite oxide and the nitrogen could be absorbed. The both results were consistent with the literature [48,52–55].

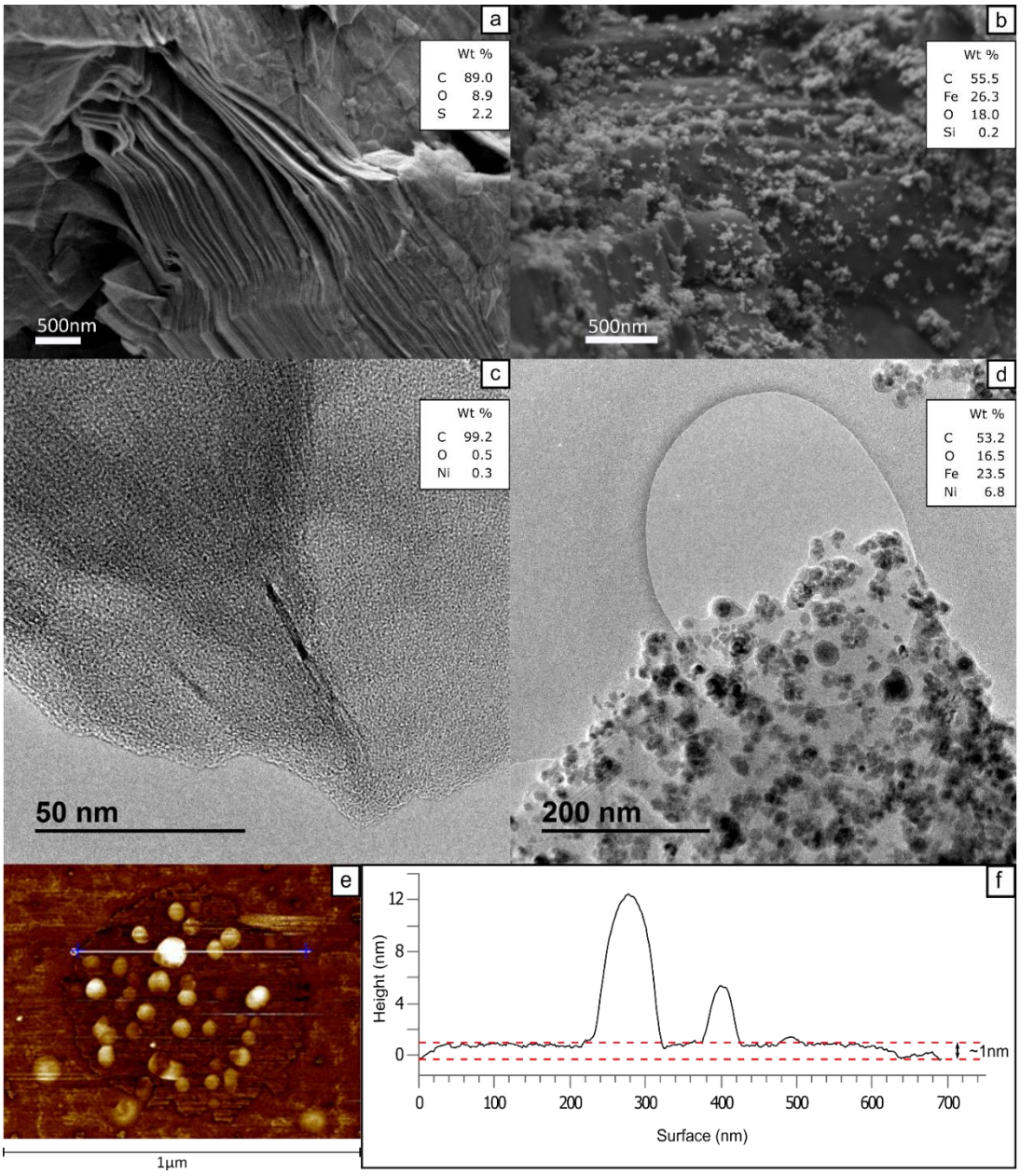

Figure 3.3. SEM images of **(a)** Graphite oxide and **(b)** Graphite oxide-magnetite. TEM images of **(c)** Graphene oxide and **(d)** Graphene oxide with

magnetic nanoparticles (GO-MNP). AFM image of **(e)** Biocatalyst (GO-MNP-Enz) and **(f)** height profile obtained from the indicated line in the AFM image.

Evaluation of the immobilization process

The enzyme immobilization process, using different initial protein loads and a constant mass of GO-MNP (mg of protein per g of GO-MNP), was evaluated to determine the yield of protein immobilization (Figure 3.4a). Higher yields of protein immobilization were observed when low protein loads (up to 50 mg) were applied, which corresponds to approximately 47 mg of protein per g of GO-MNP. When the initial protein load was greater than 50 mg, the yield decreased, but the total amount of protein bound to GO-MNP increased, reaching approximately 140 mg of protein per g of GO-MNP. The amount of protein bounded per g of support using the methodology of EDC-NHS was higher than values reported by previous immobilization studies using other synthetic routes, reaching values between 2.5–52.4 mg of protein per g of support [24,56–58]. Thus, GO-MNP was able to bind a greater amount of protein in its structure when there is an increase in the initial protein load, but excess protein caused a decrease in the yield of protein immobilization. However, despite the fact that the amount of enzyme on GO-MNP increased, the total cellulase activity of the biocatalyst stayed constant at roughly 44 $FPU.g^{-1}$ after an initial protein load of approximately 50 mg per g of GO-MNP. Similar behavior was reported by Alftrén and Hobley [26] using Cellic CTec 2 immobilized in cyanuric chloride-activated magnetic particles, but the activity of its biocatalyst stayed stable at approximately 15.5 $FPU.g^{-1}$ (almost 3x lower than reported herein).

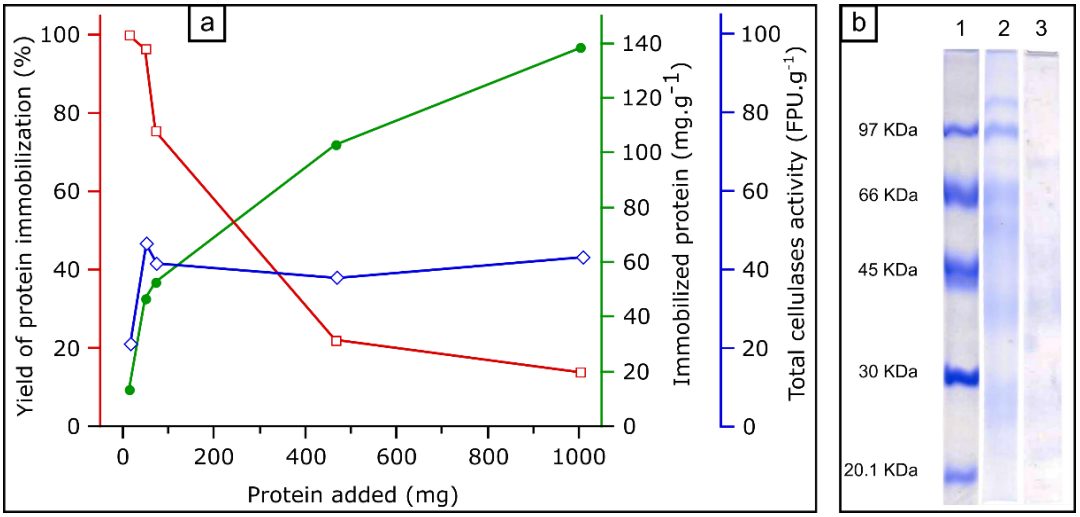

Figure 3.4. (a) Yield of protein immobilization (%) (□, red), amount of immobilized protein per gram of support (mg.g^{-1}) (●, green) and activity of total cellulases per gram of support (FPU.g^{-1}) (◇, blue) as a function of the protein load of enzymatic preparation Cellic CTec 2. **(b)** Sodium dodecyl sulfate-polyacrylamide gel electrophoresis (SDS-PAGE). Lane 1: molecular weight standards; Lane 2: supernatant before immobilization; Lane 3: supernatant after immobilization.

Sodium dodecyl sulfate-polyacrylamide gel electrophoresis (SDS-PAGE) of the supernatant before and after immobilization is demonstrated in Figure 3.4b. Using an initial protein load of about 50 mg per g of GO-MNP did not leave meaningful amounts of residual supernatant protein after the immobilization process, confirming the immobilization effectiveness and supporting the protein immobilization yield results.

In summary, starting the immobilization with a protein load of 50 mg of protein per g of GO-MNP led to a yield of 96.5% (Figure 3.4a). However, because the commercial enzymatic preparation Cellic CTec 2 is a blend of several enzymes (predominantly cellulases and xylanases) and comprises various enzyme activities, it is important to determine the yield of immobilization according to each enzyme activity under the condition of 50 mg

of protein per g of GO-MNP. For this purpose, assays for the enzymatic activities of total cellulase, endoglucanase, xylanase, β-glucosidase, and β-xylosidase were performed in the supernatant (before and after immobilization) and biocatalyst. The assays evaluated the yields of immobilization, efficiency, and activity recovery, ranking between 27%–97%, 37%–113%, and 15%–110%, respectively (Table 3.1).

Table 3.1. Yield, efficiency and activity recovery in the immobilization process of enzyme preparation Cellic CTec 2 onto graphene oxide with magnetic nanoparticles (GO-MNP) in the condition with protein load of 50 mg of protein per gram of GO-MNP. Enzymatic activity of the biocatalyst.

Enzyme	Yield of Immobilization (%)	Efficiency (%)	Activity recovery (%)	Biocatalyst activity ($U.g^{-1}$)
Total cellulases	71.1	69.0	49.1	44.1*
Endoglucanase	63.4	37.6	23.8	299.9
Xylanase	27.0	55.2	14.9	1034.0
β-glucosidase	97.2	113.0	109.8	4500.2
β-xylosidase	91.6	86.6	79.3	33.3

* $FPU.g^{-1}$

Xylanase showed the lowest immobilization yield at 27%, indicating that this enzyme is poorly immobilized onto GO-MNP using the method chosen in the present study. However, the enzymatic activity assays showed that the other enzymes were successfully immobilized, presenting immobilization yields of 71%, 63%, 97%, and 92% for total cellulase, endoglucanase, β-glucosidase, and β-xylosidase, respectively.

The efficiency describes the percentage of bound enzyme activity that is verified in the biocatalyst (GO-MNP-Enz) [37]. This value is usually below 100%, likely because of mass transfer limitations, tertiary structure modifications, decreased accessibility of active sites, and solubility of the specific substrate for each enzyme assay. That was the case for all assessed

activities except β-glucosidase, which reached 113% efficiency and thus showed improvement in its immobilized form. β-xylosidase also showed a high efficiency (86.6%), indicating that these enzymes are less sensitive to mass transfer issues, presumably because of the high solubility of the specific substrates. β-glucosidase and β-xylosidase are responsible for the hydrolysis of cellobiose into glucose and xylobiose into xylose, respectively, during the final step of lignocellulose biomass hydrolysis. Therefore, these results are very important for producing a hydrolyzate rich in monomeric sugars.

The activity recovery relates to enzyme activity levels of the biocatalyst (GO-MNP-Enz) compared to the total starting activity of the free enzyme used for immobilization. This number gives an idea of the success of the total immobilization process. The commercial preparation Cellic CTec 2 comprises various enzymatic activities, and the immobilization results of each enzyme were different; β-glucosidase and β-xylosidase presented the best results (110% and 78%, respectively) while xylanase displayed the worst (15%).

The units (μmol.min^{-1}) of enzyme activity per g of biocatalyst were determined (Table 3.1). The total cellulase activity of the biocatalyst was 44.1 FPU.g^{-1} while the activities of endoglucanase, xylanase, β-glucosidase, and β-xylosidase were 299, 1034, 4500, and 33 U.g^{-1}, respectively. The enzymatic activity assay for exoglucanase was performed using microcrystalline cellulose as the substrate; however, no activity was detected. This could be due to the low activity of the exoglucanase present in commercial enzyme preparation Cellic CTec 2 (0.5 U.mg^{-1} of protein) associated with the dilution that was used for immobilization.

Evaluation of GO-MNP-Enz recyclability

The main objective of the enzyme immobilization was the possibility of reusing the biocatalyst. For this reason, the relative activities of endoglucanase, xylanase, β-glucosidase, and β-xylosidase after ten hydrolysis cycles of GO-MNP-Enz on their specific substrates were evaluated (Figure 3.5). GO-MNP-Enz showed relative activities of endoglucanase and xylanase above 85% until the sixth cycle. Furthermore, the endoglucanase activity remained stable at approximately 80% until the ninth cycle and diminished to 70% in the tenth cycle (Figure 3.5a). The relative enzyme activity of xylanase diminished gradually after the fifth cycle, reaching 66% in the tenth cycle (Figure 3.5b). The relative activity of β-glucosidase showed an excellent trend, remaining at values above 95% until the ninth cycle and 88% in the last cycle (Figure 3.5c). The relative activity of β-xylosidase remained stable above 95% until the fifth cycle but then gradually diminished to reach 70% in the tenth cycle (Figure 3.5d).

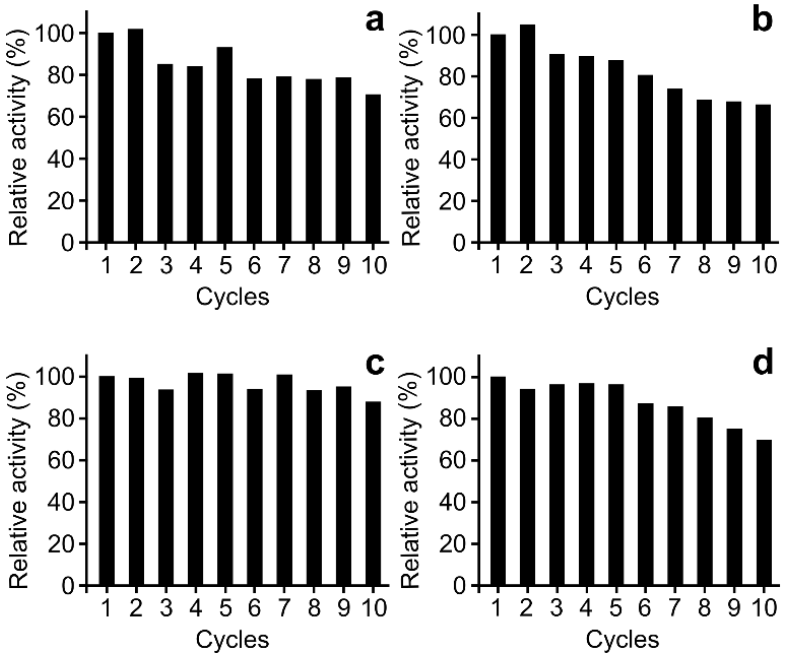

Figure 3.5. Relative enzyme activity of biocatalyst (GO-MNP-Enz) about their substrates as a function of cycles number of hydrolysis (ten cycles). **(a)** Endoglucanase, **(b)** Xylanase, **(c)** β-glucosidase and **(d)** β-xylosidase.

In order to put the obtained results into perspective, they were confronted with other results recently reported by other authors about the relative activities of endoglucanase, xylanase, β-glucosidase, and β-xylosidase on reuse assays (Table 3.2).

Several studies have reported about the reuse of β-glucosidase and β-xylosidase immobilized using different strategies and supports [59–68]. A general conclusion obtained by many of those studies is that β-glucosidase can be used for 10 consecutive cycles, conserving between 67%–95% of its initial activity. Also, for β-xylosidase, a relative activity between 39%–95% after 10 cycles of hydrolysis has been identified. These data are in accordance with the findings of this study.

In addition, we can highlight the work by Gao *et al.* [56], who managed to maintain a relative endoglucanase activity of 80% after 9 cycles while Lim *et al.* [69] produced a biocatalyst that maintained a 60% relative xylanase activity after 10 cycles. However, none of the referred systems presented magnetic properties, and deep centrifugation is required before reuse in each experiment. On the other hand, Abraham *et al.*[70] immobilized cellulases on purely magnetite nanoparticles using glutaraldehyde, and the relative activity fell to approximately 30% after 10 cycles of hydrolysis. Gokhale *et al.* [24] and Han *et al.* [71] have used GO-MNP as a support for cellulase immobilization via different routes, but the relative activity of the biocatalyst they obtained fell to approximately 50% after 4 and 7 cycles, respectively. Compared to the results previously reported in the literature for endoglucanase and xylanase reuse, GO-MNP-Enz proved to be stable for more cycles and maintained a greater relative activity.

In addition, the calculated TOF (g of sugar per g of biocatalyst per hour) of the previous reported works are considerably lower than those obtained with our biocatalyst (see Table 3.2). As can be seen in Table 3.2, the biocatalyst presented in this work showed a TOF several times higher, reaching 0.40, 2.30, 4.94, and 0.11 h^{-1} using carboxymethylcellulose (CMC), xylan, 4-Nitrophenyl β-D-glucopyranoside (*p*-NPG), and 4-Nitrophenyl β-D-xylopyranoside (*p*-NPG) as substrates, respectively. These values are especially relevant from the point of view of large-scale production of fermentable sugars.

The main reasons for the superior performance of the biocatalyst presented herein, in comparison to other biocatalysts reported in the literature, are the following: i) the commercial enzyme preparation Cellic CTec 2 is resistant to hydrolysis conditions; ii) the GO kept a high quality (few-layers/high surface area and structural quality) throughout the process; iii) the immobilization method used in combination with the highly hydrophilic characteristics of the high quality GO obtained a consistently supported biocatalyst. Altogether, the resulting GO-MNP-Enz presented not just one but rather all necessary enzymatic activities for lignocellulosic biomass hydrolysis.

Table 3.2. Literature survey about the relative activity of endocellulase, xylanase β-glucosidase and β-xylosidase after several reuse cycles.

Support	Immobilization route	Number of cycles	Substrate	Relative activity at last cycle (%)	TOF	Reference
MNP	GA	10	CMC	30	0.2586	[70]
GO	SESA	9	CMC	80	0.1193	[56]
MNP	GA	10	CMC	62	0.0026	[57]
GO-MNP	PAA-EDC	4	CMC	55	-	[24]
GO-MNP	PEG10K-GA	7	CMC	45	-	[71]
GO-MNP	EDC-NHS	10	CMC	70	0.4020	This work
Mesoporous cellulose foam	APTES	10	Xylan	60	0.5885	[69]
Zeolite	Adsorption	6	Xylan	56	0.0105	[72]
GO-MNP	PEGA	8	Xylan	10	0.0418	[19]
GO-MNP	EDC-NHS	10	Xylan	66	2.3070	This work
MNP	GA	10	*p*-NPG	86	0.0201	[59]
MNP	APTES-GA	10	*p*-NPG	67	0.3980	[61]
AMNPs	ECH-IDA-Co^{2+}	10	*p*-NPG	95	0.0858	[62]
APEPMOs	Adsorption	10	*p*-NPG	70	-	[63]
GO-MNP	EDC-NHS	10	*p*-NPG	88	4.9450	This work
Chitosan	GA	25	*p*-NPX	94	0.0003	[66]
Agarose	Glyoxyl-PEG	10	*p*-NPX	70	0.0005	[67]
Agarose	Glyoxyl	8	*p*-NPX	40	0.0001	[68]
PAM	Adsorption	10	*p*-NPX	55	-	[65]
GO-MNP	EDC-NHS	10	*p*-NPX	70	0.1133	This work

AMNPs: Agarose coupled to magnetic nanoparticles; APEPMOs: aminopropyl-functionalized ethane-bridged bifunctional periodic mesoporous organosilicas; APTES: (3-Aminopropyl)triethoxysilane; CMC: Sodium carboxymethylcellulose; EDC: 1-ethyl-3-(3-dimethylaminopropyl) carbodiimide; EDH: epichlorohydrin; GA: Glutaraldehyde; GO: Graphene oxide; IDA: iminodiacetatic acid; MCC: Microcrystalline cellulose; MNP: Magnetic nanoparticles; NHS: n-Hydroxysuccinimide; PAA: Polyacrylic acid; PAM: Polyamide membrane; PEG: Polyethylene glycol; PEG10K: 10K-4-arm-PEG-NH_2; PEGA: Poly(ethylene glycol) bis(amine); p-NPG: 4-Nitrophenyl β-D-glucopyranoside; p-NPX: 4-Nitrophenyl β-D-xylopyranoside; SESA: p-β-sulfuric acid ester ethyl sulfone aniline; TOF: Turnover Frequency; WSN: Wrinkled silica nanoparticles; XOs: Xylo-oligosaccharides.

Enzymatic hydrolysis of PSB using GO-MNP-Enz

In order to assess the GO-MNP-Enz performance for a real-life application (compared to its *in vitro* activity), this system was applied to the hydrolysis of PSB, and its conversion was evaluated for 10 reuse cycles (Figure 3.6). The chemical composition of PSB was determined and reported in Table 3.S1. The enzymatic hydrolysis of PSB reached a 72% conversion of cellulose to glucose in the first cycle. However, the conversion decreased progressively to 56%, 43%, 37%, and 34% in the following four cycles. From the sixth to the ninth cycles, the cellulose conversion to glucose remained stable at approximately 27% (Figure 3.6).

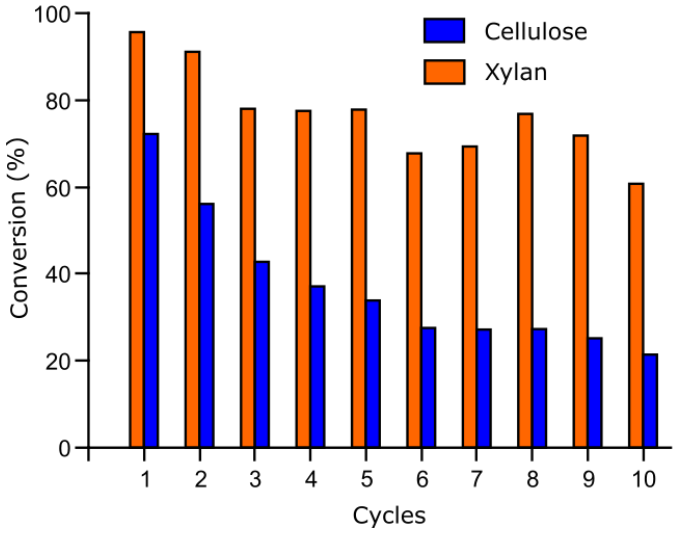

Figure 3.6. Hydrolysis of sugarcane bagasse pretreated with sulfite-alkali (PSB) with the application of the biocatalyst (GO-MNP-Enz). Cellulose and xylan conversion into glucose and xylose, respectively.

Xylan conversion of PSB to xylose presented more promising results, reaching 96% conversion in the first cycle, 91% in the second cycle, and remaining stable at approximately 78% in the third, fourth, and fifth cycles. From the sixth to the ninth cycles, the conversion remained between 77%–

68%, ultimately declining to 61% in the tenth cycle (Figure 3.6). These results suggested that the biocatalyst presented here kept approximately 50% and 80% of its efficiency for cellulose and xylan hydrolysis, respectively, after 5 hydrolysis cycles. This efficiency was decreased to approximately 65% after 10 cycles of xylan hydrolysis. In general, the loss in efficiency of an enzyme biocatalyst is due to degradation by heat. However, in this work the hydrolysis of sugarcane bagasse was carried out at a moderate temperature (30°C), which probably does not affect the stability of the biocatalyst. A plausible explanation for the loss in efficiency could be small biocatalyst losses in each cycle.

In total, 21 mg of glucose and 20 mg of xylose were produced from 100 mg of PSB after 10 hydrolysis cycles (10 mg of PSB per cycle). Altogether, the biocatalyst presented a satisfactory efficiency, especially for xylan hydrolysis, and is suitable for a cost-effective reuse process.

Previous studies have reported on similar approaches to hydrolyze lignocellulosic biomass; however, some of them applied different pretreatments, such as Ingle *et al.* [73] using cellulase immobilized on MNPs (without GO) for acid PSB and finding a cellulose conversion to glucose of 52%, 47%, and 27% in the first, second, and third cycles, respectively. This means a loss of biocatalyst efficiency of almost 50% by the third cycle. Alftrén and Hobley [26] immobilized the commercial enzymatic preparation Cellic CTec 2 onto MNPs (without GO) activated with cyanuric chloride for hydrolyzing hydrothermally-pretreated wheat straw (50 °C for 72 h) and identified a cellulose conversion to glucose of 82% in the first hydrolysis cycle

and 66% in the second cycle. However, this biocatalyst was only used for two cycles. In another work, cellulases from *Trichoderma reesei* were immobilized in chitosan-coated MNPs and used to hydrolyze *Agave atrovirens* biomass. This biocatalyst was used for 5 hydrolysis cycles, reaching a cellulose conversion to glucose of 22.4% in the first cycle and decreasing to 10.1% in the fifth cycle. This means a loss of biocatalyst efficiency of 55% by the fifth cycle and a production of 6.1 mg of glucose from 100 mg of biomass [74].

The biocatalyst presented in this work reached higher conversion levels and maintained an overall better efficiency. Nonetheless, very few studies have been conducted on biocatalyst reuse in the hydrolysis of real lignocellulosic biomass. Most studies evaluating biocatalyst reuse only utilize model substrates, such as carboxymethyl cellulose (CMC) or microcrystalline cellulose (MCC) [24,56–58,70,71,75–78]. The biocatalyst presented here was capable of being reused for 10 consecutive hydrolysis cycles using real lignocellulosic biomass (PSB). Consequently, GO-MNP-Enz offers an important advantage in the total conversion per biocatalyst life-cycle and could be a prospective candidate for application in industries such as biorefineries.

CONCLUSION

In this study, a commercial enzymatic blend containing cellulases and xylanases was successfully immobilized onto the surface of a GO-magnetite by covalent attachment, producing a biocatalyst (GO-MNP-Enz). The yield, efficiency, and relative activity of the immobilization process ranked from 27%–97%, 37%–113%, and 24%–110%, respectively, for the different enzymatic

activities assessed. This biocatalyst presented a stable behavior when evaluated for the different catalytic activities over several cycles of use, reaching relative endoglucanase, xylanase, β-glucosidase, and β-xylosidase activities of 70%, 66%, 88%, and 70%, respectively, after 10 cycles of hydrolysis. Consequently, the TOF of the GO-MNP-Enz biocatalyst was several times higher than those of other biocatalysts reported in the literature, meaning that more product can be obtained per unit of biocatalyst per h. When GO-MNP-Enz was used multiple times in the hydrolysis of PSB, cellulose conversion to glucose was diminished in comparison to the initial cycles. On the other hand, xylan conversion to xylose, despite decreasing progressively, remained high and stable at levels greater than 60% until the tenth cycle.

Finally, the use of GO-MNP-Enz has been demonstrated as a cost-effective strategy for more competitive hydrolysis of sugarcane bagasse, potentializing its application to the production of second-generation ethanol, where the cost of enzymes is considered the main bottleneck that prevents its economic viability.

DECLARATIONS SECTION

List of abbreviations

(AFM) Atomic force microscopy; (ATR-FTIR) Attenuated total reflection-Fourier Transform Infrared; (CMC) Sodium carboxymethylcellulose; (EDC) 1-ethyl-3-(3-dimethylaminopropyl) carbodiimide; (EDX) Energy-dispersive X-ray; (FPU) Filter paper units; (GO) Graphene oxide; (GO-MNP) Graphene oxide-magnetite; (GO-MNP-Enz) biocatalyst; (NHS) *N*-hydroxy-succinimide; (PSB)

Pretreated sugarcane bagasse; (SEM) Scanning electron microscopy; (SDS-PAGE) sodium dodecyl sulfate–polyacrylamide gel electrophoresis; (TEM) Transmission electron microscopy; (TOF) Turnover frequency.

Ethical Approval and Consent to participate

Not applicable.

Consent for publication

All authors read and approved the final manuscript.

Availability of supporting data

We are providing a document with supplementary information.

Conflicts of interest

There are no conflicts to declare.

Funding

São Paulo State Research Support Foundation (FAPESP) contract number 2018/06241-3 funding this work. Coordination of Improvement of Higher Education Personnel (CAPES) funding the doctoral scholarship of Fernando Roberto Paz-Cedeno in Brazil and in the Universitat Politècnica de València (UPV), Institute of Chemical Technology (ITQ), Valencia, Spain. Authors acknowledge financial support from PGC2018-097277-B-

100(MCIU/AEI/FEDER,UE) project and Severo Ochoa Program (SEV-2016-0683).

CRediT authorship contribution statement

Fernando Roberto Paz Cedeno: Conceptualization, Investigation, Methodology, Writing - original draft, Writing - review & editing. **Jose Miguel Carceller:** Methodology, Writing - review & editing. **Sara Iborra:** Supervision, Funding acquisition, Resources, Writing - review & editing. **Ricardo Keitel Donato:** Supervision, Writing - review & editing. **Anna Paula Godoy:** Methodology, Writing - review & editing. **Ariela Veloso de Paula:** Writing - review & editing. **Rubens Monti:** Writing - review & editing. **Avelino Corma:** Supervision, Funding acquisition, Writing - review & editing. **Fernando Masarin:** Conceptualization, Supervision, Funding acquisition, Resources, Writing - review & editing.

Acknowledgements

FAPESP, contract number 2018/06241-3 funding this paper. Coordination of Improvement of Higher Education Personnel (CAPES) financed the doctoral scholarship of Fernando Roberto Paz-Cedeno in Brazil and in the Universitat Politècnica de València (UPV), Institute of Chemical Technology (ITQ), Valencia, Spain. Authors acknowledge financial support from PGC2018-097277-B-100 (MCIU/AEI/FEDER,UE) project and Program Severo Ochoa (SEV-2016-0683).

REFERENCES

[1] Renewable Fuel Association, 2020 Pocket Guide to Ethanol, 2020. https://ethanolrfa.org/wp-content/uploads/2020/02/2020-Outlook-Pocket-Guide-for-Web.pdf.

[2] UNICA, Moagem de cana-de-açúcar e produção de açúcar e etanol - safra 2018/2019, (2020). http://unicadata.com.br/historico-de-producao-e-moagem.php (accessed February 25, 2020).

[3] V.L. Sirisha, A. Jain, A. Jain, Enzyme Immobilization: An Overview on Methods, Support Material, and Applications of Immobilized Enzymes, Adv. Food Nutr. Res. 79 (2016) 179–211. doi:10.1016/bs.afnr.2016.07.004.

[4] C. Aragon, Imobilização multipontual covalente de xilanases: seleção de derivados ativos e estabilizados, Universidade Estadual Paulista Julio de Mesquita Filho, 2013.

[5] S. Lei, Y. Xu, G. Fan, M. Xiao, S. Pan, Immobilization of naringinase on mesoporous molecular sieve MCM-41 and its application to debittering of white grapefruit, Appl. Surf. Sci. 257 (2011) 4096–4099. doi:10.1016/j.apsusc.2010.12.003.

[6] J.M. Guisán, Immobilization of enzymes on glyoxyl agarose – Strategies for enzyme stabilization by multipoint attachment, in: G.F. BICKERSTAFF (Ed.), Immobil. Enzym. Cells, 1st ed., Humana Press, Totowa, 1997: pp. 277–287. doi:10.1385/0896033864.

[7] J.M. Guisan, Aldehyde-agarose gels as activated supports for immobilization-stabilization of enzymes, Enzyme Microb. Technol. 10

(1988) 375–382. doi:10.1016/0141-0229(88)90018-X.

[8] J. Jiang, J. Zhao, C. He, B. Cui, J. Xiong, H. Jiang, J. Ao, G. Xiang, Recyclable magnetic carboxymethyl chitosan/calcium alginate – cellulase bioconjugates for corn stalk hydrolysis, Carbohydr. Polym. 166 (2017) 358–364. doi:10.1016/j.carbpol.2017.03.003.

[9] E. Poorakbar, A. Shafiee, A.A. Saboury, B.L. Rad, K. Khoshnevisan, L. Ma'mani, H. Derakhshankhah, M.R. Ganjali, M. Hosseini, Synthesis of magnetic gold mesoporous silica nanoparticles core shell for cellulase enzyme immobilization: Improvement of enzymatic activity and thermal stability, Process Biochem. 71 (2018) 92–100. doi:10.1016/j.procbio.2018.05.012.

[10] N.R. Mohamad, N. Haziqah, C. Marzuki, N.A. Buang, R.A. Wahab, An overview of technologies for immobilization of enzymes and surface analysis techniques for immobilized enzymes, Biotechnol. Biotechnol. Equip. 29 (2015) 205–220. doi:10.1080/13102818.2015.1008192.

[11] I. Díaz Carretero, R.M. Blanco Martín, M. Sánchez Sánchez, C. Márquez Álvarez, Biocatalysis on porous materials, in: V. Blay, L.F. Bobadilla, A. Cabrera-García (Eds.), Zeolites Met. Fram. From Lab to Ind., Amsterdam University Press, 2018: pp. 149–174. http://hdl.handle.net/10261/164226.

[12] J.M. Carceller, R. Monti, J.C. Bassan, M. Filice, J. Yu, S. Iborra, Covalent immobilization of naringinase over two-dimensional 2D zeolites and its applications in a continuous process to produce citrus flavonoids and for debittering of juices, ChemCatChem. (2020).

doi:10.1002/cctc.202000320.

[13] P. Miró, M. Audiffred, T. Heine, An atlas of two-dimensional materials, Chem. Soc. Rev. 43 (2014) 6537–6554. doi:10.1039/c4cs00102h.

[14] P. Montes-Navajas, N.G. Asenjo, R. Santamaría, R. Menéndez, A. Corma, H. García, Surface Area Measurement of Graphene Oxide in Aqueous Solutions, Langmuir. 29 (2013) 13443–13448. doi:10.1021/la4029904.

[15] J. Zhang, J. Zhang, F. Zhang, H. Yang, X. Huang, H. Liu, S. Guo, Graphene oxide as a matrix for enzyme immobilization, Langmuir. 26 (2010) 6083–6085. doi:10.1021/la904014z.

[16] J.M. Carceller, J.P. Martínez Galán, R. Monti, J.C. Bassan, M. Filice, S. Iborra, J. Yu, A. Corma, Selective synthesis of citrus flavonoids prunin and naringenin using heterogeneized biocatalyst on graphene oxide, Green Chem. 21 (2019) 839–849. doi:10.1039/c8gc03661f.

[17] E. Doustkhah, S. Rostamnia, Covalently bonded sulfonic acid magnetic graphene oxide: Fe3O4@GO-Pr-SO3H as a powerful hybrid catalyst for synthesis of indazolophthalazinetriones, J. Colloid Interface Sci. 478 (2016) 280–287. doi:10.1016/j.jcis.2016.06.020.

[18] M. Heidarizadeh, E. Doustkhah, S. Rostamnia, P.F. Rezaei, F.D. Harzevili, B. Zeynizadeh, Dithiocarbamate to modify magnetic graphene oxide nanocomposite (Fe3O4-GO): A new strategy for covalent enzyme (lipase) immobilization to fabrication a new nanobiocatalyst for enzymatic hydrolysis of PNPD, Int. J. Biol. Macromol. 101 (2017) 696–702. doi:10.1016/j.ijbiomac.2017.03.152.

[19] V. Mehnati-Najafabadi, A. Taheri-Kafrani, A.K. Bordbar, Xylanase immobilization on modified superparamagnetic graphene oxide nanocomposite: Effect of PEGylation on activity and stability, Int. J. Biol. Macromol. 107 (2018) 418–425. doi:10.1016/j.ijbiomac.2017.09.013.

[20] C.G.C.M. Netto, H.E. Toma, L.H. Andrade, Superparamagnetic nanoparticles as versatile carriers and supporting materials for enzymes, J. Mol. Catal. B Enzym. 85–86 (2013) 71–92. doi:10.1016/j.molcatb.2012.08.010.

[21] W. Huang, S. Pan, Y. Li, L. Yu, R. Liu, Immobilization and Characterization of cellulase on hydroxy and aldehyde functionalized magnetic Fe2O3/Fe3O4 nanocomposites prepared via a novel rapid combustion process, Int. J. Biol. Macromol. 162 (2020) 845–852. doi:https://doi.org/10.1016/j.ijbiomac.2020.06.209.

[22] R. Liu, W. Huang, S. Pan, Y. Li, L. Yu, D. He, Covalent immobilization and characterization of penicillin G acylase on magnetic Fe2O3/Fe3O4 heterostructure nanoparticles prepared via a novel solution combustion and gel calcination process, Int. J. Biol. Macromol. 162 (2020) 1587–1596. doi:10.1016/j.ijbiomac.2020.07.283.

[23] K. Khoshnevisan, F. Vakhshiteh, M. Barkhi, H. Baharifar, E. Poor-Akbar, N. Zari, H. Stamatis, A.K. Bordbar, Immobilization of cellulase enzyme onto magnetic nanoparticles: Applications and recent advances, Mol. Catal. 442 (2017) 66–73. doi:10.1016/j.mcat.2017.09.006.

[24] A.A. Gokhale, J. Lu, I. Lee, Immobilization of cellulase on magnetoresponsive graphene nano-supports, J. Mol. Catal. B Enzym.

90 (2013) 76–86. doi:10.1016/j.molcatb.2013.01.025.

[25] Y. Lin, X. Liu, Z. Xing, Y. Geng, J. Wilson, D. Wu, H. Kong, Preparation and characterization of magnetic Fe3O4–chitosan nanoparticles for cellulase immobilization, Cellulose. 24 (2017) 5541–5550. doi:10.1007/s10570-017-1520-6.

[26] J. Alftrén, T.J. Hobley, Immobilization of cellulase mixtures on magnetic particles for hydrolysis of lignocellulose and ease of recycling, Biomass and Bioenergy. 65 (2014) 72–78. doi:10.1016/j.biombioe.2014.03.009.

[27] R. Ahmad, M. Sardar, Immobilization of cellulase on TiO2 nanoparticles by physical and covalent methods: A comparative study, Indian J. Biochem. Biophys. 51 (2014) 314–320.

[28] H. Liao, D. Chen, L. Yuan, M. Zheng, Y. Zhu, X. Liu, Immobilized cellulase by polyvinyl alcohol/Fe2O3magnetic nanoparticle to degrade microcrystalline cellulose, Carbohydr. Polym. 82 (2010) 600–604. doi:10.1016/j.carbpol.2010.05.021.

[29] M. Sakata, A. Funatsu, S. Sonoda, T. Ogata, T. Taniguchi, Y. Matsumoto, Immobilization of Trypsin on Graphene Oxide Nanosheets for Increased Proteolytic Stability, Chem. Lett. 41 (2012) 1625–1627. doi:10.1246/cl.2012.1625.

[30] J. Shen, M. Shi, B. Yan, H. Ma, N. Li, Y. Hu, M. Ye, Covalent attaching protein to graphene oxide via diimide-activated amidation, Colloids Surfaces B Biointerfaces. 81 (2010) 434–438. doi:10.1016/j.colsurfb.2010.07.035.

[31] Q. Yu, Z. Wang, Y. Zhang, R. Liu, Covalent immobilization and

characterization of penicillin G acylase on amino and GO functionalized magnetic Ni0.5Zn0.5Fe2O4@SiO2 nanocomposite prepared via a novel rapid-combustion process, Int. J. Biol. Macromol. 134 (2019) 507–515. doi:10.1016/j.ijbiomac.2019.05.066.

[32] W.S. Hummers, R.E. Offeman, Preparation of Graphitic Oxide, J. Am. Chem. Soc. 80 (1958) 1339–1339. doi:10.1021/ja01539a017.

[33] T.K. Ghose, Measurement of cellulase activities, Pure Appl. Chem. 59 (1987) 257–268. doi:10.1351/pac198759020257.

[34] M. Tanaka, M. Taniguchi, R. Matsuno, T. Kamikubo, Purification and Properties of Cellulases from Eupencillium javanicum : Studies on the Re-utilization of Cellulosic Resources(VII), J. Ferment. Technol. 59 (1981) 177–183. http://ci.nii.ac.jp/naid/110002672575/en/ (accessed July 26, 2016).

[35] M.J. Bailey, P. Biely, K. Poutanen, Interlaboratory testing of methods for assay of xylanase activity, J. Biotechnol. 23 (1992) 257–270. doi:10.1016/0168-1656(92)90074-J.

[36] L.U.L. Tan, P. Mayers, J.N. Saddler, Purification and characterization of a thermostable xylanase from a thermophilic fungus Thermoascus aurantiacus, Can. J. Microbiol. (1987) 689–691. doi:10.1139/m87-120.

[37] R.A. Sheldon, S. van Pelt, Enzyme immobilisation in biocatalysis: Why, what and how, Chem. Soc. Rev. 42 (2013) 6223–6235. doi:10.1039/c3cs60075k.

[38] F.M. Mendes, G. Siqueira, W. Carvalho, A. Ferraz, A.M.F. Milagres, Enzymatic hydrolysis of chemithermomechanically pretreated

sugarcane bagasse and samples with reduced initial lignin content, Biotechnol. Prog. 27 (2011) 395–401. doi:10.1002/btpr.553.

[39] F.R. Paz-Cedeno, E.G. Solórzano-Chávez, L.E. de Oliveira, V.C. Gelli, R. Monti, S.C. de Oliveira, F. Masarin, Sequential Enzymatic and Mild-Acid Hydrolysis of By-Product of Carrageenan Process from Kappaphycus alvarezii, BioEnergy Res. 12 (2019) 419–432. doi:10.1007/s12155-019-09968-7.

[40] E.G. Solorzano-Chavez, F.R. Paz-Cedeno, L. Ezequiel de Oliveira, V.C. Gelli, R. Monti, S. Conceição de Oliveira, F. Masarin, Evaluation of the Kappaphycus alvarezii growth under different environmental conditions and efficiency of the enzymatic hydrolysis of the residue generated in the carrageenan processing, Biomass and Bioenergy. 127 (2019). doi:10.1016/j.biombioe.2019.105254.

[41] F. Masarin, F.R.P. Cedeno, E.G.S. Chavez, L.E. de Oliveira, V.C. Gelli, R. Monti, Chemical analysis and biorefinery of red algae Kappaphycus alvarezii for efficient production of glucose from residue of carrageenan extraction process, Biotechnol. Biofuels. 9 (2016) 122. doi:10.1186/s13068-016-0535-9.

[42] Q. Zhang, J. Kang, B. Yang, L. Zhao, Z. Hou, B. Tang, Immobilized cellulase on Fe3O4nanoparticles as a magnetically recoverable biocatalyst for the decomposition of corncob, Cuihua Xuebao/Chinese J. Catal. 37 (2016) 389–397. doi:10.1016/S1872-2067(15)61028-2.

[43] P.J. Huang, K.L. Chang, J.F. Hsieh, S.T. Chen, Catalysis of rice straw hydrolysis by the combination of immobilized cellulase from aspergillus

niger on β -Cyclodextrin-Fenanoparticles and ionic liquid, Biomed Res. Int. 2015 (2015). doi:10.1155/2015/409103.

[44] X. Yang, X. Zhang, Y. Ma, Y. Huang, Y. Wang, Y. Chen, Superparamagnetic graphene oxide-Fe3O4 nanoparticles hybrid for controlled targeted drug carriers, J. Mater. Chem. 19 (2009) 2710–2714. doi:10.1039/b821416f.

[45] M.I. Khalil, Co-precipitation in aqueous solution synthesis of magnetite nanoparticles using iron(III) salts as precursors, Arab. J. Chem. 8 (2015) 279–284. doi:10.1016/j.arabjc.2015.02.008.

[46] U. Han, M. Choi, J. Hong, Immobilization of basic fibroblast growth factor on heparin/EDC-methiodide nano-aggregates to maintain its continuous signaling, J. Ind. Eng. Chem. 53 (2017) 404–410. doi:10.1016/j.jiec.2017.05.012.

[47] M. Bagherzadeh, M.A. Amrollahi, S. Makizadeh, Decoration of Fe3O4magnetic nanoparticles on graphene oxide nanosheets, RSC Adv. 5 (2015) 105499–105506. doi:10.1039/c5ra22315f.

[48] M. Puche Panadero, Nanomateriales híbridos basados en complejos de metales de transición anclados sobre óxido de grafeno. Aplicaciones catalíticas., Universitat Politècnica de València, 2017. doi:10.4995/Thesis/10251/86211.

[49] M.A. Pimenta, G. Dresselhaus, M.S. Dresselhaus, L.G. Cançado, A. Jorio, R. Saito, Studying disorder in graphite-based systems by Raman spectroscopy, Phys. Chem. Chem. Phys. 9 (2007) 1276–1290. doi:10.1039/B613962K.

[50] D.C. Elias, R.R. Nair, T.M.G. Mohiuddin, S. V Morozov, P. Blake, M.P. Halsall, A.C. Ferrari, D.W. Boukhvalov, M.I. Katsnelson, A.K. Geim, K.S. Novoselov, Control of Graphene Properties by Reversible Hydrogenation: Evidence for Graphane, Science (80-.). 323 (2009) 610 LP – 613. doi:10.1126/science.1167130.

[51] C. Xu, X. Wang, J. Zhu, Graphene−Metal Particle Nanocomposites, J. Phys. Chem. C. 112 (2008) 19841–19845. doi:10.1021/jp807989b.

[52] T. Szabó, E. Tombácz, E. Illés, I. Dékány, Enhanced acidity and pH-dependent surface charge characterization of successively oxidized graphite oxides, Carbon N. Y. 44 (2006) 537–545. doi:10.1016/j.carbon.2005.08.005.

[53] S. Zhang, H. Wang, J. Liu, C. Bao, Measuring the specific surface area of monolayer graphene oxide in water, Mater. Lett. 261 (2020) 127098. doi:10.1016/j.matlet.2019.127098.

[54] S. Yusan, Preparation and characterization of magnetic graphene oxide nanocomposite (GO-Fe3O4) for removal of strontium and cesium from aqueous solutions, Compos. Mater. Res. 7 (2018). doi:10.18282/cmr.v7i1.89.

[55] P. Wang, X. Zhou, Y. Zhang, L. Wang, K. Zhi, Y. Jiang, Synthesis and application of magnetic reduced graphene oxide composites for the removal of bisphenol A in aqueous solution—a mechanistic study, RSC Adv. 6 (2016) 102348–102358. doi:10.1039/C6RA23542E.

[56] J. Gao, C.-L. Lu, Y. Wang, S.-S. Wang, J.-J. Shen, J.-X. Zhang, Y.-W. Zhang, Rapid immobilization of cellulase onto graphene oxide with a

hydrophobic spacer, Catalysts. 8 (2018) 1–12. doi:10.3390/catal8050180.

[57] K. Selvam, M. Govarthanan, D. Senbagam, S. Kamala-Kannan, B. Senthilkumar, T. Selvankumar, Activity and stability of bacterial cellulase immobilized on magnetic nanoparticles, Cuihua Xuebao/Chinese J. Catal. 37 (2016) 1891–1898. doi:10.1016/S1872-2067(16)62487-7.

[58] J. Jordan, C.S.S.R. Kumar, C. Theegala, Preparation and characterization of cellulase-bound magnetite nanoparticles, J. Mol. Catal. B Enzym. 68 (2011) 139–146. doi:10.1016/j.molcatb.2010.09.010.

[59] Y. Zhou, S. Pan, X. Wei, L. Wang, Y. Liu, Immobilization of β-glucosidase onto magnetic nanoparticles and evaluation of the enzymatic properties, BioResources. 8 (2013) 2605–2619. doi:10.15376/biores.8.2.2605-2619.

[60] V. Califano, F. Sannino, A. Costantini, J. Avossa, S. Cimino, A. Aronne, Wrinkled Silica Nanoparticles: Efficient Matrix for β-Glucosidase Immobilization, J. Phys. Chem. C. 122 (2018) 8373–8379. doi:10.1021/acs.jpcc.8b00652.

[61] H.J. Park, A.J. Driscoll, P.A. Johnson, The development and evaluation of B-glucosidase immobilized magnetic nanoparticles as recoverable biocatalysts, Biochem. Eng. J. 133 (2018) 66–73. doi:10.1016/j.bej.2018.01.017.

[62] T. Chen, W. Yang, Y. Guo, R. Yuan, L. Xu, Y. Yan, Enhancing catalytic performance of β-glucosidase via immobilization on metal ions chelated

magnetic nanoparticles, Enzyme Microb. Technol. 63 (2014) 50–57. doi:10.1016/j.enzmictec.2014.05.008.

[63] L. Guan, B. Di, M. Su, J. Qian, Immobilization of β-glucosidase on bifunctional periodic mesoporous organosilicas, Biotechnol. Lett. 35 (2013) 1323–1330. doi:10.1007/s10529-013-1208-4.

[64] A. Morana, A. Mangione, L. Maurelli, I. Fiume, O. Paris, R. Cannio, M. Rossi, Immobilization and characterization of a thermostable β-xylosidase to generate a reusable biocatalyst, Enzyme Microb. Technol. 39 (2006) 1205–1213. doi:10.1016/j.enzmictec.2006.03.010.

[65] G. Delcheva, G. Dobrev, I. Pishtiyski, Performance of Aspergillus niger B 03 β-xylosidase immobilized on polyamide membrane support, J. Mol. Catal. B Enzym. 54 (2008) 109–115. doi:10.1016/j.molcatb.2007.12.019.

[66] M. Guerfali, I. Maalej, A. Gargouri, H. Belghith, Catalytic properties of the immobilized Talaromyces thermophilus β-xylosidase and its use for xylose and xylooligosaccharides production, J. Mol. Catal. B Enzym. 57 (2009) 242–249. doi:10.1016/j.molcatb.2008.09.011.

[67] C.R.F. Terrasan, M. Romero-Fernández, A.H. Orrego, S.M. Oliveira, B.C. Pessela, E.C. Carmona, J.M. Guisan, Immobilization and Stabilization of Beta-Xylosidases from Penicillium janczewskii, Appl. Biochem. Biotechnol. 182 (2017) 349–366. doi:10.1007/s12010-016-2331-1.

[68] C.R.F. Terrasan, C.C. Aragon, D.C. Masui, B.C. Pessela, G. Fernandez-Lorente, E.C. Carmona, J.M. Guisan, β-xylosidase from Selenomonas

ruminantium: Immobilization, stabilization, and application for xylooligosaccharide hydrolysis, Biocatal. Biotransformation. 34 (2016) 161–171. doi:10.1080/10242422.2016.1247817.

[69] H.K. Lim, N.-J. Park, Y.K. Hwang, K.-I. Lee, T. Hwang, Improvement and Immobilization of a new Endo-β-1,4-xylanases KRICT PX1 from Paenibacillus sp. HPL-001, J. Bioprocess. Biotech. 05 (2015) 1–8. doi:10.4172/2155-9821.1000215.

[70] R.E. Abraham, M.L. Verma, C.J. Barrow, M. Puri, Suitability of magnetic nanoparticle immobilised cellulases in enhancing enzymatic saccharification of pretreated hemp biomass, Biotechnol. Biofuels. 7 (2014) 1–12. doi:10.1186/1754-6834-7-90.

[71] J. Han, P. Luo, Y. Wang, L. Wang, C. Li, W. Zhang, J. Dong, L. Ni, The development of nanobiocatalysis via the immobilization of cellulase on composite magnetic nanomaterial for enhanced loading capacity and catalytic activity, Int. J. Biol. Macromol. 119 (2018) 692–700. doi:10.1016/j.ijbiomac.2018.07.176.

[72] J. Na'imah, S. Prasetyawan, A. Srihardyastutie, In Vitro and In Silico Studies of Immobilized Xylanase on Zeolite Matrix Activated with Hydrochloric Acid, J. Pure Appl. Chem. Res. 6 (2017) 181–188. doi:10.21776/ub.jpacr.2017.006.03.335.

[73] A.P. Ingle, J. Rathod, R. Pandit, S.S. da Silva, M. Rai, Comparative evaluation of free and immobilized cellulase for enzymatic hydrolysis of lignocellulosic biomass for sustainable bioethanol production, Cellulose. 24 (2017) 5529–5540. doi:10.1007/s10570-017-1517-1.

[74] J. Sánchez-Ramírez, J.L. Martínez-Hernández, P. Segura-Ceniceros, G. López, H. Saade, M.A. Medina-Morales, R. Ramos-González, C.N. Aguilar, A. Ilyina, Cellulases immobilization on chitosan-coated magnetic nanoparticles: application for Agave Atrovirens lignocellulosic biomass hydrolysis, Bioprocess Biosyst. Eng. 40 (2017) 9–22. doi:10.1007/s00449-016-1670-1.

[75] J. Han, L. Wang, Y. Wang, J. Dong, X. Tang, L. Ni, L. Wang, Preparation and characterization of Fe3O4-NH2@4-arm-PEG-NH2, a novel magnetic four-arm polymer-nanoparticle composite for cellulase immobilization, Biochem. Eng. J. 130 (2018) 90–98. doi:10.1016/j.bej.2017.11.008.

[76] T. Alahakoon, J.W. Koh, X.W.C. Chong, W.T.L. Lim, Immobilization of cellulases on amine and aldehyde functionalized Fe2O3magnetic nanoparticles, Prep. Biochem. Biotechnol. 42 (2012) 234–248. doi:10.1080/10826068.2011.602800.

[77] J. Xu, Z. Sheng, X. Wang, X. Liu, J. Xia, P. Xiong, B. He, Enhancement in ionic liquid tolerance of cellulase immobilized on PEGylated graphene oxide nanosheets: Application in saccharification of lignocellulose, Bioresour. Technol. 200 (2016) 1060–1064. doi:10.1016/j.biortech.2015.10.070.

[78] M.R. Ladole, J.S. Mevada, A.B. Pandit, Ultrasonic hyperactivation of cellulase immobilized on magnetic nanoparticles, Bioresour. Technol. 239 (2017) 117–126. doi:10.1016/j.biortech.2017.04.096.

ANNEX: Electronic Supplementary Information

Magnetic graphene oxide as a platform for the immobilization of cellulases and xylanases: ultrastructural characterization and assessment of lignocellulosic biomass hydrolysis

Fernando Roberto Paz-Cedeno,[*a] Jose Miguel Carceller,[b] Sara Iborra,[b] Ricardo Keitel Donato,[c] Anna Paula Godoy,[d] Ariela Veloso de Paula,[a] Rubens Monti,[a] Avelino Corma[*b] and Fernando Masarin[a]

[a]São Paulo State University (UNESP), School of Pharmaceutical Science (FCF), Department of Bioprocess Engineering and Biotechnology. Araraquara-SP, Brazil. 14800-903

[b]Universitat Politècnica de València (UPV), Institute of Chemical Technology (ITQ), Valencia, Spain. 46022

[c]Institute of Macromolecular Chemistry, Czech Academy of Sciences, Prague, Czech Republic.162 06

[d]Graphene and Nanomaterials Research Center, Mackenzie Presbyterian University, São Paulo, Brazil. 01302-907

(*) Corresponding author

Email addresses:

FRPC: fernando.paz@unesp.br
JMC: jocarca8@upvnet.upv.es
SI: siborra@itq.upv.es
RKD: donato@imc.cas.cz
APG: apaulasgodoy@gmail.com
AVP: ariela.veloso@unesp.br
RM: rubens.monti@unesp.br
AC: acorma@itq.upv.es
FM: fernando.masarin@unesp.br

Raman and EDX spectroscopy

Raman spectroscopy can be used as a quick and unambiguous method to determine the structural quality as well as the number of layers of carbonaceous materials, e.g., graphite, graphene, GO, rGO, and carbon nanotubes. The spectrum is mainly characterized by the presence of D, G, and 2D bands. The D band (at 1350 cm^{-1}) involves the collective vibration of six carbon atoms (denominated breathing mode) and is active in Raman due the presence of defects in the graphene lattice as heteroatoms and edge effects with incomplete bonds. At 1580 cm^{-1}, the G band corresponds to the in-plane vibrational mode (or stretching mode) of two sp^2 hybridized carbon atoms, and its position is highly sensitive to the number of layers of material. Its widening depicts a high heterogeneity or structural disorder. The characteristic band of graphitic materials denoted by 2D (or G' at 2700 cm^{-1}) has been widely used as a simple and efficient way to confirm the presence of single layer graphene [1,2]. The 2D band is associated with the second harmonic of the D band, and it is present even if the D band has low intensity. It is also attributed to the structural organization of the bidimensional plane of graphene (stacking) [3–5]. Additionally, the intensity ratio, I_D/I_G, provides insight regarding the structural disorder degree and quality of graphene where the defect-free graphene ratio is equal to 2 [6,7].

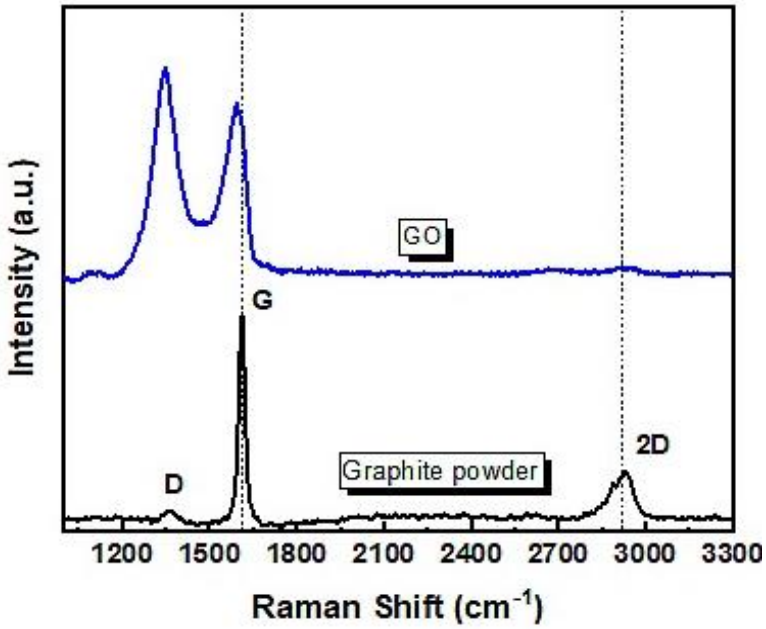

Figure 3.S1. Raman spectra of GO and graphite powder.

The EDX spectroscopy technique was used in conjunction with SEM (SEM-EDX) (Figure 3.S2a and b) and TEM (TEM-EDX) (Figures 3.S2c and d) to characterize the GO. EDX is a fast qualitative analysis method of the main elements in a sample [8,9]. Two types of X-ray photon emission from the X-ray spectrum are produced by beam-specimen interaction: characteristic X-rays, whose specific energies provide a fingerprint to each element, and continuum X-rays, which occur at all photon energies from the measurement threshold, thus producing a background beneath the characteristic X-rays. The generated spectrum can be used to identify and quantify the specific elements over a wide range of concentrations (0.1%–1%) [10,11].

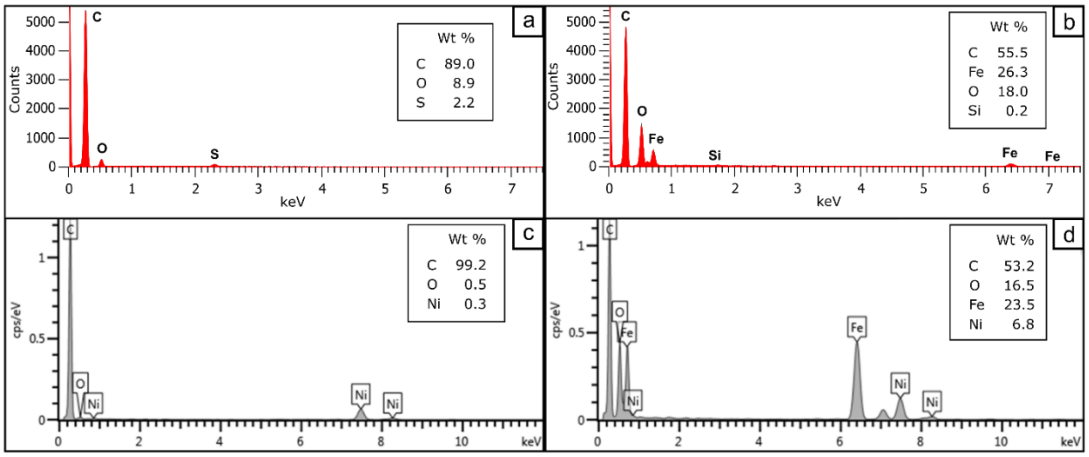

Figure 3.S2. Energy-dispersive X-ray spectroscopy (SEM-EDX) of **(a)** Graphite oxide. **(b)** Graphite oxide-magnetite. Energy-dispersive X-ray spectroscopy (TEM-EDX) of **(c)** Graphene oxide (GO) and **(d)** Graphene oxide with magnetic nanoparticles (GO-MNP).

The spectrum in Figure 3.S2a showed that the produced GO is mainly composed of the following: C (99.2%), O (8.9%) from oxygenated groups attached to the graphene skeleton, and S (2.2%) from the oxidation method using H_2SO_4. With the addition of magnetic particles (Figure 3.S2b), the concentrations of C and O were 55.5% and 18%, respectively. The increasing O concentration and appearance of Fe on the spectrum confirmed that the magnetic particles were successfully attached to the GO. In the TEM-EDX (Figure 3.S2c) analysis, it was determined that GO was composed of C (99.2%) and O (0.5%). In Figure 3.S2d, the element concentrations of C, O, and Fe were 53.5%, 16.5%, and 23.5%, respectively. The two latter because of the presence of magnetic particles. The presences of Ni and Si were attributed to the substrate.

Chemical composition of sugarcane bagasse

Table 3.S1. Chemical composition of original and pretreated sugarcane bagasse.

Treatment	Yield (g/100g of SB)	Components of Sugarcane Bagasse (g/100g of material)				
		Cellulose (%)	Xylan (%)	Arabinosyl groups (%)	Acetyl groups (%)	Lignin (%)
Untreated	-	37.5 ± 2.7	22.1 ± 1.8	1.7 ± 0.1	2.8 ± 0.3	23.7 ± 0.6
NaOH-Sulfite	64.9	48.4 ± 2.9	23.0 ± 2.0	2.4 ± 0.2	0.0 ± 0.0	9.8 ± 1.0

REFERENCES

[1] J.C. Meyer, C. Kisielowski, R. Erni, M.D. Rossell, M.F. Crommie, A. Zettl, Direct Imaging of Lattice Atoms and Topological Defects in Graphene Membranes, Nano Lett. 8 (2008) 3582–3586. doi:10.1021/nl801386m.

[2] K. Erickson, R. Erni, Z. Lee, N. Alem, W. Gannett, A. Zettl, Determination of the Local Chemical Structure of Graphene Oxide and Reduced Graphene Oxide, Adv. Mater. 22 (2010) 4467–4472. doi:10.1002/adma.201000732.

[3] A.C. Ferrari, J.C. Meyer, V. Scardaci, C. Casiraghi, M. Lazzeri, F. Mauri, S. Piscanec, D. Jiang, K.S. Novoselov, S. Roth, A.K. Geim, Raman Spectrum of Graphene and Graphene Layers, Phys. Rev. Lett. 97 (2006) 187401. doi:10.1103/PhysRevLett.97.187401.

[4] A.C. Ferrari, D.M. Basko, Raman spectroscopy as a versatile tool for studying the properties of graphene, Nat. Nanotechnol. 8 (2013) 235–246. doi:10.1038/nnano.2013.46.

[5] A.C. Ferrari, Raman spectroscopy of graphene and graphite: Disorder, electron–phonon coupling, doping and nonadiabatic effects, Solid State Commun. 143 (2007) 47–57. doi:https://doi.org/10.1016/j.ssc.2007.03.052.

[6] A. Jorio, Raman Spectroscopy in Graphene-Based Systems: Prototypes for Nanoscience and Nanometrology, ISRN Nanotechnol. 2012 (2012) 234216. doi:10.5402/2012/234216.

[7] M.A. Pimenta, G. Dresselhaus, M.S. Dresselhaus, L.G. Cançado, A.

Jorio, R. Saito, Studying disorder in graphite-based systems by Raman spectroscopy, Phys. Chem. Chem. Phys. 9 (2007) 1276–1290. doi:10.1039/B613962K.

[8] J.I. Goldstein, D.E. Newbury, J.R. Michael, N.W.M. Ritchie, J.H.J. Scott, D.C. Joy, Scanning Electron Microscopy and X-Ray Microanalysis, 4th ed., Springer Nature, New York, 2018. doi:10.1007/978-1-4939-6676-9.

[9] N. Seifollah, H. Shokrollah, Modern analytical techniques in failure analysis of aerospace, chemical, and oil and gas industries, in: A.S.H. Makhlouf, M. Aliofkhazraei (Eds.), Handb. Mater. Fail. Anal. with Case Stud. from Oil Gas Ind., 1st ed., Butterworth-Heinemann, 2016: pp. 39–54. doi:10.1016/B978-0-08-100117-2.00010-8.

[10] M.S. Eluyemi, M.A. Eleruja, A. V. Adedeji, B. Olofinjana, O. Fasakin, O.O. Akinwunmi, O.O. Ilori, A.T. Famojuro, S.A. Ayinde, E.O.B. Ajayi, Synthesis and Characterization of Graphene Oxide and Reduced Graphene Oxide Thin Films Deposited by Spray Pyrolysis Method, Graphene. 05 (2016) 143–154. doi:10.4236/graphene.2016.53012.

[11] H. Kharkwal, H.C. Joshi, K.P. Singh, Fabrication and Characterization of Layered Graphene Oxide Biocompatible Nano-Film by Various Methods, Int. J. Biochem. Biophys. 6 (2018) 1–19. doi:10.13189/ijbb.2018.060101.

ELSEVIER

Publishing Agreement

Elsevier Ltd

Magnetic graphene oxide as a platform for the immobilization of cellulases and xylanases: Ultrastructural characterization and assessment of lignocellulosic biomass hydrolysis

Corresponding author	Mr. Fernando Roberto Paz-Cedeno
E-mail address	fernando.paz@unesp.br
Journal	Renewable Energy
Our reference	RENE14208
PII	S0960-1481(20)31484-1

Your Status

- I am one author signing on behalf of all co-authors of the manuscript

Assignment of Copyright

I hereby assign to Elsevier Ltd the copyright in the manuscript identified above (where Crown Copyright is asserted, authors agree to grant an exclusive publishing and distribution license) and any tables, illustrations or other material submitted for publication as part of the manuscript (the "Article"). This assignment of rights means that I have granted to Elsevier Ltd, the exclusive right to publish and reproduce the Article, or any part of the Article, in print, electronic and all other media (whether now known or later developed), in any form, in all languages, throughout the world, for the full term of copyright, and the right to license others to do the same, effective when the Article is accepted for publication. This includes the right to enforce the rights granted hereunder against third parties.

Supplemental Materials

"Supplemental Materials" shall mean materials published as a supplemental part of the Article, including but not limited to graphical, illustrative, video and audio material.

With respect to any Supplemental Materials that I submit, Elsevier Ltd shall have a perpetual worldwide, non-exclusive right and license to publish, extract, reformat, adapt, build upon, index, redistribute, link to and otherwise use all or any part of the Supplemental Materials in all forms and media (whether now known or later developed), and to permit others to do so.

Research Data

"Research Data" shall mean the result of observations or experimentation that validate research findings and that are published separate to the Article, which can include but are not limited to raw data, processed data, software, algorithms, protocols, and methods.

With respect to any Research Data that I wish to make accessible on a site or through a service of Elsevier Ltd, Elsevier Ltd shall have a perpetual worldwide, non-exclusive right and license to publish, extract, reformat, adapt, build upon, index, redistribute, link to and otherwise use all or any part of the Research Data in all forms and media (whether now known or later developed) and to permit others to do so. Where I have selected a specific end user license under which the Research Data is to be made available on a site or through a service, the publisher shall apply that end user license to the Research Data on that site or service.

Reversion of rights

Articles may sometimes be accepted for publication but later rejected in the publication process, even in some cases after public posting in "Articles in Press" form, in which case all rights will revert to the author (see https://www.elsevier.com/about/our-business/policies/article-withdrawal).

Revisions and Addenda

I understand that no revisions, additional terms or addenda to this Journal Publishing Agreement can be accepted without Elsevier Ltd's express written consent. I understand that this Journal Publishing Agreement supersedes any previous agreements I have entered into with Elsevier Ltd in relation to the Article from the date hereof.

Author Rights for Scholarly Purposes

I understand that I retain or am hereby granted (without the need to obtain further permission) the Author Rights (see description below), and that no rights in patents, trademarks or other intellectual property rights are transferred to Elsevier Ltd.
The Author Rights include the right to use the Preprint , Accepted Manuscript and the Published Journal Article for Personal Use and Internal Institutional Use . They also include the right to use these different versions of the Article for Scholarly Sharing purposes, which include sharing:

- the Preprint on any website or repository at any time;
- the Accepted Manuscript on certain websites and usually after an embargo period;
- the Published Journal Article only privately on certain websites, unless otherwise agreed by Elsevier Ltd.

In the case of the Accepted Manuscript and the Published Journal Article the Author Rights exclude Commercial Use (unless expressly agreed in writing by Elsevier Ltd), other than use by the author in a subsequent compilation of the author's works or to extend the Article to book length form or re-use by the author of portions or excerpts in other works (with full acknowledgment of the original publication of the Article).

Author Representations / Ethics and Disclosure / Sanctions

I affirm the Author Representations noted below, and confirm that I have reviewed and complied with the relevant Instructions to Authors, Ethics in Publishing policy, Declarations of Interest disclosure and information for authors from countries affected by sanctions (Iran, Cuba, Sudan, Burma, Syria, or Crimea). Please note that some journals may require that all co-authors sign and submit Declarations of Interest disclosure forms. I am also aware of the publisher's policies with respect to retractions and withdrawal (https://www.elsevier.com/about/our-business/policies/article-withdrawal).

For further information see the publishing ethics page at https://www.elsevier.com/about/our-business/policies/publishing-ethics and the journal home page. For further information on sanctions, see https://www.elsevier.com/about/our-business/policies/trade-sanctions

Author representations

- The Article I have submitted to the journal for review is original, has been written by the stated authors and has not been previously published.
- The Article was not submitted for review to another journal while under review by this journal and will not be submitted to any other journal.
- The Article and the Supplemental Materials do not infringe any copyright, violate any other intellectual property, privacy or other rights of any person or entity, or contain any libellous or other unlawful matter.
- I have obtained written permission from copyright owners for any excerpts from copyrighted works that are included and have credited the sources in the Article or the Supplemental Materials.
- Except as expressly set out in this Journal Publishing Agreement, the Article is not subject to any prior rights or licenses and, if my or any of my co-authors' institution has a policy that might restrict my ability to grant the rights required by this Journal Publishing Agreement (taking into account the Author Rights permitted hereunder, including Internal Institutional Use), a written waiver of that policy has been obtained.
- If I and/or any of my co-authors reside in Iran, Cuba, Sudan, Burma, Syria, or Crimea, the Article has been prepared in a personal, academic or research capacity and not as an official representative or otherwise on behalf of the relevant government or institution.
- If I am using any personal details or images of patients, research subjects or other individuals, I have obtained all consents required by applicable law and complied with the publisher's policies relating to the use of such images or personal information. See https://www.elsevier.com/about/our-business/policies/patient-consent for further information.
- Any software contained in the Supplemental Materials is free from viruses, contaminants or worms.
- If the Article or any of the Supplemental Materials were prepared jointly with other authors, I have informed the co-author(s) of the terms of this Journal Publishing Agreement and that I am signing on their behalf as their agent, and I am

authorized to do so.

Governing Law and Jurisdiction

This Agreement will be governed by and construed in accordance with the laws of the country or state of Elsevier Ltd ("the Governing State"), without regard to conflict of law principles, and the parties irrevocably consent to the exclusive jurisdiction of the courts of the Governing State.

For information on the publisher's copyright and access policies, please see http://www.elsevier.com/copyright.
For more information about the definitions relating to this agreement click here.

I have read and agree to the terms of the Journal Publishing Agreement.

18 September 2020 T-copyright-v22/2017

4. CAPÍTULO 3

Stability of Cellic CTec2 enzymatic preparation immobilized onto magnetic graphene oxide: Assessment of hydrolysis of pretreated sugarcane bagasse

This manuscript is in the final preparation phase (final review of the discussion and English language).

Stability of Cellic CTec2 enzymatic preparation immobilized onto magnetic graphene oxide: Assessment of hydrolysis of pretreated sugarcane bagasse

Fernando Roberto Paz-Cedeno[*a], Jose Miguel Carceller[b], Sara Iborra[b], Ricardo Keitel Donato[c], Eddyn Gabriel Solorzano-Chavez[a], Ismael Ulises Miranda Roldán[a], Ariela Veloso de Paula[a], Avelino Corma[b] and Fernando Masarin[a]

[a]São Paulo State University (UNESP), School of Pharmaceutical Science (FCF), Department of Bioprocess Engineering and Biotechnology. Araraquara-SP, Brazil. 14800-903

[b]Universitat Politècnica de València (UPV), Institute of Chemical Technology (ITQ), Valencia, Spain. 46022

[c]National University of Singapore, Center for advanced 2D materials. Singapore. 117546

(*) Corresponding author

Email addresses:

FRPC: fernando.paz@unesp.br
JMC: jocarca8@upvnet.upv.es
SI: siborra@itq.upv.es
RKD: donato@ nus.edu.sg
EGSC: eddyn.solorzano@unesp.br
IUMR: imiranda_3@hotmail.com
AVP: ariela.veloso@unesp.br
AC: acorma@itq.upv.es
FM: fernando.masarin@unesp.br

ABSTRACT

In this study, pretreated sugarcane bagasse was subjected to enzymatic hydrolysis using Cellic CTec enzymes immobilized on graphene-oxide magnetite. Immobilized exoglucanase, endoglucanase, β-glucosidase, xylanase and β-xylosidase were evaluated for their operational stability, half-life, and effects of temperature and pH. The biocatalyst obtained showed similar performance in a wide range of pH and temperature, compared to the free enzymes. The half-life of the immobilized enzymes was longer than the free enzymes at temperatures above 45 °C, with the exception of endoglucanase. After 45 days of cold storage, the biocatalyst showed relative enzymatic activities greater than 65% for all assessed enzymes. The sugarcane bagasse was subjected to pretreatments to reduce recalcitrance to hydrolysis, generating SSB (sulfite-NaOH pretreated sugarcane bagasse) and CSB (chlorite pretreated sugarcane bagasse). The enzymatic hydrolysis of SSB and CSB was evaluated using free and immobilized enzymes. The hydrolysis rate of SSB using free enzymes was higher compared to immobilized enzymes, however, after 72 h of hydrolysis, the cellulose and xylan conversions into glucose and xylose was similar with the use of enzymes in free or immobilized form. This did not occur in the hydrolysis of CSB, in which at the end of 72 h, the cellulose and xylan conversions obtained with immobilized enzymes did not reach the levels obtained with free enzymes. The biocatalyst was successfully reused in several SSB hydrolysis cycles, maintaining an efficiency of approximately 80% in the last cycle. Finally, these results show that the immobilization of cellulases and xylanases improves its

operational stability and the biocatalyst obtained has the capacity to be used for several cycles in the hydrolysis of lignocellulosic biomass.

KEYWORDS: Sugarcane by-product; Enzyme immobilization; Enzymatic hydrolysis; Biocatalyst reuse; Second-generation ethanol.

HIGHLIGHTS

- The biocatalyst showed high relative activities after 45 days of storage
- The half-life of the immobilized enzymes was longer than the free enzymes
- Cellulose and xylan conversion reached the same level with free or immobilized enzymes
- The biocatalyst maintained 80% of its efficiency after several cycles of hydrolysis of sugarcane bagasse

INTRODUCTION

Due to its abundance and wide availability, lignocellulosic biomass is an alternative to reduce dependence on petroleum derivatives in the manufacture of fuels and chemical products. The most abundant lignocellulosic biomass in Brazil is sugarcane bagasse (SB). In the 2019/2020 season, the sugarcane crop was 643 million tons (dry basis), of which SB represents approximately 14% [1]. Several studies show that SB is an economical and sustainable biomass for obtaining value-added products, such as bioethanol [2–6], biodiesel [7], biobutanol [8,9], biohydrogen [10–12], xylitol [13–16], citric acid

[17], succinic acid [18], itaconic acid [19], lactic acid [20], butyric acid [21], gluconic acid [22], furfural [23], oligosaccharides [24–26], reducing sugars [27–29], among others.

Enzymatic hydrolysis represents an important step in obtaining bioproducts from SB; however, the use of free enzymes can increase production costs. A strategy that has been proven technically feasible to minimize this problem is the immobilization of enzymes onto solid supports and their reuse in several hydrolysis cycles [29]. The immobilization of enzymes confers several advantages to the biocatalyst such as reuse of the enzymes, increased stability and ease in the separation of the product [30]. On the other hand, despite being possible the enzymatic hydrolysis of untreated SB, several studies have shown that the application of pretreatments that partially remove the lignin from the SB reduces recalcitrance and improves the results of enzymatic hydrolysis [28,31].

In this work, the immobilization of an enzymatic cocktail on the surface of a solid magnetic support formed by graphene oxide-magnetite (GO-MNP) was evaluated. The biocatalyst obtained (GO-MNP-Enz), with endoglucanase, exoglucanase, β-glucosidase, xylanase and β-xylosidase activities, was evaluated in terms of its operational stability, half-life and effects of temperature and pH. Additionally, the SB was subjected to two different pretreatments with the intention of reducing its recalcitrance before enzymatic hydrolysis. These pretreatments resulted in SSB (sugarcane bagasse pretreated with sulfite-NaOH) and CSB (sugarcane bagasse pretreated with sodium chlorite) biomass. Enzymatic hydrolysis was performed with free

enzymes and GO-MNP-Enz, and the performance of the biocatalyst in several hydrolysis cycles of SSB and CSB was evaluated.

EXPERIMENTAL METHODS

Synthesis of support and immobilization of Cellic CTec 2 enzymatic preparation

The first step was the synthesis of the graphene oxide (GO). Thus, graphite powder (99.99%; <150 μm; Sigma-Aldrich, St Louis, MO, USA), sulfuric acid (95-97% v/v) and potassium permanganate were mixed, following the method reported by Hummers' [29,32]. The solid obtained was suspended in ultrapure water (1 $mg.mL^{-1}$) and sonicated for 2h to obtain the GO. For GO magnetization, $FeCl•6H_2O$ and $FeCl_2•4H_2O$ (molar ratio 2:1) were mixed in acetic acid solution (3% v/v) under vigorous stirring and the GO dispersion (5 $mg.mL^{-1}$) was added. The temperature was raised to 80 °C and ammonia (25% v/v) was added to raise the pH. After 20 min, the reaction was stopped and, with the help of an external magnetic field, the solid was recovered and washed several times with methanol and ultrapure water. This solid was oven dried at 40 °C and stored. This material was exposed to sonication in aqueous suspension before use, to be exfoliated in GO-MNP.

The commercial Cellic CTec 2 enzymatic preparation was covalently immobilized on the surface of the GO-MNP support, forming a biocatalyst that was named GO-MNP-Enz. For this, the functionalization of the support (20 mL of GO-MNP dispersion at 0.5 $mg.mL^{-1}$) with NHS (20 mg) and EDC (24 mg) was carried out for 3 h. The functionalized support was washed and

resuspended in sodium acetate buffer (pH 4.8). The Cellic CTec 2 enzyme extract was added and the suspension was kept on a roller shaker for 12 h. An external magnet was used to recover the biocatalyst, which was washed and then resuspended in sodium acetate buffer (pH 4.8) [29].

Enzyme activity assays and protein determination

Cellic CTec2 enzymatic preparation contains several enzymes necessary for the hydrolysis of lignocellulosic biomass, such as endoglucanase, exoglucanase, xylanase, β-glucosidase and β-xylosidase.

Endoglucanase activity was determined following the methodology described by Tanaka et al. [33]. Thus, a 0.1 mL volume of diluted Cellic CTec 2 was added to 0.9 mL of 0.44% (w/v) sodium carboxymethylcellulose (CMC) (≥95%; Carbosynth, USA) and kept at 50 °C in a thermal bath for 1 h. Xylanase activity was measured following the methodology described by Bailey et al. [34]. Then, a 0.1 mL volume of diluted Cellic CTec 2 was added to 0.9 mL of 1% (w/v) xylan (≥90%; Sigma-Aldrich, USA) and kept at 50 °C in a thermal bath for 5 min. Total cellulases were determined according describe by Ghose [35]. A strip of Whatman N°1 filter paper was placed in a tube with 1mL of 0.05 M sodium acetate buffer (pH 4.8). Then 0.5 mL of Cellic CTec 2 (properly diluted) was added to the tubes and kept at 50 °C for 1 h. The reactions of endoglucanase, xylanase and total cellulase were stopped by adding 3,5-dinitrosalicylic acid (DNS) and boiling for 5 min. After cooling, the readings were taken in a spectrophotometer at 540 nm.

Exoglucanase, β-glucosidase and β-xylosidase activities were measured following the methodology described by Tan et al. [36]. Accordingly, 0.8 mL of 0.1% (w/v) 4-nitrophenyl β-D-glucopyranoside (≥98%; Sigma-Aldrich, USA) or 4-nitrophenyl β-D-xylopyranoside (≥98%; Sigma-Aldrich, USA) or 4-nitrophenyl β-D-cellobioside (≥98%; Sigma-Aldrich, USA) was added to 0.2 mL of diluted Cellic CTec 2 and kept at 50 °C in a thermal bath for 30 min. The reactions were stopped by adding 2 mL of 10% (w/v) $NaHCO_3$, and the respective absorbance was read at 410 nm.

The protein content of Cellic CTec 2 was determined using the methodology described by Bradford [37]. Accordingly, a volume of properly diluted enzyme preparation was mixed with the Bradford reagent and absorbance was taken in a spectrophotometer at 595 nm. Bovine serum albumin (BSA) (Sigma-Aldrich, USA) was employed as protein standard.

According to Sheldon and Van Pelt [38], the most used parameters to determine the success of enzyme immobilization are: immobilization yield, immobilization efficiency and activity recovery. In this context, we have calculated these parameters according with the following Equations:

$$Yield = \left(\frac{A_i - A_f}{A_i}\right) * 100\% \quad (1)$$

$$Efficiency = \left(\frac{A_b}{A_i - A_f}\right) * 100\% \quad (2)$$

$$Activity\ recovery = \left(\frac{A_b}{A_i}\right) * 100\% \quad (3)$$

Where A_i: total activity on the enzyme preparation solution before immobilization; A_f: total activity on the supernatant after immobilization; and A_b: total activity on the biocatalyst.

Determination of maximum activity temperature and pH

The assays to determine the maximum activity temperature and pH were conducted in the manner described in previous item (Enzyme activity assays and protein determination). To find out the maximum activity temperature, the tests were carried out at temperatures between 30-80 °C with intervals of 10 °C. To find out the maximum activity pH, the tests were performed at pH 3-8 at the maximum activity temperature previously defined. The data were presented in the form of relative activity, considering 100% the highest activity obtained.

Thermal and pH stability

The thermal stability of endoglucanase, exoglucanase, β-glucosidase, xylanase and β-xylosidase was determined by incubating the enzyme (free and immobilized) to temperatures of 30, 40, 50 and 60 °C for 72 h. The residual activity of the enzymes was measured at different intervals of time. The stability in various pH buffers was determined similarly by incubating the enzyme (free or immobilized) at 4 °C in buffers with pH between 3-8 and determining the residual activity. Additionally, storage stability of immobilized endoglucanase, exoglucanase, β-glucosidase, xylanase and β-xylosidase was determined by incubating the biocatalyst at 4 °C in sodium acetate buffer pH 4.8 0.05 M during

45 days and measuring the residual activity of the enzymes at several intervals of time. The data were presented as relative activity, considering 100% the activity observed immediately after immobilization.

Half-life and enzyme deactivation

For thermal deactivation studies, it is common to use a first-order kinetic model to correlate enzymatic activity with time at a specific temperature [39]. Considering this, Equations 4 and 5 were used to calculate the thermal deactivation kinetic constant (K_d) and half-life time ($t_{1/2}$) of each immobilized enzyme at different temperatures.

$$Ln\left(\frac{A}{A_0}\right) = -K_d \quad (4)$$

$$t_{\frac{1}{2}} = \frac{ln\left(\frac{1}{2}\right)}{K_d} \quad (5)$$

Where A: final enzymatic activity of free or immobilized enzyme; A_0: initizl enzymatic activity; K_d: thermal deactivation kinetic constant (h^{-1}); $t_{1/2}$: half-life time of the free or immobilized enzyme (h)

Pretreatment of sugarcane bagasse

Sugarcane bagasse was separately subjected to two different pretreatments [28]. For the first pretreatment, 50 g (dry basis) of SB were placed in a 1.5 L reactor (AU/E-20, Regmed). Then, 250 mL of a 1% (w/v) NaOH solution and 250 mL of a 2% (w/v) Na_2SO_3 solution were added. The reactor was configured to operate at 140 °C for 30 minutes with a horizontal

rotation of 4 rpm. The material obtained was washed with tap water until the pH was neutralized and was dried in an oven at 40 °C for 24 h. This material was denominated sulfite-pretreated sugarcane bagasse (SSB).

For the second pretreatment, 20 g (dry basis) of SB were placed in a beaker and 640 mL of ultrapure water, 6 g of sodium chlorite and 2 mL of acetic acid were added. The reaction was kept at 70 °C for 4 h. At each hour of reaction, 6 g of sodium chlorite and 2 mL of acetic acid were added. After pretreatment, the mixture was filtered through porous glass filters (Schott #3, Germany) and washed with distilled water until the pH was neutral. The treated SB retained in filters were washed with 200 mL of pure acetone after the neutralization step [40]. The material was separated and oven dried for 24h at 40 °C. This material was named chlorite-pretreated sugarcane bagasse (CSB).

The yield of pretreatments was determined by gravimetry (percentage in relation to initial mass and mass after pretreatment, dry basis).

Chemical composition

To determine the chemical composition of the SB, SSB and CSB, the samples were ground using a knife mill and sieve of 20 mesh (0.84 mm screen). Lignin and carbohydrate contents were determined by acid hydrolysis [41]. For this, SBs were mixed with 72 % (w/w) H_2SO_4 for 1 h at 30 °C and then the H_2SO_4 was diluted until reaching a concentration of 4 % (w/w) and the reaction was maintained for 1 h at 121 °C. The hydrolysate was filtered through porous glass filters (Schott #3, Germany) and the retained material was washed with ultrapure water, dried, and weighed. This material corresponds to

insoluble lignin. An aliquot of the filtrate was used to determine soluble lignin by spectrophotometry at 205 nm. The filtrate was injected into a high-performance liquid chromatography (HPLC) system to determine the structural carbohydrates. Chromatographic analyses were performed using an HPX87H column (Bio-Rad, Hercules, CA, USA) at 60 °C with 0.005 M H_2SO_4 at 0.6 $mL.min^{-1}$. Detection was performed using a refractive index detector at 60 °C (Shimadzu, model C-R7A) [28,41,42]. Cellulose and hemicellulose contents in the SB were calculated from glucose, xylose, arabinose, and acetic acid data.

Structural characterization

The SBs were oven dried, milled, and screened through a 0.84 mm screen. The dried samples were subjected to infrared analysis using attenuated total reflection with a Fourier transform infrared (ATR-FTIR) spectrometer (Platinum- ATR Alpha; Bruker) with a single reflection diamond module at 25 °C. X-ray diffractograms (XRDs) of the dried samples were obtained in a Siemens Kristalloflex diffractometer running at a power output of 40 kV with a current of 30 mA and Ka Cu radiation (λ = 1.5406 Å) at 25 °C within an angle range of 5°- 70° 2Θ (Bragg Angle) and a scan speed of 2° min^{-1}. The crystallinity index (CrI) of the samples was calculated from the XRD by the deconvolution method (curve fitting). For peak fitting, PeaKFit software version 4.12 was used, assuming Gaussian functions to approximate each peak [28,43–45]. The CrI was calculated using Equation 6 as follows:

$$CrI\ (\%) = \left(\frac{A_c}{A_c + A_a}\right) * 100\% \quad (6)$$

Where, A_c is the area of the crystalline region; and A_a is the area of the amorphous regions.

Scanning electron microscopy (SEM) images were taken using an JSM-7500F Field Emission Scanning Electron Microscope (JEOL, Japan). For this purpose, the samples were thoroughly oven dried for 24 h at 50 °C, homogenized and placed on a conductive carbon adhesive tape.

The ground and dried samples of sugarcane bagasse were used for determination of molecular absorption spectrophotometry in the UV and visible regions on a Varian Cary 5000 UV- Vis-NIR spectrophotometer with a Cary Praying Mantis diffuse reflectance accessory for dried powder samples. The samples were analyzed at wavelengths from 200 to 700 nm using MgO as a reference substance.

Enzymatic hydrolysis of pretreated sugarcane bagasse and recycling

Pretreated sugarcane bagasse was hydrolyzed using both, free and immobilized Cellic CTec 2 enzymatic preparation. For this purpose, 100 mg of SBs (SSB or CSB) were placed in a beaker and added 10 mL of acetate buffer (pH 4.8) containing the appropriate amount of GO-MNP-Enz to reach an enzyme load of 10 and 20 FPU per gram of SB (dry basis). The reaction was carried out in thermal shaker at 45 °C and 150 rpm during 72 h. Aliquots were withdrawn at certain time intervals and were injected into an HPLC system using an HPX87H column (Bio-Rad, Hercules, CA, USA) at 60 °C with in the isocratic mode using 0.005 M H_2SO_4 at 0.6 $mL.min^{-1}$. Detection was performed using a refractive index detector at 60 °C (Shimadzu, model C-R7A). The

cellulose and xylan conversions were determined by Equations 7 and 8, respectively.

$$Cellulose\ conversion\ (\%) = \left(\frac{M_g * 0.90}{F_C + M_B}\right) * 100\% \quad (7)$$

$$Xylan\ conversion\ (\%) = \left(\frac{M_x * 0.88}{F_X + M_B}\right) * 100\% \quad (8)$$

where M_g: mass of glucose (mg); 0.9: conversion factor of glucose to cellulose; F_C: cellulose fraction in the pretreated SB ($g.g^{-1}$); M_B: mass of pretreated SB at the start of the reaction (mg); M_x: mass of xylose (mg); 0.88: conversion factor of xylose to xylan; and F_X: xylan fraction in the pretreated SB ($g.g^{-1}$).

Operational stability of GO-MNP-Enz was assessed by using the biocatalyst in several cycles of hydrolysis of pretreated sugarcane bagasse. The hydrolysis was conducted under the same conditions established above but for 24 h. After this time, the biocatalyst was retained with the help of an external magnet and the supernatant was removed from the reaction. 100 mg of SB and 10 mL of acetate buffer were added again, placed in a shaker at 45 °C and 150 rpm to start the new hydrolysis cycle.

Estimation of kinetic parameters

A model based on saturation kinetics was used to interpret the glucose and xylose concentration obtained during enzymatic hydrolysis assays [28,46–48]. For this purpose, the Equation 9 was used.

$$C = C_{Max}(1 - e^{-kt}) \quad (9)$$

Where C: sugar concentration ($g.L^{-1}$); C_{Max}: asymptotic maximum sugar concentration ($g.L^{-1}$); k: kinetic constant of sugar accumulation (h^{-1}); t: hydrolysis time (h).

RESULTS AND DISCUSSION

Synthesis of graphene oxide magnetite for immobilization of Cellic CTec2

Following the methodology described above, graphene oxide was obtained from graphite and then used to form the graphene oxide-magnetite nanocomposite. This nanocomposite was functionalized to serve as an immobilization support for the enzymes contained in the commercial enzymatic preparation Cellic CTec 2. After immobilization, the biocatalyst obtained showed activity of exoglucanase, endoglucanase, β-glucosidase, xylanase and β-xylosidase of 763, 300, 4500, 1034 and 33 $U.g^{-1}$, respectively, while the total cellulases activity was 44 $FPU.g^{-1}$. The immobilization yield is used to describe the percentage of total enzyme activity from the free enzyme solution that is immobilized. Most of the enzymes evaluated in this study obtained a high immobilization yield, ranging between 63-97%, with the exception of xylanase, which showed 27% of immobilization yield. The immobilization efficiency is described as the percentage of bound enzyme activity that is verified in the biocatalyst. Most of the time this value is less than 100% likely because of mass transfer limitations, tertiary structure modifications, decreased accessibility of active sites, and solubility of the specific substrate for each enzyme assay [49,50]. In this study exoglucanase and β-glucosidase showed efficiency values greater than 100% (136 and 113%, respectively) indicating that these enzymes are less sensitive to mass transfer issues, presumably because of the high solubility of the specific substrates. Lastly, the activity recovery compares the activity verified in the biocatalyst to that of the

total starting activity of the free enzyme and gives an idea of the success of the immobilization process. The values presented in Table 4.1 were published in a previous article by our research group, with the exception of the values referring to exoglucanase [29].

Table 4.1. Biocatalyst activity, yield of immobilization, efficiency and activity recovery in the immobilization process of Cellic CTec 2 onto graphene oxide-magnetite.

	Biocatalyst activity ($U.g^{-1}$)	**Immobilization yield (%)**	**Immobilization efficiency (%)**	**Activity recovery (%)**
Exoglucanase	763	96.4	136.0	131.1
*Endoglucanase	300	63.4	37.6	23.8
*β-glucosidase	4500	97.2	113.0	109.8
*Xylanase	1034	27.0	55.2	14.9
*β-xylosidase	33	91.6	86.6	79.3
*Total cellulases	44[#]	71.1	69.0	49.1

** From Paz-Cedeno et al. 2021* [29]. *[#] FPU.g^{-1}*

Optimal temperature, pH and stability (thermal, pH and storage)

Cellic CTec 2 enzymes in free and immobilized form were evaluated for the optimal temperature and pH in response to enzyme activity (Figure 4.1). Endoglucanase and xylanase activities showed differences in relation to optimal temperature in free and immobilized form. For these enzymes, optimal temperature was 60 °C for free, but decreased to 50 °C for immobilized form. Exoglucanase, β-glucosidase and β-xylosidase did not show differences for the free and immobilized forms, optimal temperature being 60 °C for exoglucanase, 50-60 °C for β-glucosidase and 50 °C for β-xylosidase. These results are in agreement with the literature since several studies show little or no difference in optimal temperature between immobilized and free cellulases and xylanases [51–57].

The optimum pH of all the enzymes was the same in the free or immobilized form except for endoglucanase, which showed an optimum pH of

4 in free form and 5 in immobilized form. The literature shows conflicting results in this regard. Huang et al. [58] immobilized endoglucanase in magnetic Fe_2O_3/Fe_3O_4 nanocomposites and reported a decrease in the optimal pH from 5 to 4, compared with the free form, while Ying et al. [52] immobilized endoglucanase in polyurea microspheres and did not observe an optimal pH change between free and immobilized enzyme, remaining pH 5 as optimal. On the other hand, Wang et al. [53] verified an optimal pH shift of 4 to 5 after immobilizing endoglucanases in magnetic gold mesoporous silica nanoparticles. In the case of xylanase, the relative activity at all pH is similar in the free and immobilized form, with the exception of pH 3 in which the enzyme in the immobilized form maintains a relative activity close to 100%, while in the free form relative activity is about 35%.

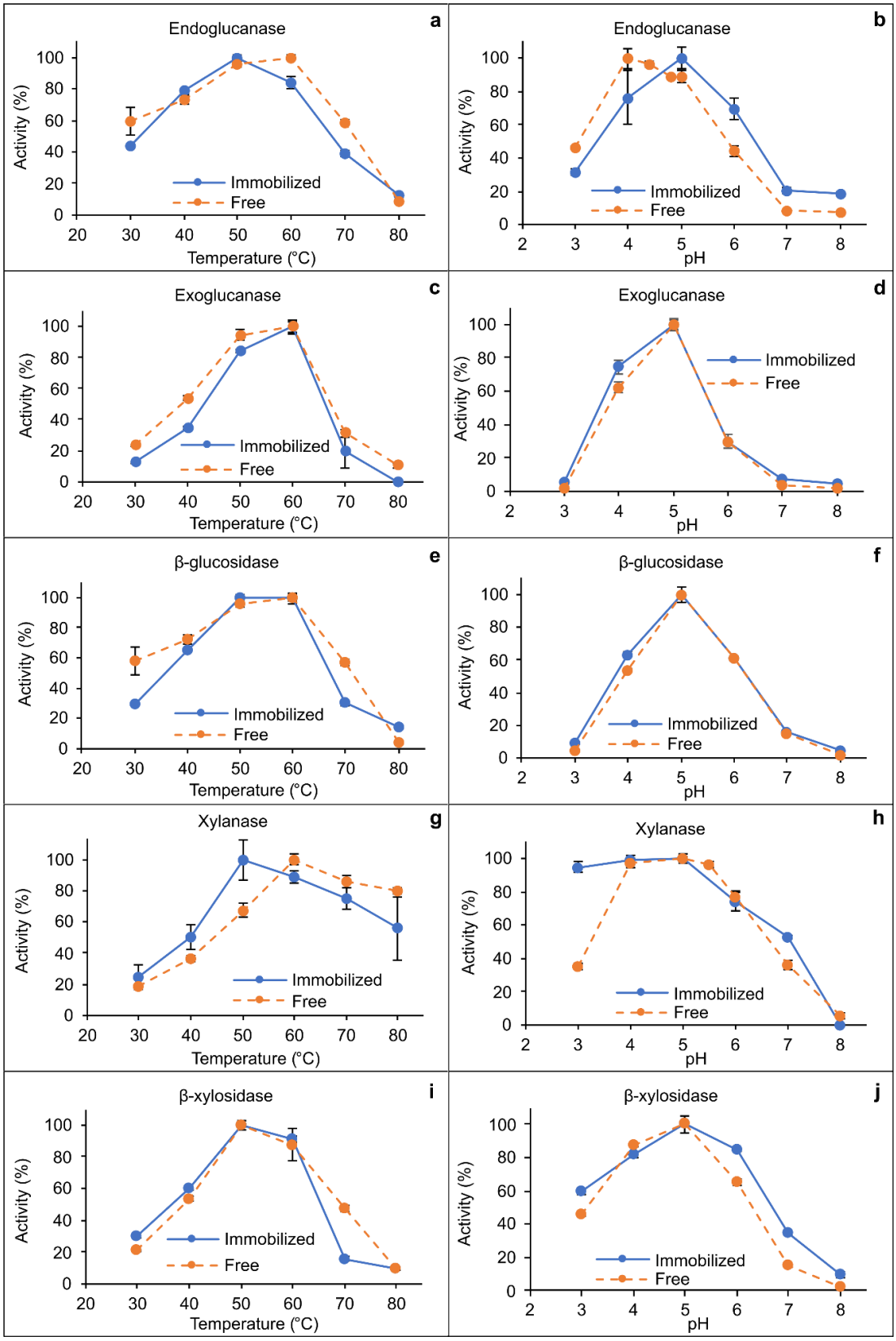

Figure 4.1. Optimal temperature and pH of free and immobilized endoglucanase **(a-b)**, exoglucanase **(c-d)**, β-glucosidase **(e-f)**, xylanase **(g-h)**, β-xylosidase **(i-j)**.

The storage stability of biocatalyst was assessed. A suspension of biocatalyst (1 mg.mL^{-1}) was kept refrigerated (4 °C) and the residual activity was measured. It was found that after 45 days the enzymatic activities remained between 65 and 82% (Figure 4.2). Additionally, the storage stability of the dry biocatalyst was evaluated. For this, the biocatalyst was dried under vacuum conditions at a temperature of 40 °C and then resuspended to measure its enzymatic activity. The biocatalyst immediately showed a great loss of activity, probably due to the difficulty of forming a dispersion again. In future tests, the storage stability in a more concentrated dispersion will be evaluated, in order to reduce the amount of water in storage.

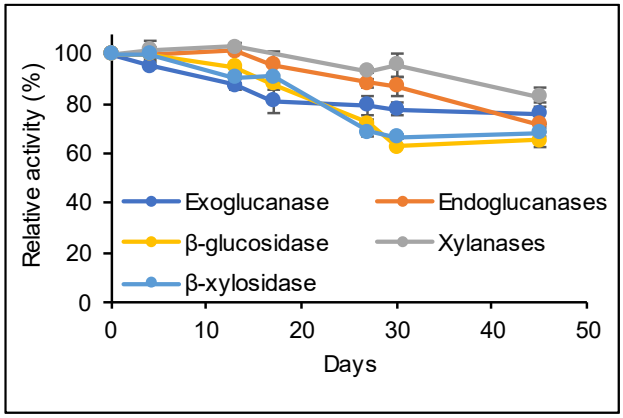

Figure 4.2. Storage stability of immobilized endoglucanase, exoglucanase, β-glucosidase, xylanase and β-xylosidase.

The thermal stability of enzymes is a vital parameter from the point of view of industrial application. In this work we evaluate the thermal stability of endoglucanase, exoglucanase, β-glucosidase, xylanase and β-xylosidase in a temperature range of 30 to 60 ° C for 72 h (Figure 4.3). It was possible to verify that the immobilization of the enzymes in GO-MNP played an important role in the improvement of the thermal stability of the enzymes at temperatures up to

45 °C, however this effect was less at temperatures above 50 °C and this was reflected in the half-life time (Figure 4.4). The half-life time was calculated at temperatures between 30 and 60 °C for the enzymes in the free and immobilized form. At a low temperature (30 °C), the half-life of the free enzymes is longer than the immobilized enzymes, with the exception of xylanase, which showed a significant improvement in the half-life in the immobilized form compared to the free form. However, we verified that from 45 °C, the half-life of immobilized enzymes is longer compared to free enzymes in all cases, with the exception of endoglucanase, where the half-life time in the free form was greater than 200 h. Additionally, it is possible to verified that the half-life time decreases dramatically at 50 °C compared to 45 °C, indicating that in an enzymatic hydrolysis assay, the enzymes will maintain their activity for a longer time at 45 °C.

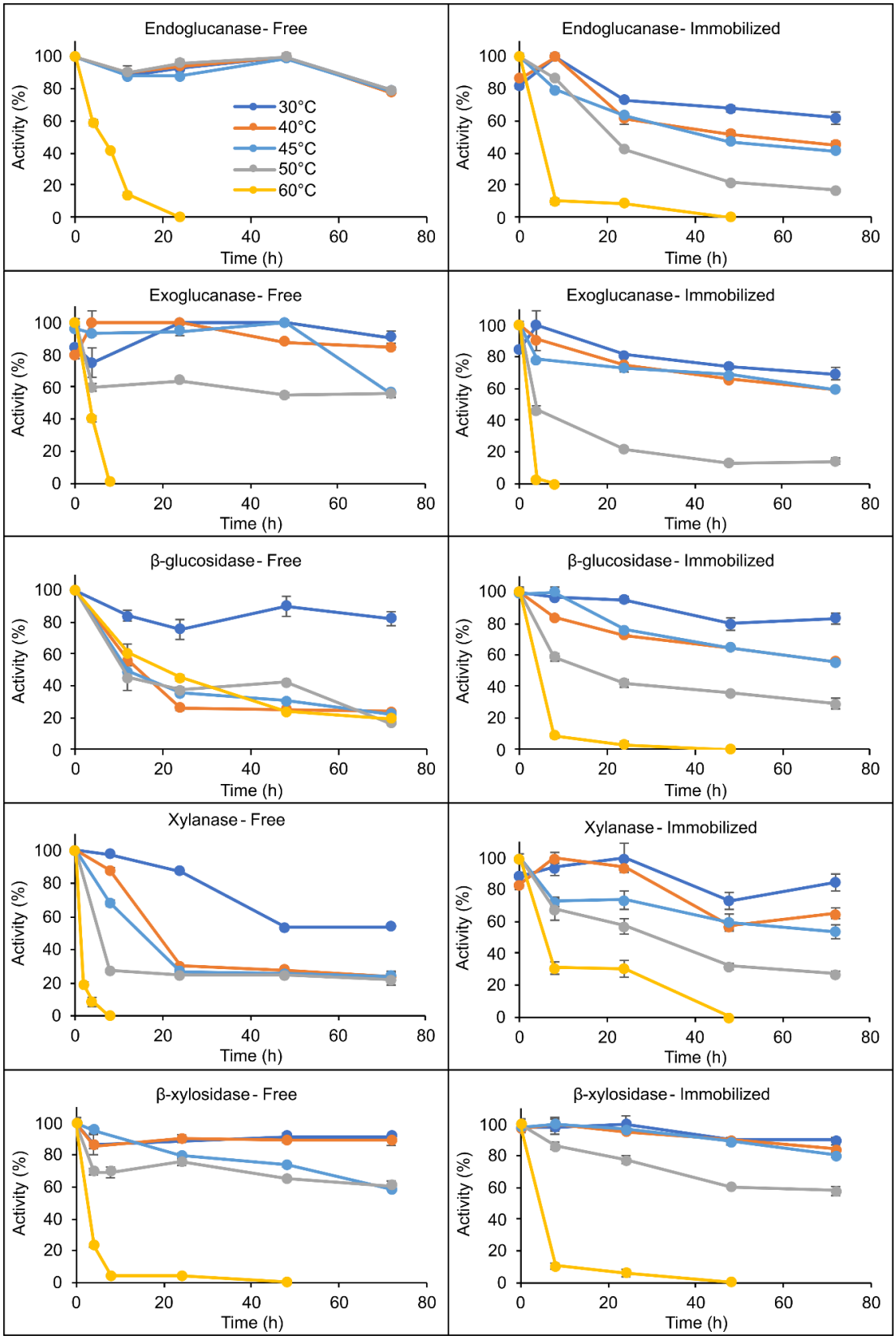

Figure 4.3. Thermal stability of free and immobilized endoglucanase, exoglucanase, β-glucosidase, xylanase and β-xylosidase.

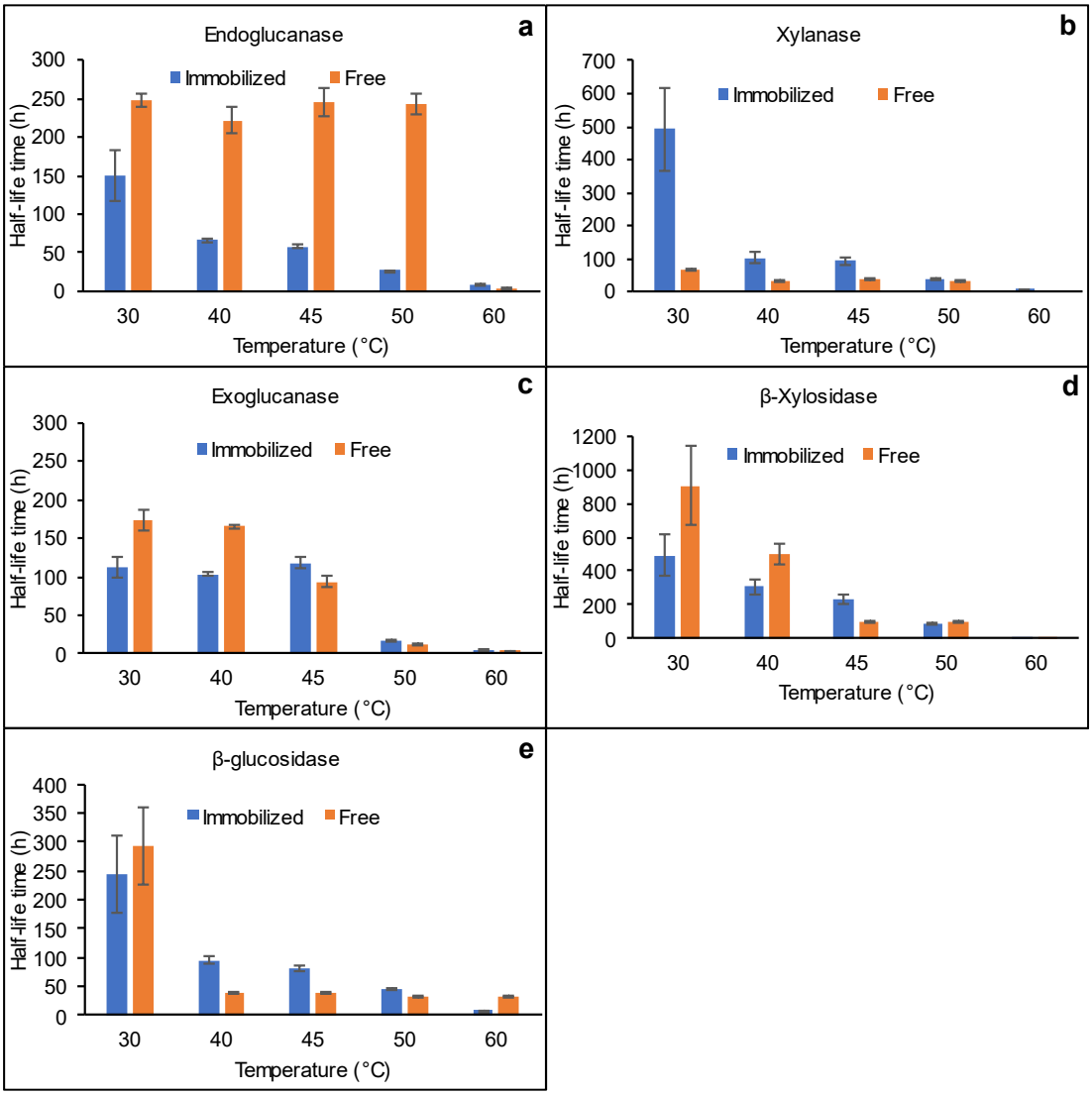

Figure 4.4. Half-life time of free and immobilized endoglucanase (a), xylanase (b), exoglucanase (c), β-xylosidase (d) and β-glucosidase (e).

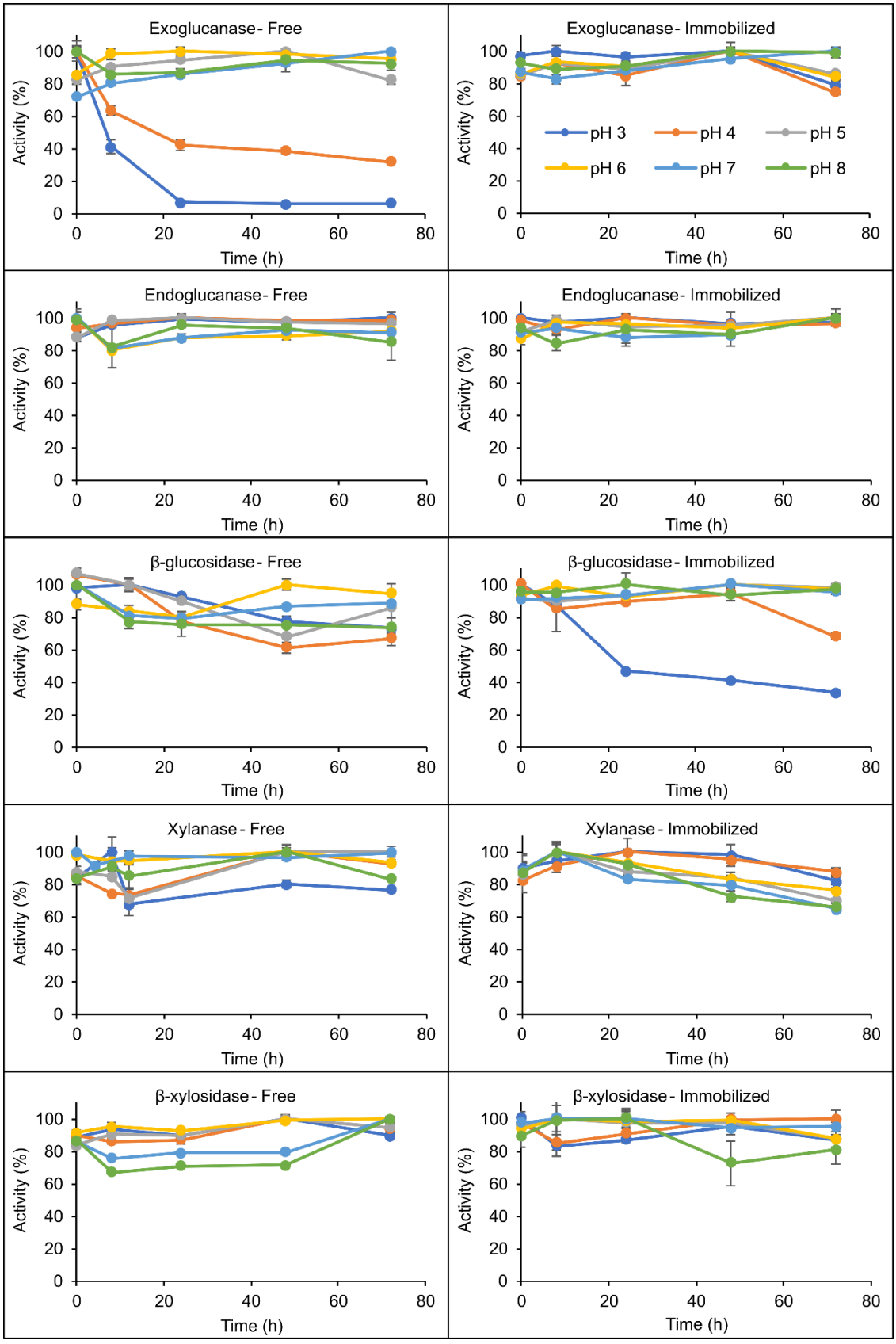

Figure 4.5. pH stability of free and immobilized endoglucanase, exoglucanase, β-glucosidase, xylanase and β-xylosidase.

The free and immobilized enzymes were incubated in buffer with a pH between 3 and 8 in order to evaluate their stability (Figure 4.5). Free and immobilized endoglucanase maintained a relative activity greater than 80% at all pH's. The immobilized β-glucosidase presented a better stability in relation to the free one at pH of 5, 6, 7 and 8, however at pH 3 it lost 60% of its activity. The xylanase and β-xylosidase enzymes showed a relative activity greater than 60% at all pH after 72 h.

Chemical composition and structural analysis of pretreated sugarcane bagasse

The literature shows that enzymatic hydrolysis on lignocellulosic biomass untreated is inefficient and there is a need to subject the biomass to a pretreatment in order to reduce the recalcitrance presented by these materials [28,40,59]. Untreated sugarcane bagasse contains 34.6% of cellulose, 25.3% of hemicellulose and 21.9% of lignin (Table 4.2).

Table 4.2. Chemical composition of untreated and pretreated sugarcane bagasse.

		Sugarcane Bagasse components (g/100g of material)		
Biomass	**Yield (g/100g of SB)**	**Cellulose (%)**	**Hemicellulose (%)**	**Lignin (%)**
Untreated	-	34.6 ± 2.5	25.3 ± 1.8	21.9 ± 0.6
SSB	64.2	48.4 ± 2.9	23.0 ± 2.0	9.8 ± 1.0
CSB	76.7	42.0 ± 0.6	25.1 ± 0.4	10.8 ± 0.8
		% of components loss (biomass components as g/100g of untreated SB)		
		Cellulose (%)	**Hemicellulose (%)**	**Lignin (%)**
Untreated		- (34.6)[a]	- (25.3)[a]	- (21.9)[a]
SSB		10.2 (31.1)[a]	33.3 (16.9)[b]	71.3 (6.3)[c]
CSB		6.9 (32.2)[a]	3.8 (24.4)[a]	61.0 (8.2)[b]

**Values that do not share a letter are significantly different. Extractives in the untreated sample: 7.8% (grams per 100 grams of sugarcane bagasse, dry basis). SSB: Sulfite-NaOH pretreated sugarcane bagasse. CSB: Chlorite pretreated sugarcane bagasse.*

The sugarcane bagasse was subjected to two different pretreatments using sulfite-NaOH and sodium chlorite. The visual aspect of bagasse sugarcane changed, leaving the pretreated samples clearer compared to the untreated sample (Figure 4.S1). After the pretreatments, the percentages of the components of the sugarcane bagasse changed, the main result being the removal of lignin, falling to approximately 10% (raw material, Table 4.2). The data presented in Table 4.2 show that there was no significant loss of cellulose content after pretreatments. However, there was a significant loss of hemicellulose in the sulfite-NaOH pretreatment (33%). In relation to lignin, it was verified that the two pretreatments were successful in removing it, being that the pretreatment with sulfite-NaOH reduced more (71.3%) than the pretreatment with chlorite (61.0%). Mendes et al [59] subjected sugarcane bagasse to pretreatment with sulfite-NaOH at 120 °C for 1 h and reported a 53.3% removal of lignin. Applying a pretreatment with sodium chlorite in sugarcane bagasse, Siqueira et al. [60] reported a 70 % decrease in lignin content, a result consistent with that presented in this study.

The ATR-FTIR spectra of SB, SSB and CSB are depicted in Figure 4.6a. The spectra show characteristic bands of cellulose (bands g, h, j and k), hemicellulose (band c) and lignin (band a, b, d, e, f, i and l). A detailed description of bands is presented in Table 4.S1. In this study, the spectra were compared to corroborate the chemical composition. In this sense, it is possible to verified that the characteristic bands of cellulose are present in all the spectra, confirming that the pretreatments did not degrade it. Band c, typical of hemicellulose, is present in the SB and CSB spectra; however, in the SSB

spectrum this band is not found, confirming the decrease in the hemicellulosic fraction in SSB shown in Table 4.2. Regarding lignin, a decrease in the intensity of the characteristic bands was observed in the spectra of SSB and CSB compared to the spectrum of SB, confirming the decrease of this component in the pretreated bagasse.

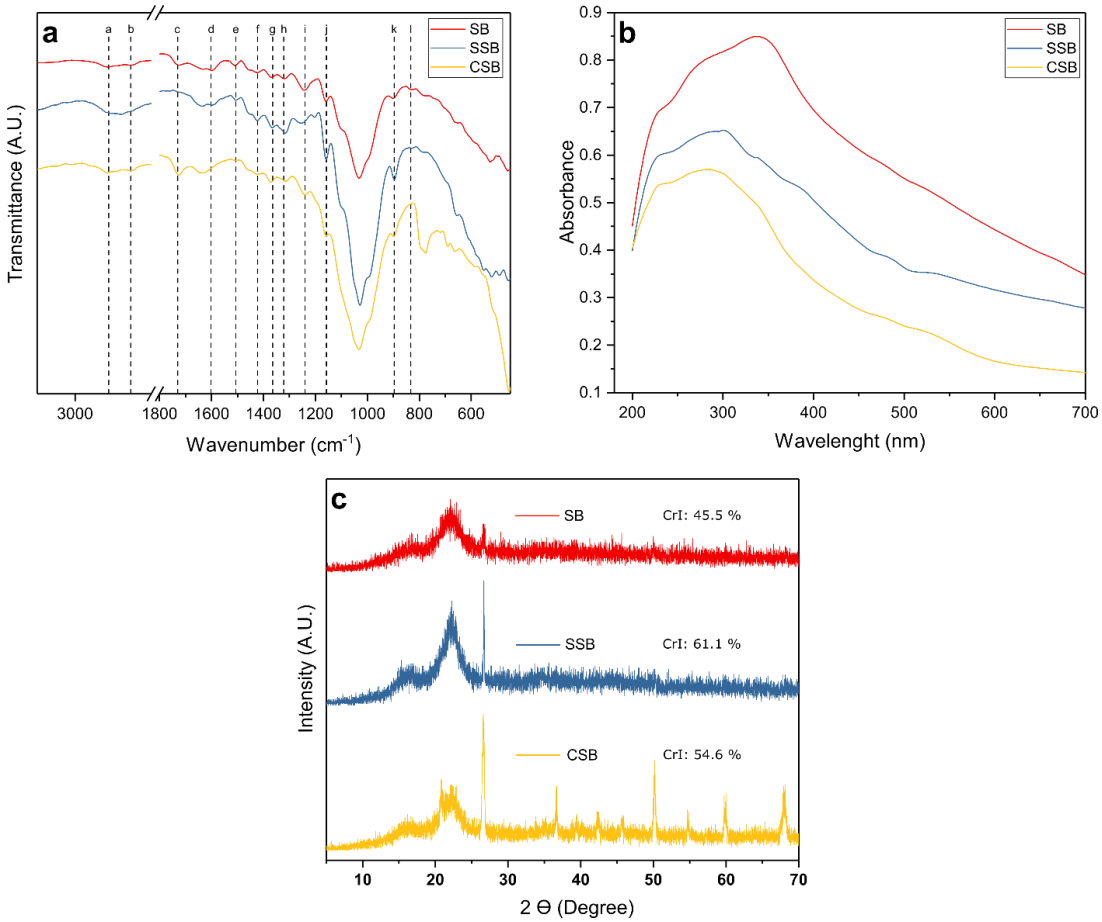

Figure 4.6. (a) Attenuated total reflectance in the infrared with Fourier transform (ATR-FTIR) spectra, (b) UV-Vis spectra and (c) X-ray diffraction spectra of sugarcane bagasse before (SB) and after sulfite-NaOH (SSB) and chlorite (CSB) pretreatments.

The UV-Vis spectra of the samples under study are presented in Figure 4.6b. According to the literature, bands at 280 and 350 nm correspond to non-conjugated and conjugated phenolic groups present in biomass containing

lignin, respectively [61,62]. SB shows a maximum absorption peak at approximately 350 nm that can be attributed to coniferyl aldehyde structures, ρ-coumaric and ferulic acids in lignin [63,64]. The SSB and CSB spectra show a shift of the region of maximum absorbance from 350 nm to 280-310nm, compared to SB, indicating that the characteristic components of 350 nm region (conjugated phenolic groups) were partially removed. The SSB and CSB maximum absorbance region (280-310 nm) is related to lignin rich in guaiacyl-syringyl and hydroxycinnamic acids bound to lignin [40,62]. This result indicates a partial decrease in the lignin content, corroborating the results of the chemical composition.

Figure 4.6c presents the XRD spectra and crystallinity index (CrI) of SB, SSB and SCB. The SB presented a CrI of 45.5%, consistent with that reported in the literature [28,45]. After the pretreatments, an increase in CrI was verified, being that the SSB was 61.1% and the CSB 54.6%. Lignin and hemicellulose have amorphous structures and its removal favors an increase in the crystallinity index of the biomass under study. These results are in agreement with that reported in Table 4.2, confirming that there was a removal of lignin and hemicellulose in SSB while in CSB, despite having a removal of lignin, the hemicellulose remained intact, which is reflected in a CrI lower than SSB.

The SEM images show the morphological differences between untreated and pretreated sugarcane bagasse. Figure 4.S2a shows a mostly smooth and uniform structure, characteristic of untreated sugarcane bagasse, while Figures 4.S2b and 4.S2c show rough and irregular structures, which are

the result of the deconstruction of the fibers caused by the pretreatments (SSB and CSB, respectively).

Enzymatic hydrolysis of pretreated sugarcane bagasse

Untreated sugarcane bagasse can be subjected to enzymatic hydrolysis directly. However, as is widely demonstrated in the literature, this biomass exhibits a high recalcitrance against enzymatic hydrolysis which generally leads to cellulose and xylan conversion values of approximately 20% or less. Several works have confirmed that enzymatic hydrolysis has a better performance when SB has been subjected to a pretreatment [28,59,65–67]. In this study, the hydrolysis was carried out on SB pretreated with sulfite-NaOH (SSB) and sodium chlorite (CSB). The profile of enzymatic hydrolysis of SSB and CSB using free and immobilized Cellic CTec 2 is presented in Figure 4.7.

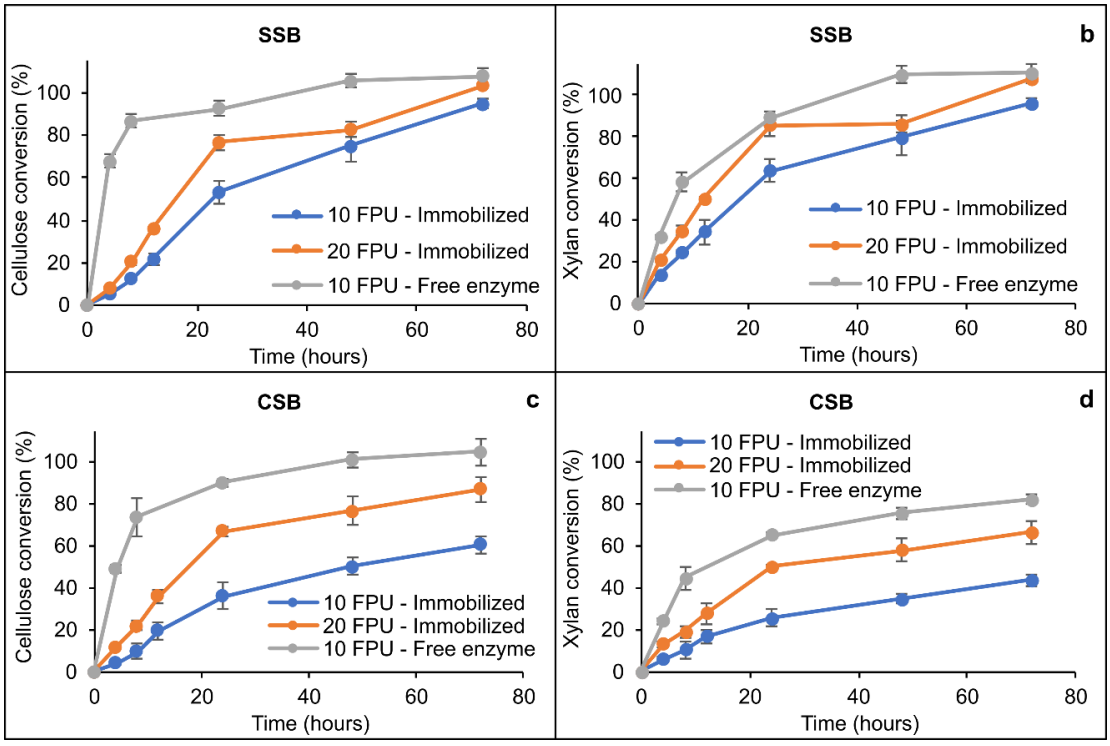

Figure 4.7. Hydrolysis of sulfite-NaOH (SSB) **(a-b)** and chlorite (CSB) **(c-d)** pretreated sugarcane bagasse using free and immobilized enzymes.

The cellulose conversion into glucose and xylan into xylose was faster in tests performed with the enzyme in its free form compared to the immobilized form. This is probably due to the mass transfer limitation problems faced by immobilized enzymes [49]. After 72 h of hydrolysis, the cellulose conversion reaches 100% in both the SSB and CSB. In the case of the xylan conversion, we verified that after 72 h of hydrolysis of SSB it reaches 100% conversion, but in the CSB it reaches approximately 80%.

The results of hydrolysis of SSB using immobilized enzymes show that, despite the fact that in the first hours, the conversion is lower compared to hydrolysis with free enzymes, after 72 h the conversion of cellulose and xylan reaches high levels, being approximately 90% and 100% with loads of 10 and 20 $FPU.g^{-1}$, respectively. Meanwhile, the results of the hydrolysis of CSB show that although an increase in the load of immobilized enzymes (from 10 to 20 $FPU.g^{-1}$) manages to increase the cellulose conversion (from 60 to 87%) and xylan (from 44 to 67%), it is not enough to reach the levels of conversion achieved by the free enzyme. These differences may be due to the fact that the sulfite-containing pretreatment (SSB) promotes a sulfonation of lignin, which increases the swelling of the fibers and, in this way, increases the exposure of cellulose and hemicellulose to the active sites of the enzymes [28,59]. Additionally, the sulfonated lignin is more hydrophilic and present less unproductive adsorption of the enzymes, which makes the reuse of the biocatalyst more efficient [68,69]. Siqueira et al. [40] subjected sugarcane bagasse to a pretreatment with chlorite and verified the response in enzymatic hydrolysis with free enzymes. The data presented by the authors are lower

than those found in this work, reaching a cellulose conversion into glucose of 60% and of xylan into xylose of 55% after 72 h of hydrolysis.

The kinetic parameters calculated from the experimental data, using a previously reported mathematical model [46–48], help us to understand the differences in the kinetics of free and immobilized enzymes (Table 4.3). In all cases, the maximum rate of product formation was higher in free enzymes compared to immobilized enzymes. However, it is verified that in the case of SSB hydrolysis, there was no significant difference in the maximum rate of glucose formation between hydrolysis with an enzyme load of 10 and 20 $FPU.g^{-1}$, but there was a difference in the maximum rate of xylose formation, being that of 20 $FPU.g^{-1}$ higher. On the other hand, there was a significant difference between the hydrolysis of CSB that used 10 and 20 $FPU.g^{-1}$, being that the one with 20 $FPU.g^{-1}$ had a higher rate of both glucose and xylose formation.

Table 4.3. Kinetic parameters of enzymatic hydrolysis of pretreated sugarcane bagasse using free and immobilized enzymes.

Biomass	Bioproduct	Biocatalyst	k (h^{-1})	C_{Max} ($g.L^{-1}$)	*Maximum rate of product formation ($g.L^{-1}.h^{-1}$)	R^2
SSB	Glucose	Free (10 $FPU.g^{-1}$)	0.242 ± 0.016	5.238 ± 0.212	1.269 ± 0.084[a]	0.907
		Immobilized (10 $FPU.g^{-1}$)	0.025 ± 0.007	5.826 ± 1.502	0.137 ± 0.004[b]	0.975
		Immobilized (20 $FPU.g^{-1}$)	0.030 ± 0.008	6.765 ± 1.517	0.196 ± 0.015[b]	0.961
	Xylose	Free (10 $FPU.g^{-1}$)	0.072 ± 0.002	2.890 ± 0.087	0.209 ± 0.008[a]	0.973
		Immobilized (10 $FPU.g^{-1}$)	0.045 ± 0.011	2.393 ± 0.463	0.105 ± 0.008[b]	0.986
		Immobilized (20 $FPU.g^{-1}$)	0.050 ± 0.010	2.939 ± 0.446	0.143 ± 0.013[c]	0.962
CSB	Glucose	Free (10 $FPU.g^{-1}$)	0.160 ± 0.010	4.482 ± 0.043	0.715 ± 0.040[a]	0.939
		Immobilized (10 $FPU.g^{-1}$)	0.033 ± 0.005	3.047 ± 0.193	0.099 ± 0.009[b]	0.982
		Immobilized (20 $FPU.g^{-1}$)	0.042 ± 0.009	4.276 ± 0.423	0.177 ± 0.018[c]	0.984
	Xylose	Free (10 $FPU.g^{-1}$)	0.085 ± 0.012	2.203 ± 0.054	0.187 ± 0.024[a]	0.953
		Immobilized (10 $FPU.g^{-1}$)	0.034 ± 0.016	1.447 ± 0.370	0.045 ± 0.013[b]	0.988
		Immobilized (20 $FPU.g^{-1}$)	0.049 ± 0.010	1.931 ± 0.204	0.094 ± 0.009[c]	0.987

** The values with the same superscripts do not differ among themselves at a significance level of 0.05 (Tukey test). SSB: Sulfite-NaOH pretreated sugarcane bagasse. CSB: Chlorite pretreated sugarcane bagasse.*

Operational stability of immobilized enzyme

The main objective of the immobilization of enzymes is the reuse of the biocatalyst in several cycles of hydrolysis. For this reason, enzymatic hydrolysis tests of SSB and CSB were performed using immobilized enzymes, and after the hydrolysis cycle was finished, the biocatalyst was recovered with the aid of an external magnet and reused in a new hydrolysis cycle (Figure 4.8).

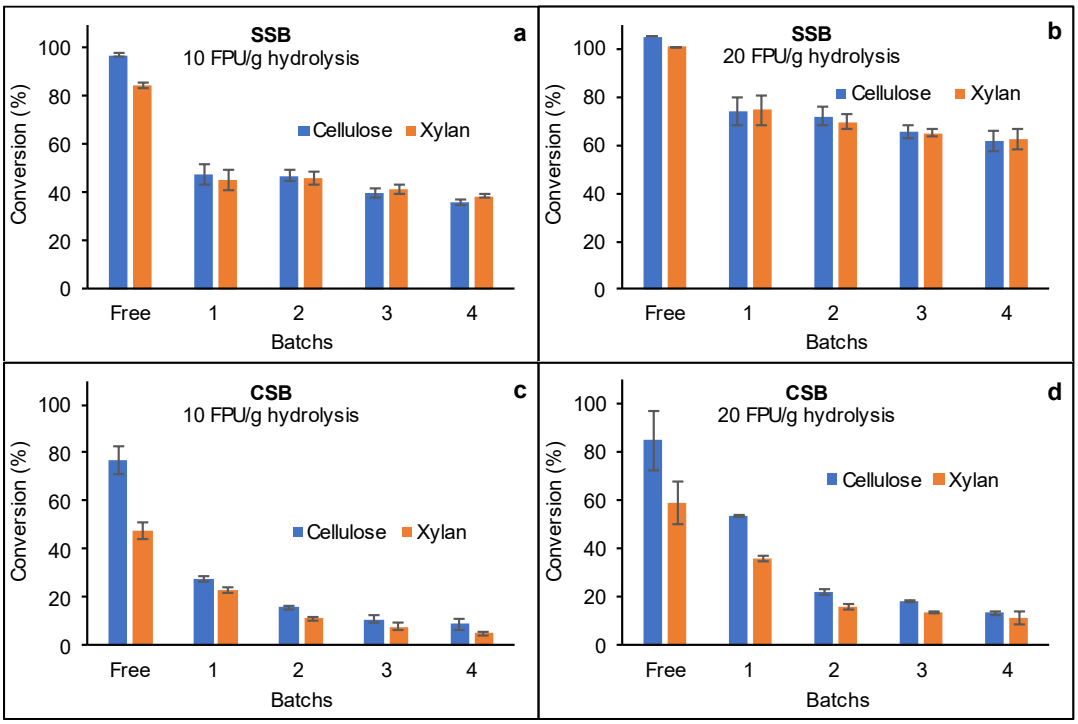

Figure 4.8. Recycling hydrolysis of sulfite-NaOH (SSB) **(a-b)** and chlorite (CSB) **(c-d)** pretreated sugarcane bagasse.

The hydrolysis of SSB with immobilized enzymes (enzyme load 10 FPU.g^{-1}) achieved a cellulose conversion into glucose of 47% in the first cycle and remained at a similar level until the fourth cycle when it reached 36% (Figure 4.8a). Xylan conversion into xylose in the same test was 45% in the first cycle and 39% in the last. Although these values are not high, a very low

loss of biocatalyst efficiency is confirmed between hydrolysis cycles, maintaining an efficiency of 76 and 86% in the cellulose and xylan conversions, respectively, compared to the first cycle. Carrying out the same hydrolysis test but with a higher enzymatic load (20 FPU.g-1), it was verified that the cellulose conversion was 74% in the first cycle and remained at a similar level until the fourth cycle in which it reached 62% (Figure 4.8b). In the same test, the xylan conversion in the first cycle was 74% and 63% in the fourth cycle. This indicates an efficiency of the biocatalyst of approximately 84% after 4 cycles of hydrolysis compared to the first cycle. From these SSB hydrolysis tests we can show that the cellulose and xylan conversions in each hydrolysis cycle increases with the increase in enzymatic load, however, the catalyst efficiency reached similar levels in the tests with 10 and 20 $FPU.g^{-1}$.

CSB hydrolysis had inferior performance compared to SSB hydrolysis. Using 10 $FPU.g^{-1}$, the cellulose conversion in the first cycle reached 28% and 9% in the last. While the xylan conversion in the first cycle was 23% and in the fourth it was 5% (Figure 4.8c). This indicates that the efficiency of the biocatalyst fell 68% for cellulose conversion and 79% for xylan conversion. The increase in the enzymatic load for 20 $FPU.g^{-1}$ led to an increase in the cellulose and xylan conversions, reaching 54% and 36% in the first cycle, respectively. However, in the fourth cycle, the cellulose conversion barely reached 13% and xylan conversion was 11% (Figure 4.8d). This indicates that there was a loss of catalyst efficiency of 75% in the case of cellulose conversion and 69% for xylan conversion, compared to the first cycle.

These differences in bioconversion of SSB and CSB may be due to the fact that the pretreatment with sulfite-NaOH reduces hydrophobic interactions between lignin and the enzyme, achieving less unproductive adsorption and additionally causes a swelling between the fibers that facilitates the access of the biocatalyst and therefore increases the conversion during the hydrolysis [59,69]. Moreover, a higher cellulose and xylan conversions facilitates the separation of the biocatalyst at the time of finishing one hydrolysis cycle and starting the next, since there is less insoluble matter that can adhere to the biocatalyst. Figure 4.9 shows scanning electronic microscopy images of SSB and CSB before use and after several cycles of hydrolysis using the biocatalyst GO-MNP-Enz. It is possible to observe the GO-MNP-Enz deposited on the surface of the fibers. In addition, we can verify that, although initially the dispersion of GO-MNP-Enz is homogeneous, this biocatalyst can be more or less concentrated in different portions of the biomass.

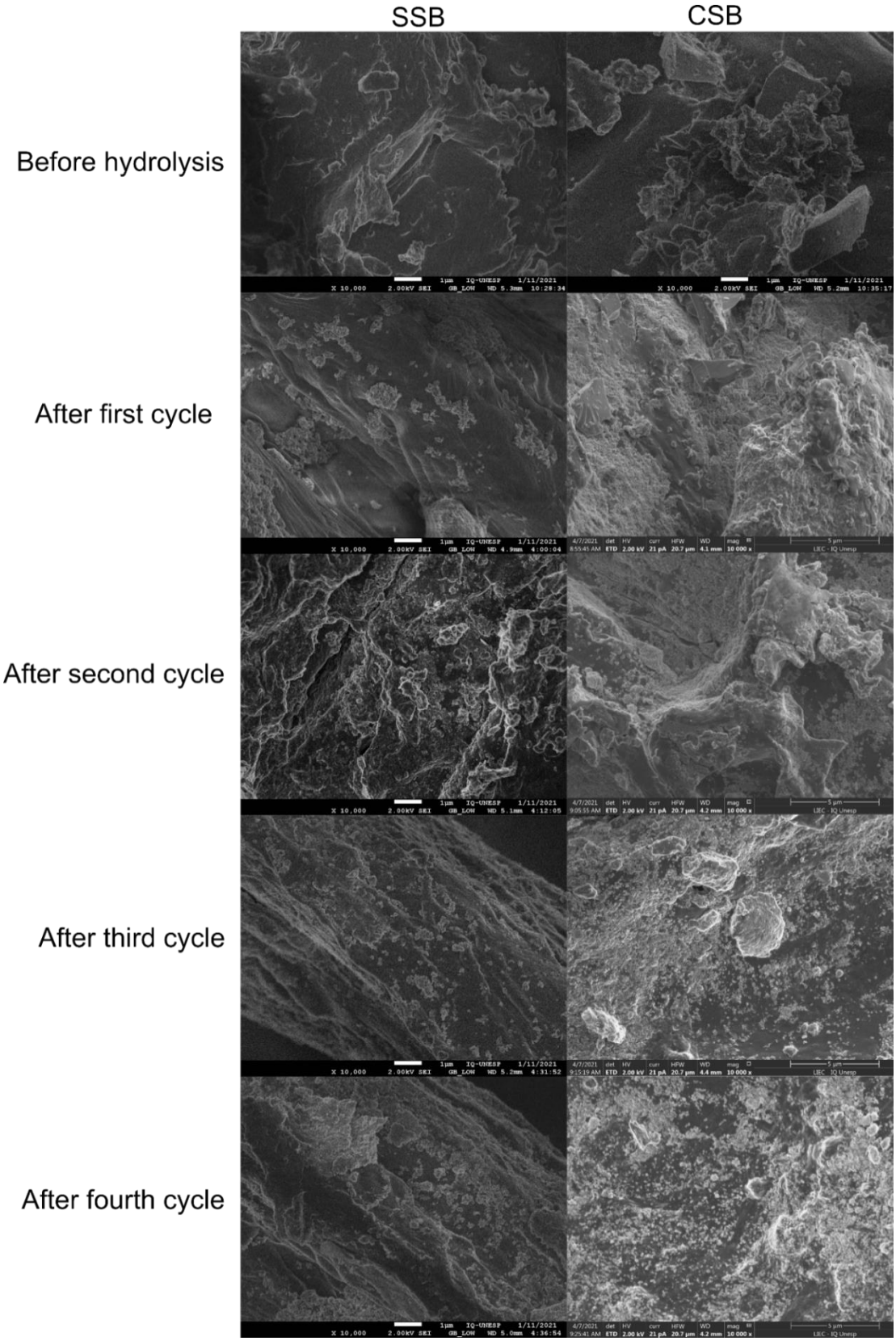

Figure 4.9. Scanning electronic microscopy images (SEM) of sulfite-NaOH pretreated (SSB) and chlorite pretreated (CSB) sugarcane bagasse (SB) before and after several hydrolysis cycles using biocatalyst GO-MNP-Enz.

CONCLUSION

The enzymes contained in the commercial Cellic CTec 2 preparation immobilized in graphene oxide-magnetite showed a similar behavior in a wide range of pH and temperature compared to the free form. The biocatalyst was stable in cold storage for 45 days, with relative enzymatic activities between 65-82%. The half-life time at operational temperature (45 °C) was higher in the immobilized enzymes compared to the free form, with the exception of endoglucanase. This indicates that immobilization favors the operational stability of the enzymes evaluated. Regarding the hydrolysis of pretreated sugarcane bagasse, it was confirmed that there was a better performance in the hydrolysis of SSB compared to CSB. This had repercussions in the reuse tests of the biocatalyst, in which it was found that after several cycles of hydrolysis of SSB, the efficiency of the biocatalyst remained at levels between 76-86%, while in the hydrolysis of CSB, the efficiency of the catalyst after four cycles of hydrolysis was between 25-32%.

Ultimately, the immobilization of enzymes in graphene oxide-magnetite showed an improvement in the operational stability of the evaluated enzymes and the biocatalyst obtained maintained a high efficiency after several hydrolysis cycles, being therefore a technically viable strategy for the hydrolysis of pretreated SB.

DECLARATIONS SECTION

List of abbreviations

(ATR-FTIR) Attenuated total reflection-Fourier Transform Infrared; (CMC) Sodium carboxymethylcellulose; (CrI) Crystallinity index; (CSB) Chlorite pretreated sugarcane bagasse; (EDC) 1-ethyl-3-(3-dimethylaminopropyl) carbodiimide; (EDX) Energy-dispersive X-ray; (FPU) Filter paper units; (GO) Graphene oxide; (GO-MNP) Graphene oxide-magnetite nanocomposite; (NHS) *N*-hydroxy-succinimide; (SEM) Scanning electron microscopy; (SB) Sugarcane bagasse *in natura*; (SSB) Sulfite-NaOH pretreated sugarcane bagasse; (XRD) X-ray diffractogram.

Ethical Approval and Consent to participate

Not applicable.

Consent for publication

All authors read and approved the final manuscript.

Availability of supporting data

We are providing a document with supplementary information.

Conflicts of interest

There are no conflicts to declare.

Funding

São Paulo State Research Support Foundation (FAPESP) contract number 2018/06241-3 funding this work. Coordination of Improvement of Higher Education Personnel (CAPES) funding the doctoral scholarship of Fernando Roberto Paz-Cedeno in Brazil and in the Universitat Politècnica de València (UPV), Institute of Chemical Technology (ITQ), Valencia, Spain. Authors acknowledge financial support from PGC2018-097277-B-100(MCIU/AEI/FEDER,UE) project and Severo Ochoa Program (SEV-2016-0683).

CRediT authorship contribution statement

Fernando Roberto Paz Cedeno: Conceptualization, Investigation, Methodology, Writing - original draft, Writing - review & editing. **Jose Miguel Carceller:** Methodology, Writing - review & editing. **Sara Iborra:** Supervision, Funding acquisition, Resources, Writing - review & editing. **Ricardo Keitel Donato:** Supervision, Writing - review & editing. **Eddyn Gabriel Solorzano-Chavez:** Methodology, Writing - review & editing. **Ismael Ulises Miranda Roldán:** Methodology, Writing - review & editing. **Ariela Veloso de Paula:** Writing - review & editing. **Avelino Corma:** Supervision, Funding acquisition, Writing - review & editing. **Fernando Masarin:** Conceptualization, Supervision, Funding acquisition, Resources, Writing - review & editing.

Acknowledgements

FAPESP, contract number 2018/06241-3 funding this paper. Coordination of Improvement of Higher Education Personnel (CAPES) financed the doctoral scholarship of Fernando Roberto Paz-Cedeno in Brazil and in the Universitat Politècnica de València (UPV), Institute of Chemical Technology (ITQ), Valencia, Spain. Authors acknowledge financial support from PGC2018-097277-B-100 (MCIU/AEI/FEDER,UE) project and Program Severo Ochoa (SEV-2016-0683).

REFERENCES

[1] CONAB, Acompanhamento da Safra Brasileira de Cana-de-açucar Safra 2019/20, Brasilia, 2020. doi:2318-7921.

[2] D. da S. Dos Santos, A.C. Camelo, K.C.P. Rodrigues, L.C. Carlos, N. Pereira, Ethanol Production from Sugarcane Bagasse by Zymomonas mobilis Using Simultaneous Saccharification and Fermentation (SSF) Process, Appl. Biochem. Biotechnol. 161 (2010) 93–105. doi:10.1007/s12010-009-8810-x.

[3] X. Zhao, Y. Song, D. Liu, Enzymatic hydrolysis and simultaneous saccharification and fermentation of alkali/peracetic acid-pretreated sugarcane bagasse for ethanol and 2,3-butanediol production, Enzyme Microb. Technol. 49 (2011) 413–419. doi:https://doi.org/10.1016/j.enzmictec.2011.07.003.

[4] Y. Jugwanth, Y. Sewsynker-Sukai, E.B. Gueguim Kana, Valorization of sugarcane bagasse for bioethanol production through simultaneous

saccharification and fermentation: Optimization and kinetic studies, Fuel. 262 (2020) 116552. doi:https://doi.org/10.1016/j.fuel.2019.116552.

[5] N. Sritrakul, S. Nitisinprasert, S. Keawsompong, Evaluation of dilute acid pretreatment for bioethanol fermentation from sugarcane bagasse pith, Agric. Nat. Resour. 51 (2017) 512–519. doi:https://doi.org/10.1016/j.anres.2017.12.006.

[6] Alokika, Anu, A. Kumar, V. Kumar, B. Singh, Cellulosic and hemicellulosic fractions of sugarcane bagasse: Potential, challenges and future perspective, Int. J. Biol. Macromol. 169 (2021) 564–582. doi:https://doi.org/10.1016/j.ijbiomac.2020.12.175.

[7] P. Rattanapoltee, P. Kaewkannetra, Utilization of Agricultural Residues of Pineapple Peels and Sugarcane Bagasse as Cost-Saving Raw Materials in Scenedesmus acutus for Lipid Accumulation and Biodiesel Production, Appl. Biochem. Biotechnol. 173 (2014) 1495–1510. doi:10.1007/s12010-014-0949-4.

[8] H. Su, G. Liu, M. He, F. Tan, A biorefining process: Sequential, combinational lignocellulose pretreatment procedure for improving biobutanol production from sugarcane bagasse, Bioresour. Technol. 187 (2015) 149–160. doi:https://doi.org/10.1016/j.biortech.2015.03.107.

[9] H. Li, L. Xiong, X. Chen, C. Wang, G. Qi, C. Huang, M. Luo, X. Chen, Enhanced enzymatic hydrolysis and acetone-butanol-ethanol fermentation of sugarcane bagasse by combined diluted acid with oxidate ammonolysis pretreatment, Bioresour. Technol. 228 (2017) 257–263. doi:https://doi.org/10.1016/j.biortech.2016.12.119.

[10] Z. Lai, M. Zhu, X. Yang, J. Wang, S. Li, Optimization of key factors affecting hydrogen production from sugarcane bagasse by a thermophilic anaerobic pure culture, Biotechnol. Biofuels. 7 (2014) 119. doi:10.1186/s13068-014-0119-5.

[11] R.P. Ratti, T.P. Delforno, I.K. Sakamoto, M.B.A. Varesche, Thermophilic hydrogen production from sugarcane bagasse pretreated by steam explosion and alkaline delignification, Int. J. Hydrogen Energy. 40 (2015) 6296–6306. doi:https://doi.org/10.1016/j.ijhydene.2015.03.067.

[12] D. Jiang, Z. Fang, S.X. Chin, X.F. Tian, T.C. Su, Biohydrogen Production from Hydrolysates of Selected Tropical Biomass Wastes with Clostridium Butyricum, Sci. Rep. 6 (2016) 1–11. doi:10.1038/srep27205.

[13] G. Prakash, A.J. Varma, A. Prabhune, Y. Shouche, M. Rao, Microbial production of xylitol from d-xylose and sugarcane bagasse hemicellulose using newly isolated thermotolerant yeast Debaryomyces hansenii, Bioresour. Technol. 102 (2011) 3304–3308. doi:https://doi.org/10.1016/j.biortech.2010.10.074.

[14] S. Kamat, M. Khot, S. Zinjarde, A. RaviKumar, W.N. Gade, Coupled production of single cell oil as biodiesel feedstock, xylitol and xylanase from sugarcane bagasse in a biorefinery concept using fungi from the tropical mangrove wetlands, Bioresour. Technol. 135 (2013) 246–253. doi:https://doi.org/10.1016/j.biortech.2012.11.059.

[15] L. Xu, L. Liu, S. Li, W. Zheng, Y. Cui, R. Liu, W. Sun, Xylitol Production by Candida tropicalis 31949 from Sugarcane Bagasse Hydrolysate, Sugar Tech. 21 (2019) 341–347. doi:10.1007/s12355-018-0650-y.

[16] W.G. Morais Junior, T.F. Pacheco, D. Trichez, J.R.M. Almeida, S.B. Gonçalves, Xylitol production on sugarcane biomass hydrolysate by newly identified Candida tropicalis JA2 strain, Yeast. 36 (2019) 349–361. doi:https://doi.org/10.1002/yea.3394.

[17] D. Kumar, V.K. Jain, G. Shanker, A. Srivastava, Citric acid production by solid state fermentation using sugarcane bagasse, Process Biochem. 38 (2003) 1731–1738. doi:https://doi.org/10.1016/S0032-9592(02)00252-2.

[18] E.R. Borges, N. Pereira Jr., Succinic acid production from sugarcane bagasse hemicellulose hydrolysate by Actinobacillus succinogenes, J. Ind. Microbiol. Biotechnol. 38 (2011) 1001–1011. doi:10.1007/s10295-010-0874-7.

[19] M. Nieder-Heitmann, K.F. Haigh, J.F. Görgens, Process design and economic analysis of a biorefinery co-producing itaconic acid and electricity from sugarcane bagasse and trash lignocelluloses, Bioresour. Technol. 262 (2018) 159–168. doi:https://doi.org/10.1016/j.biortech.2018.04.075.

[20] L. Peng, N. Xie, L. Guo, L. Wang, B. Yu, Y. Ma, Efficient Open Fermentative Production of Polymer-Grade L-Lactate from Sugarcane Bagasse Hydrolysate by Thermotolerant Bacillus sp. Strain P38, PLoS One. 9 (2014) e107143. https://doi.org/10.1371/journal.pone.0107143.

[21] D. Wei, X. Liu, S.-T. Yang, Butyric acid production from sugarcane bagasse hydrolysate by Clostridium tyrobutyricum immobilized in a fibrous-bed bioreactor, Bioresour. Technol. 129 (2013) 553–560.

doi:https://doi.org/10.1016/j.biortech.2012.11.065.

[22] X. Zhou, Y. Xu, Integrative process for sugarcane bagasse biorefinery to co-produce xylooligosaccharides and gluconic acid, Bioresour. Technol. 282 (2019) 81–87. doi:https://doi.org/10.1016/j.biortech.2019.02.129.

[23] Q. Li, C.-L. Ma, P.-Q. Zhang, Y.-Y. Li, X. Zhu, Y.-C. He, Effective conversion of sugarcane bagasse to furfural by coconut shell activated carbon-based solid acid for enhancing whole-cell biosynthesis of furfurylamine, Ind. Crops Prod. 160 (2021) 113169. doi:https://doi.org/10.1016/j.indcrop.2020.113169.

[24] J. Bragatto, F. Segato, F.M. Squina, Production of xylooligosaccharides (XOS) from delignified sugarcane bagasse by peroxide-HAc process using recombinant xylanase from Bacillus subtilis, Ind. Crops Prod. 51 (2013) 123–129. doi:https://doi.org/10.1016/j.indcrop.2013.08.062.

[25] F. Mandelli, L.B. Brenelli, R.F. Almeida, R. Goldbeck, L.D. Wolf, Z.B. Hoffmam, R. Ruller, G.J.M. Rocha, A.Z. Mercadante, F.M. Squina, Simultaneous production of xylooligosaccharides and antioxidant compounds from sugarcane bagasse via enzymatic hydrolysis, Ind. Crops Prod. 52 (2014) 770–775. doi:https://doi.org/10.1016/j.indcrop.2013.12.005.

[26] F.C. Barbosa, E. Kendrick, L.B. Brenelli, H.S. Arruda, G.M. Pastore, S.C. Rabelo, A. Damasio, T.T. Franco, D. Leak, R. Goldbeck, Optimization of cello-oligosaccharides production by enzymatic hydrolysis of hydrothermally pretreated sugarcane straw using cellulolytic and

oxidative enzymes, Biomass and Bioenergy. 141 (2020) 105697. doi:https://doi.org/10.1016/j.biombioe.2020.105697.

[27] J. de Cassia Pereira Scarpa, N. Paganini Marques, D. Alves Monteiro, G.M. Martins, A.V. de Paula, M. Boscolo, R. da Silva, E. Gomes, D. Alonso Bocchini, Saccharification of pretreated sugarcane bagasse using enzymes solution from Pycnoporus sanguineus MCA 16 and cellulosic ethanol production, Ind. Crops Prod. 141 (2019) 111795. doi:https://doi.org/10.1016/j.indcrop.2019.111795.

[28] F.R. Paz-Cedeno, L.R. Henares, E.G. Solorzano-Chavez, M. Scontri, F.P. Picheli, I.U. Miranda Roldán, R. Monti, S. Conceição de Oliveira, F. Masarin, Evaluation of the effects of different chemical pretreatments in sugarcane bagasse on the response of enzymatic hydrolysis in batch systems subject to high mass loads, Renew. Energy. 165 (2020). doi:10.1016/j.renene.2020.10.092.

[29] F.R. Paz-Cedeno, J.M. Carceller, S. Iborra, R.K. Donato, A.P. Godoy, A.V. De Paula, R. Monti, A. Corma, F. Masarin, Magnetic graphene oxide as a platform for the immobilization of cellulases and xylanases: ultrastructural characterization and assessment of lignocellulosic biomass hydrolysis, Renew. Energy. (2020). doi:10.1016/j.renene.2020.09.059.

[30] C. Aragon, Imobilização multipontual covalente de xilanases: seleção de derivados ativos e estabilizados, Universidade Estadual Paulista Julio de Mesquita Filho, 2013.

[31] S. Lu, Q. Wang, Z. Liang, W. Wang, C. Liang, Z. Wang, Z. Yuan, P. Lan,

W. Qi, Saccharification of sugarcane bagasse by magnetic carbon-based solid acid pretreatment and enzymatic hydrolysis, Ind. Crops Prod. 160 (2021) 113159. doi:https://doi.org/10.1016/j.indcrop.2020.113159.

[32] W.S. Hummers, R.E. Offeman, Preparation of Graphitic Oxide, J. Am. Chem. Soc. 80 (1958) 1339–1339. doi:10.1021/ja01539a017.

[33] M. Tanaka, M. Taniguchi, R. Matsuno, T. Kamikubo, Purification and Properties of Cellulases from Eupencillium javanicum : Studies on the Re-utilization of Cellulosic Resources(VII), J. Ferment. Technol. 59 (1981) 177–183. http://ci.nii.ac.jp/naid/110002672575/en/ (accessed July 26, 2016).

[34] M.J. Bailey, P. Biely, K. Poutanen, Interlaboratory testing of methods for assay of xylanase activity, J. Biotechnol. 23 (1992) 257–270. doi:10.1016/0168-1656(92)90074-J.

[35] T.K. Ghose, Measurement of cellulase activities, Pure Appl. Chem. 59 (1987) 257–268. doi:10.1351/pac198759020257.

[36] L.U.L. Tan, P. Mayers, J.N. Saddler, Purification and characterization of a thermostable xylanase from a thermophilic fungus Thermoascus aurantiacus, Can. J. Microbiol. (1987) 689–691. doi:10.1139/m87-120.

[37] M.M. Bradford, A Rapid and Sensitive Method for the Quantitation Microgram Quantities of Protein Utilizing the Principle of Protein-Dye Binding, Anal. Biochem. 254 (1976) 248–254. doi:10.1016/0003-2697(76)90527-3.

[38] R.A. Sheldon, S. van Pelt, Enzyme immobilisation in biocatalysis: Why,

what and how, Chem. Soc. Rev. 42 (2013) 6223–6235. doi:10.1039/c3cs60075k.

[39] E.P. Melo, Estabilidade de proteínas, in: J.M.S. Cabral, M.R. Aires-barros, M. Gama (Eds.), Eng. Enzimática, Lidel, Lisbon, 2003: pp. 67–120.

[40] G. Siqueira, A.M.F. Milagres, W. Carvalho, G. Koch, A. Ferraz, Topochemical distribution of lignin and hydroxycinnamic acids in sugar-cane cell walls and its correlation with the enzymatic hydrolysis of polysaccharides, Biotechnol. Biofuels. 4 (2011) 7. doi:10.1186/1754-6834-4-7.

[41] F. Masarin, D.B. Gurpilhares, D.C. Baffa, M.H. Barbosa, W. Carvalho, A. Ferraz, A.M. Milagres, Chemical composition and enzymatic digestibility of sugarcane clones selected for varied lignin content, Biotechnol. Biofuels. 4 (2011) 55. doi:10.1186/1754-6834-4-55.

[42] F. Masarin, F.R.P. Cedeno, E.G.S. Chavez, L.E. de Oliveira, V.C. Gelli, R. Monti, Chemical analysis and biorefinery of red algae Kappaphycus alvarezii for efficient production of glucose from residue of carrageenan extraction process, Biotechnol. Biofuels. 9 (2016) 122. doi:10.1186/s13068-016-0535-9.

[43] S. Park, J.O. Baker, M.E. Himmel, P.A. Parilla, D.K. Johnson, Cellulose crystallinity index: measurement techniques and their impact on interpreting cellulase performance, Biotechnol. Biofuels. 3 (2010) 10. doi:10.1186/1754-6834-3-10.

[44] N. Terinte, R. Ibbett, K. Schuster, Overview on native cellulose and

microcrystalline cellulose I structure studied by X-ray diffraction (WAXD): Comparison between measurement techniques, Lenzinger Berichte. 89 (2011).

[45] I.U.M. Roldán, A.T. Mitsuhara, J.P. Munhoz Desajacomo, L.E. de Oliveira, V.C. Gelli, R. Monti, L.V. Silva do Sacramento, F. Masarin, Chemical, structural, and ultrastructural analysis of waste from the carrageenan and sugar-bioethanol processes for future bioenergy generation, Biomass and Bioenergy. 107 (2017) 233–243. doi:10.1016/j.biombioe.2017.10.008.

[46] S.C. Oliveira, F.R. Paz-Cedeno, F. Masarin, Mathematical modeling of glucose accumulation during enzymatic hydrolysis of carrageenan waste, in: A. Silva Santos (Ed.), Avanços Científicos e Tecnológicos Em Bioprocessos, Atena Editora, 2018: pp. 97–103. doi:10.22533/at.ed.475180110.

[47] E.G. Solorzano-Chavez, F.R. Paz-Cedeno, L. Ezequiel de Oliveira, V.C. Gelli, R. Monti, S. Conceição de Oliveira, F. Masarin, Evaluation of the Kappaphycus alvarezii growth under different environmental conditions and efficiency of the enzymatic hydrolysis of the residue generated in the carrageenan processing, Biomass and Bioenergy. 127 (2019). doi:10.1016/j.biombioe.2019.105254.

[48] F.R. Paz-Cedeno, E.G. Solórzano-Chávez, L.E. de Oliveira, V.C. Gelli, R. Monti, S.C. de Oliveira, F. Masarin, Sequential Enzymatic and Mild-Acid Hydrolysis of By-Product of Carrageenan Process from Kappaphycus alvarezii, Bioenergy Res. (2019). doi:10.1007/s12155-

019-09968-7.

[49] J. Boudrant, J.M. Woodley, R. Fernandez-Lafuente, Parameters necessary to define an immobilized enzyme preparation, Process Biochem. 90 (2020) 66–80. doi:10.1016/j.procbio.2019.11.026.

[50] R.A. Sheldon, S. van Pelt, Enzyme immobilisation in biocatalysis: why, what and how, Chem Soc Rev. 42 (2013) 6223–6235. doi:10.1039/c3cs60075k.

[51] E. Poorakbar, A. Shafiee, A.A. Saboury, B.L. Rad, K. Khoshnevisan, L. Ma'mani, H. Derakhshankhah, M.R. Ganjali, M. Hosseini, Synthesis of magnetic gold mesoporous silica nanoparticles core shell for cellulase enzyme immobilization: Improvement of enzymatic activity and thermal stability, Process Biochem. 71 (2018) 92–100. doi:10.1016/j.procbio.2018.05.012.

[52] Y. Sui, Y. Cui, G. Xia, X. Peng, G. Yuan, G. Sun, A facile route to preparation of immobilized cellulase on polyurea microspheres for improving catalytic activity and stability, Process Biochem. 87 (2019) 73–82. doi:https://doi.org/10.1016/j.procbio.2019.09.002.

[53] Y. Wang, D. Chen, G. Wang, C. Zhao, Y. Ma, W. Yang, Immobilization of cellulase on styrene/maleic anhydride copolymer nanoparticles with improved stability against pH changes, Chem. Eng. J. 336 (2018) 152–159. doi:https://doi.org/10.1016/j.cej.2017.11.030.

[54] N.M. Mubarak, J.R. Wong, K.W. Tan, J.N. Sahu, E.C. Abdullah, N.S. Jayakumar, P. Ganesan, Immobilization of cellulase enzyme on functionalized multiwall carbon nanotubes, J. Mol. Catal. B Enzym. 107

(2014) 124–131. doi:10.1016/j.molcatb.2014.06.002.

[55] L. Zang, J. Qiu, X. Wu, W. Zhang, E. Sakai, Y. Wei, Preparation of magnetic chitosan nanoparticles as support for cellulase immobilization, Ind. Eng. Chem. Res. 53 (2014) 3448–3454. doi:10.1021/ie404072s.

[56] C.R.F. Terrasan, C.C. Aragon, D.C. Masui, B.C. Pessela, G. Fernandez-Lorente, E.C. Carmona, J.M. Guisan, β-xylosidase from Selenomonas ruminantium: Immobilization, stabilization, and application for xylooligosaccharide hydrolysis, Biocatal. Biotransformation. 34 (2016) 161–171. doi:10.1080/10242422.2016.1247817.

[57] T. Chen, W. Yang, Y. Guo, R. Yuan, L. Xu, Y. Yan, Enhancing catalytic performance of β-glucosidase via immobilization on metal ions chelated magnetic nanoparticles, Enzyme Microb. Technol. 63 (2014) 50–57. doi:10.1016/j.enzmictec.2014.05.008.

[58] W. Huang, S. Pan, Y. Li, L. Yu, R. Liu, Immobilization and Characterization of cellulase on hydroxy and aldehyde functionalized magnetic Fe2O3/Fe3O4 nanocomposites prepared via a novel rapid combustion process, Int. J. Biol. Macromol. 162 (2020) 845–852. doi:https://doi.org/10.1016/j.ijbiomac.2020.06.209.

[59] F.M. Mendes, G. Siqueira, W. Carvalho, A. Ferraz, A.M.F. Milagres, Enzymatic hydrolysis of chemithermomechanically pretreated sugarcane bagasse and samples with reduced initial lignin content, Biotechnol. Prog. 27 (2011) 395–401. doi:10.1002/btpr.553.

[60] G. Siqueira, A. Várnai, A. Ferraz, A.M.F. Milagres, Enhancement of cellulose hydrolysis in sugarcane bagasse by the selective removal of

lignin with sodium chlorite, Appl. Energy. 102 (2013) 399–402. doi:10.1016/j.apenergy.2012.07.029.

[61] V. Arun, E.M. Perumal, K.A. Prakash, M. Rajesh, K. Tamilarasan, Sequential fractionation and characterization of lignin and cellulose fiber from waste rice bran, J. Environ. Chem. Eng. 8 (2020) 104124. doi:https://doi.org/10.1016/j.jece.2020.104124.

[62] D. Yang, L.X. Zhong, T.Q. Yuan, X.W. Peng, R.C. Sun, Studies on the structural characterization of lignin, hemicelluloses and cellulose fractionated by ionic liquid followed by alkaline extraction from bamboo, Ind. Crops Prod. 43 (2013) 141–149. doi:10.1016/j.indcrop.2012.07.024.

[63] A.-S. Jääskeläinen, A.-M. Saariaho, J. Vyörykkä, T. Vuorinen, P. Matousek, A.W. Parker, Application of UV-Vis and resonance Raman spectroscopy to study bleaching and photoyellowing of thermomechanical pulps, 60 (2006) 231–238. doi:doi:10.1515/HF.2006.038.

[64] L. Bu, Y. Tang, Y. Gao, H. Jian, J. Jiang, Comparative characterization of milled wood lignin from furfural residues and corncob, Chem. Eng. J. 175 (2011) 176–184. doi:https://doi.org/10.1016/j.cej.2011.09.091.

[65] J. Tavares, R.M. Łukasik, T. De Paiva, F. Da Silva, Hydrothermal alkaline sulfite pretreatment in the delivery of fermentable sugars from sugarcane bagasse, New J. Chem. 42 (2018) 4474–4484. doi:10.1039/c7nj04975g.

[66] J.F. Mesquita, A. Ferraz, A. Aguiar, Alkaline-sulfite pretreatment and use of surfactants during enzymatic hydrolysis to enhance ethanol

production from sugarcane bagasse, Bioprocess Biosyst. Eng. 39 (2016) 441–448. doi:10.1007/s00449-015-1527-z.

[67] R. Terán Hilares, L. Ramos, S.S. da Silva, G. Dragone, S.I. Mussatto, J.C. dos Santos, Hydrodynamic cavitation as a strategy to enhance the efficiency of lignocellulosic biomass pretreatment, Crit. Rev. Biotechnol. 38 (2018) 483–493. doi:10.1080/07388551.2017.1369932.

[68] F.M. Mendes, D.F. Laurito, M. Bazzeggio, A. Ferraz, A.M.F. Milagres, Enzymatic digestion of alkaline-sulfite pretreated sugar cane bagasse and its correlation with the chemical and structural changes occurring during the pretreatment step, Biotechnol. Prog. 29 (2013) 890–895. doi:10.1002/btpr.1746.

[69] J.Y. Zhu, X.J. Pan, G.S. Wang, R. Gleisner, Sulfite pretreatment (SPORL) for robust enzymatic saccharification of spruce and red pine, Bioresour. Technol. 100 (2009) 2411–2418. doi:https://doi.org/10.1016/j.biortech.2008.10.057.

ANNEX: Electronic Supplementary Information

Stability of Cellic CTec2 enzymatic preparation immobilized onto magnetic graphene oxide: Assessment of hydrolysis of pretreated sugarcane bagasse

Fernando Roberto Paz-Cedeno,[*a] Jose Miguel Carceller,[b] Sara Iborra,[b] Ricardo Keitel Donato,[c] Eddyn Gabriel Solorzano-Chavez,[a] Ismael Ulises Miranda Roldán,[a] Ariela Veloso de Paula,[a] Avelino Corma[b] and Fernando Masarin[a]

[a]São Paulo State University (UNESP), School of Pharmaceutical Science (FCF), Department of Bioprocess Engineering and Biotechnology. Araraquara-SP, Brazil. 14800-903

[b]Universitat Politècnica de València (UPV), Institute of Chemical Technology (ITQ), Valencia, Spain. 46022

[c]National University of Singapore, Center for advanced 2D materials. Singapore. 117546

(*) Corresponding author

Email addresses:

FRPC: fernando.paz@unesp.br
JMC: jocarca8@upvnet.upv.es
SI: siborra@itq.upv.es
RKD: donato@nus.edu.sg
EGSC: eddyn.solorzano@unesp.br
IUMR: imiranda_3@hotmail.com
AVP: ariela.veloso@unesp.br
AC: acorma@itq.upv.es
FM: fernando.masarin@unesp.br

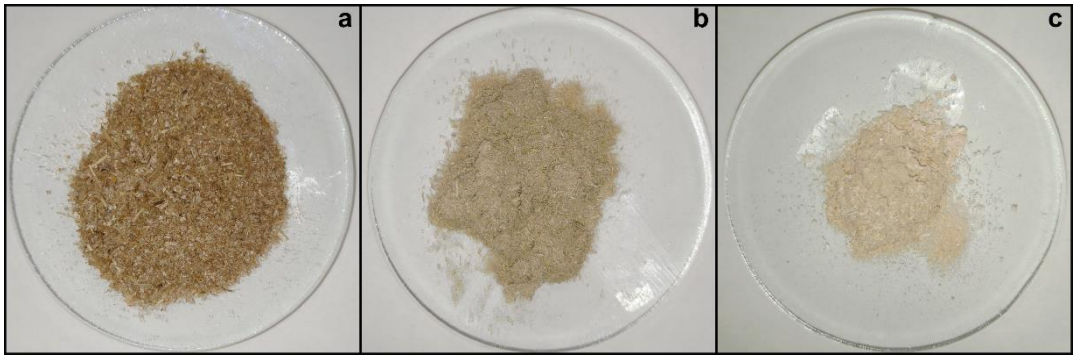

Figure 4.S1. Visual aspect of **(a)** *In natura* sugarcane bagasse (SB), **(b)** sulfite-NaOH pretreated sugarcane bagasse (SSB), **(c)** chlorite pretreated sugarcane bagasse (CSB).

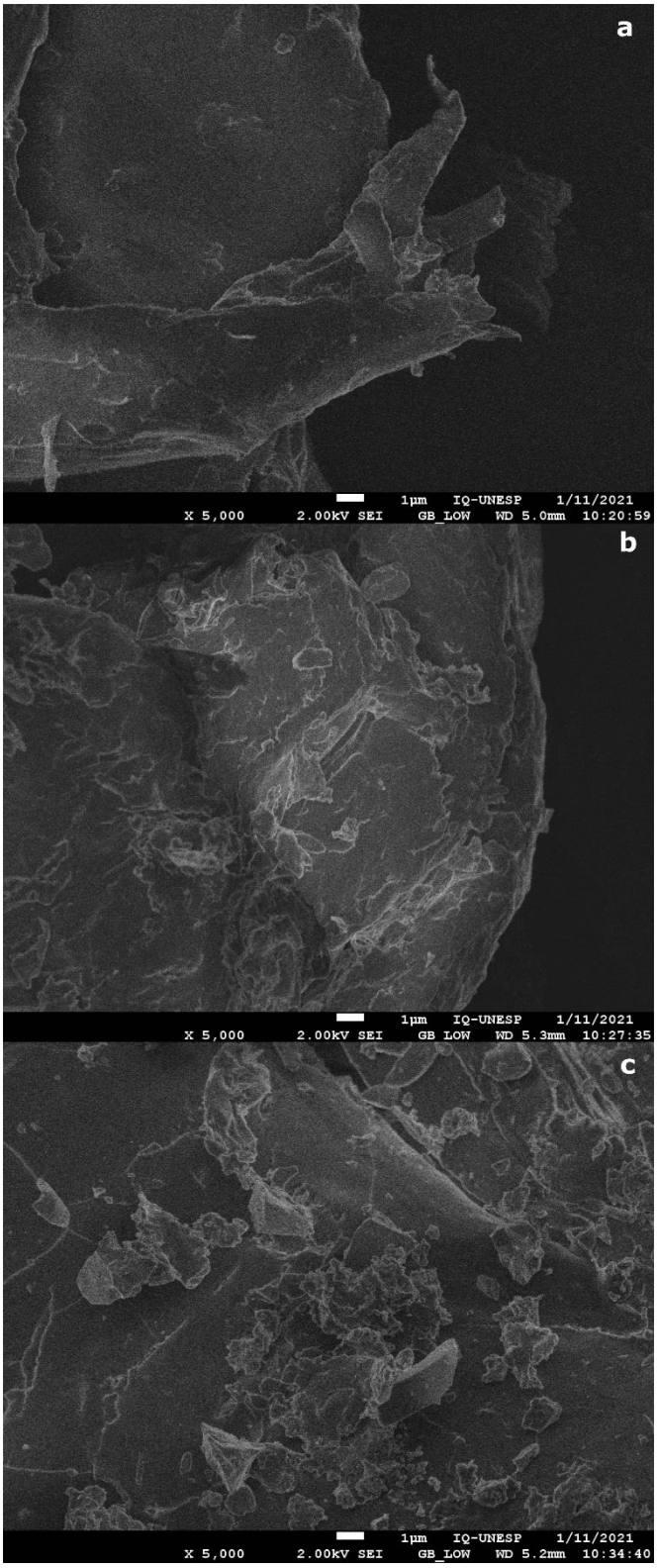

Figure 4.S2. Scanning electronic microscopy images of untreated sugarcane bagasse (SB) (a), sulfite-NaOH pretreated SB (b) and chlorite pretreated SB (c).

Table 4.S1. Characteristic bands from sugarcane bagasse (SB) in the medium infrared spectrum.

Wavenumber (cm^{-1})	Absorption band identification	Letters identifying the bands in Figure 4.4a
2924, 2854	Symmetric and asymmetric C-H (CH_2 and CH_3) stretching of alkanes, alcohols and aromatic ring	a, b
1729	Stretch C=O Hemicellulose Aldehyde/Ketone	c
1602, 1507	Lignin aromatic ring vibration C=C	d, e
1424	Aromatic skeleton combined with C-H in the plane of deformation and elongation	f
1367	Symmetrical angular deformation in the C-H plane of cellulose	g
1322	Vibration of asymmetric angular deformation (or balance) CH_2 of cellulose	h
1240	C-H in-plane deformation of lignin	i
1157	Asymmetric stretching of the C-O-C oxygen in cellulose	j
897	Glucose ring stretch, glycosidic C_1-H deformation of cellulose	k
833	Aromatic C-H out-of-plane deformation (only in GS and H lignin types)	l

5. FINAL CONSIDERATIONS

The sugarcane bagasse (SCB) was subjected to several pretreatments, of which it was possible to identify that the pretreatment with sulfite-NaOH was the one that promoted the greatest removal of lignin, considerably reducing the recalcitrance of the cellulosic fraction and hemicellulose of SCB. This allowed the enzymatic hydrolysis of SCB pretreated with sulfite-NaOH to result in better performance, both for enzymes in their free and immobilized forms.

It was possible to synthesize and characterize magnetic graphene oxide (GO-MNP) and immobilize cellulases and xylanases from the enzymatic preparation Cellic CTec 2. The biocatalyst showed a stable behavior and maintained high relative activity after 10 cycles of hydrolysis with specific substrate for endoglucanase, xylanase, β-glycosidase and β-xylosidase, with a turnover frequency higher than that reported in the literature. In addition, immobilization favored the half-life ($t_{1/2}$) of the enzymes when evaluated in their immobilized form.

The biocatalyst proved to be efficient for the hydrolysis of SCB pretreated with sulfite-NaOH, and after 4 cycles of hydrolysis, the efficiency was maintained at approximately 80%. However, when the hydrolysis of SCB pretreated with sodium chlorite was evaluated, the efficiency decreased to approximately 30%, after 4 cycles. This highlights the importance of pre-treatment for enzymatic hydrolysis.

Thus, the immobilization of cellulases and xylanases in GO-MNP by the method described in this study, proved to be technically feasible, in addition to

improving the thermal stability of the enzymes and promoting high hydrolysis efficiency after several cycles.

Collaborations

During the development of this research project, the doctoral student did an internship at the MackGraphe Graphene and Nanomaterials Research Center at Mackenzie Presbyterian University under the supervision of Professor Dr. Ricardo Keitel Donato. In addition, the doctoral student carried out an internship abroad, which allowed to expand collaboration with the research group on hybrid materials of the Institute of Chemical Technology of the Universitat Politècnica de València (ITQ-UPV). This led to the signing of a collaboration agreement between UNESP and the ITQ-UPV published in the *Diário Oficial do Estado de São Paulo* on December 22, 2020 (*Convênio 2100.0243-TA*).

Finally, it is noteworthy that, besides the published articles, this study generated the request of an application for patent entitled: *Processo de imobilização simultânea de celulases e xilanases sobre óxido de grafeno magnético e uso do mesmo*. The request was made on a joint basis between UNESP and ITQ-UPV. The request received a positive patentability opinion by the UNESP Innovation Agency (*Agência de Inovação* - AUIN) (code: 19CI202) and currently awaiting deposit at the National Institute of Industrial Property (*Instituto Nacional da Propriedade Industrial* - INPI).

6. REFERENCES

[1] CONAB, Acompanhamento da Safra Brasileira de Cana-de-açucar Safra 2019/20, Brasilia, 2020. doi:2318-7921.

[2] D. da S. Dos Santos, A.C. Camelo, K.C.P. Rodrigues, L.C. Carlos, N. Pereira, Ethanol Production from Sugarcane Bagasse by Zymomonas mobilis Using Simultaneous Saccharification and Fermentation (SSF) Process, Appl. Biochem. Biotechnol. 161 (2010) 93–105. doi:10.1007/s12010-009-8810-x.

[3] X. Zhao, Y. Song, D. Liu, Enzymatic hydrolysis and simultaneous saccharification and fermentation of alkali/peracetic acid-pretreated sugarcane bagasse for ethanol and 2,3-butanediol production, Enzyme Microb. Technol. 49 (2011) 413–419. doi:https://doi.org/10.1016/j.enzmictec.2011.07.003.

[4] Y. Jugwanth, Y. Sewsynker-Sukai, E.B. Gueguim Kana, Valorization of sugarcane bagasse for bioethanol production through simultaneous saccharification and fermentation: Optimization and kinetic studies, Fuel. 262 (2020) 116552. doi:https://doi.org/10.1016/j.fuel.2019.116552.

[5] N. Sritrakul, S. Nitisinprasert, S. Keawsompong, Evaluation of dilute acid pretreatment for bioethanol fermentation from sugarcane bagasse pith, Agric. Nat. Resour. 51 (2017) 512–519. doi:https://doi.org/10.1016/j.anres.2017.12.006.

[6] Alokika, Anu, A. Kumar, V. Kumar, B. Singh, Cellulosic and hemicellulosic fractions of sugarcane bagasse: Potential, challenges

and future perspective, Int. J. Biol. Macromol. 169 (2021) 564–582. doi:https://doi.org/10.1016/j.ijbiomac.2020.12.175.

[7] P. Rattanapoltee, P. Kaewkannetra, Utilization of Agricultural Residues of Pineapple Peels and Sugarcane Bagasse as Cost-Saving Raw Materials in Scenedesmus acutus for Lipid Accumulation and Biodiesel Production, Appl. Biochem. Biotechnol. 173 (2014) 1495–1510. doi:10.1007/s12010-014-0949-4.

[8] H. Su, G. Liu, M. He, F. Tan, A biorefining process: Sequential, combinational lignocellulose pretreatment procedure for improving biobutanol production from sugarcane bagasse, Bioresour. Technol. 187 (2015) 149–160. doi:https://doi.org/10.1016/j.biortech.2015.03.107.

[9] H. Li, L. Xiong, X. Chen, C. Wang, G. Qi, C. Huang, M. Luo, X. Chen, Enhanced enzymatic hydrolysis and acetone-butanol-ethanol fermentation of sugarcane bagasse by combined diluted acid with oxidate ammonolysis pretreatment, Bioresour. Technol. 228 (2017) 257–263. doi:https://doi.org/10.1016/j.biortech.2016.12.119.

[10] Z. Lai, M. Zhu, X. Yang, J. Wang, S. Li, Optimization of key factors affecting hydrogen production from sugarcane bagasse by a thermophilic anaerobic pure culture, Biotechnol. Biofuels. 7 (2014) 119. doi:10.1186/s13068-014-0119-5.

[11] R.P. Ratti, T.P. Delforno, I.K. Sakamoto, M.B.A. Varesche, Thermophilic hydrogen production from sugarcane bagasse pretreated by steam explosion and alkaline delignification, Int. J. Hydrogen Energy. 40 (2015)

6296–6306. doi:https://doi.org/10.1016/j.ijhydene.2015.03.067.

[12] D. Jiang, Z. Fang, S.X. Chin, X.F. Tian, T.C. Su, Biohydrogen Production from Hydrolysates of Selected Tropical Biomass Wastes with Clostridium Butyricum, Sci. Rep. 6 (2016) 1–11. doi:10.1038/srep27205.

[13] G. Prakash, A.J. Varma, A. Prabhune, Y. Shouche, M. Rao, Microbial production of xylitol from d-xylose and sugarcane bagasse hemicellulose using newly isolated thermotolerant yeast Debaryomyces hansenii, Bioresour. Technol. 102 (2011) 3304–3308. doi:https://doi.org/10.1016/j.biortech.2010.10.074.

[14] S. Kamat, M. Khot, S. Zinjarde, A. RaviKumar, W.N. Gade, Coupled production of single cell oil as biodiesel feedstock, xylitol and xylanase from sugarcane bagasse in a biorefinery concept using fungi from the tropical mangrove wetlands, Bioresour. Technol. 135 (2013) 246–253. doi:https://doi.org/10.1016/j.biortech.2012.11.059.

[15] L. Xu, L. Liu, S. Li, W. Zheng, Y. Cui, R. Liu, W. Sun, Xylitol Production by Candida tropicalis 31949 from Sugarcane Bagasse Hydrolysate, Sugar Tech. 21 (2019) 341–347. doi:10.1007/s12355-018-0650-y.

[16] W.G. Morais Junior, T.F. Pacheco, D. Trichez, J.R.M. Almeida, S.B. Gonçalves, Xylitol production on sugarcane biomass hydrolysate by newly identified Candida tropicalis JA2 strain, Yeast. 36 (2019) 349–361. doi:https://doi.org/10.1002/yea.3394.

[17] D. Kumar, V.K. Jain, G. Shanker, A. Srivastava, Citric acid production by solid state fermentation using sugarcane bagasse, Process Biochem.

38 (2003) 1731–1738. doi:https://doi.org/10.1016/S0032-9592(02)00252-2.

[18] E.R. Borges, N. Pereira Jr., Succinic acid production from sugarcane bagasse hemicellulose hydrolysate by Actinobacillus succinogenes, J. Ind. Microbiol. Biotechnol. 38 (2011) 1001–1011. doi:10.1007/s10295-010-0874-7.

[19] M. Nieder-Heitmann, K.F. Haigh, J.F. Görgens, Process design and economic analysis of a biorefinery co-producing itaconic acid and electricity from sugarcane bagasse and trash lignocelluloses, Bioresour. Technol. 262 (2018) 159–168. doi:https://doi.org/10.1016/j.biortech.2018.04.075.

[20] L. Peng, N. Xie, L. Guo, L. Wang, B. Yu, Y. Ma, Efficient Open Fermentative Production of Polymer-Grade L-Lactate from Sugarcane Bagasse Hydrolysate by Thermotolerant Bacillus sp. Strain P38, PLoS One. 9 (2014) e107143. https://doi.org/10.1371/journal.pone.0107143.

[21] D. Wei, X. Liu, S.-T. Yang, Butyric acid production from sugarcane bagasse hydrolysate by Clostridium tyrobutyricum immobilized in a fibrous-bed bioreactor, Bioresour. Technol. 129 (2013) 553–560. doi:https://doi.org/10.1016/j.biortech.2012.11.065.

[22] X. Zhou, Y. Xu, Integrative process for sugarcane bagasse biorefinery to co-produce xylooligosaccharides and gluconic acid, Bioresour. Technol. 282 (2019) 81–87. doi:https://doi.org/10.1016/j.biortech.2019.02.129.

[23] Q. Li, C.-L. Ma, P.-Q. Zhang, Y.-Y. Li, X. Zhu, Y.-C. He, Effective conversion of sugarcane bagasse to furfural by coconut shell activated carbon-based solid acid for enhancing whole-cell biosynthesis of furfurylamine, Ind. Crops Prod. 160 (2021) 113169. doi:https://doi.org/10.1016/j.indcrop.2020.113169.

[24] J. Bragatto, F. Segato, F.M. Squina, Production of xylooligosaccharides (XOS) from delignified sugarcane bagasse by peroxide-HAc process using recombinant xylanase from Bacillus subtilis, Ind. Crops Prod. 51 (2013) 123–129. doi:https://doi.org/10.1016/j.indcrop.2013.08.062.

[25] F. Mandelli, L.B. Brenelli, R.F. Almeida, R. Goldbeck, L.D. Wolf, Z.B. Hoffmam, R. Ruller, G.J.M. Rocha, A.Z. Mercadante, F.M. Squina, Simultaneous production of xylooligosaccharides and antioxidant compounds from sugarcane bagasse via enzymatic hydrolysis, Ind. Crops Prod. 52 (2014) 770–775. doi:https://doi.org/10.1016/j.indcrop.2013.12.005.

[26] F.C. Barbosa, E. Kendrick, L.B. Brenelli, H.S. Arruda, G.M. Pastore, S.C. Rabelo, A. Damasio, T.T. Franco, D. Leak, R. Goldbeck, Optimization of cello-oligosaccharides production by enzymatic hydrolysis of hydrothermally pretreated sugarcane straw using cellulolytic and oxidative enzymes, Biomass and Bioenergy. 141 (2020) 105697. doi:https://doi.org/10.1016/j.biombioe.2020.105697.

[27] J. de Cassia Pereira Scarpa, N. Paganini Marques, D. Alves Monteiro, G.M. Martins, A.V. de Paula, M. Boscolo, R. da Silva, E. Gomes, D.

Alonso Bocchini, Saccharification of pretreated sugarcane bagasse using enzymes solution from Pycnoporus sanguineus MCA 16 and cellulosic ethanol production, Ind. Crops Prod. 141 (2019) 111795. doi:https://doi.org/10.1016/j.indcrop.2019.111795.

[28] F.R. Paz-Cedeno, L.R. Henares, E.G. Solorzano-Chavez, M. Scontri, F.P. Picheli, I.U. Miranda Roldán, R. Monti, S. Conceição de Oliveira, F. Masarin, Evaluation of the effects of different chemical pretreatments in sugarcane bagasse on the response of enzymatic hydrolysis in batch systems subject to high mass loads, Renew. Energy. 165 (2020). doi:10.1016/j.renene.2020.10.092.

[29] F.R. Paz-Cedeno, J.M. Carceller, S. Iborra, R.K. Donato, A.P. Godoy, A.V. De Paula, R. Monti, A. Corma, F. Masarin, Magnetic graphene oxide as a platform for the immobilization of cellulases and xylanases: ultrastructural characterization and assessment of lignocellulosic biomass hydrolysis, Renew. Energy. (2020). doi:10.1016/j.renene.2020.09.059.

[30] F.M. Mendes, G. Siqueira, W. Carvalho, A. Ferraz, A.M.F. Milagres, Enzymatic hydrolysis of chemithermomechanically pretreated sugarcane bagasse and samples with reduced initial lignin content, Biotechnol. Prog. 27 (2011) 395–401. doi:10.1002/btpr.553.

[31] S. Lu, Q. Wang, Z. Liang, W. Wang, C. Liang, Z. Wang, Z. Yuan, P. Lan, W. Qi, Saccharification of sugarcane bagasse by magnetic carbon-based solid acid pretreatment and enzymatic hydrolysis, Ind. Crops

Prod. 160 (2021) 113159. doi:https://doi.org/10.1016/j.indcrop.2020.113159.

[32] J. Tavares, R.M. Łukasik, T. De Paiva, F. Da Silva, Hydrothermal alkaline sulfite pretreatment in the delivery of fermentable sugars from sugarcane bagasse, New J. Chem. 42 (2018) 4474–4484. doi:10.1039/c7nj04975g.

[33] M.E. Himmel, S.-Y. Ding, D.K. Johnson, W.S. Adney, M.R. Nimlos, J.W. Brady, T.D. Foust, Biomass recalcitrance: engineering plants and enzymes for biofuels production., Science. 315 (2007) 804–7. doi:10.1126/science.1137016.

[34] V.L. Sirisha, A. Jain, A. Jain, Enzyme Immobilization: An Overview on Methods, Support Material, and Applications of Immobilized Enzymes, Adv. Food Nutr. Res. 79 (2016) 179–211. doi:10.1016/bs.afnr.2016.07.004.

[35] C. Aragon, Imobilização multipontual covalente de xilanases: seleção de derivados ativos e estabilizados, Universidade Estadual Paulista Julio de Mesquita Filho, 2013.

[36] J. Zhang, J. Zhang, F. Zhang, H. Yang, X. Huang, H. Liu, S. Guo, Graphene oxide as a matrix for enzyme immobilization, Langmuir. 26 (2010) 6083–6085. doi:10.1021/la904014z.

[37] E. Doustkhah, S. Rostamnia, Covalently bonded sulfonic acid magnetic graphene oxide: Fe3O4@GO-Pr-SO3H as a powerful hybrid catalyst for synthesis of indazolophthalazinetriones, J. Colloid Interface Sci. 478

(2016) 280–287. doi:10.1016/j.jcis.2016.06.020.

[38] M. Heidarizadeh, E. Doustkhah, S. Rostamnia, P.F. Rezaei, F.D. Harzevili, B. Zeynizadeh, Dithiocarbamate to modify magnetic graphene oxide nanocomposite (Fe3O4-GO): A new strategy for covalent enzyme (lipase) immobilization to fabrication a new nanobiocatalyst for enzymatic hydrolysis of PNPD, Int. J. Biol. Macromol. 101 (2017) 696–702. doi:10.1016/j.ijbiomac.2017.03.152.

[39] de O.J.S. Pellegrini L.F., Combined production of sugar,ethanol and electricity: Thermoeconomic and environmental analysis and optimization, Energy. 36 (2011) 3704–3715. doi:10.1016/j.energy.2010.08.011.

[40] J.A. Scaramucci, C. Perin, P. Pulino, O.F.J.G. Bordoni, M.P. da Cunha, L.A.B. Cortez, Energy from sugarcane bagasse under electricity rationing in Brazil: A computable general equilibrium model, Energy Policy. 34 (2006) 986–992. doi:10.1016/j.enpol.2004.08.052.

[41] E.F. Grisi, J.M. Yusta, R. Dufo-López, Opportunity costs for bioelectricity sales in Brazilian sucro-energetic industries, Appl. Energy. 92 (2012) 860–867. doi:10.1016/j.apenergy.2011.08.045.

[42] D. Mohan, C.U. Pittman, P.H. Steele, Pyrolysis of wood/biomass for bio-oil: A critical review, Energy and Fuels. 20 (2006) 848–889. doi:10.1021/ef0502397.

[43] M.J. Taherzadeh, K. Karimi, Pretreatment of lignocellulosic wastes to improve ethanol and biogas production: A review, 2008.

doi:10.3390/ijms9091621.

[44] F.A. Santos, J.H. De Queiróz, J.L. Colodette, S.A. Fernandes, V.M. Guimaraes, S.T. Rezende, Potential of sugarcane straw for ethanol production , Potencial Da Palha Cana-de-Açúcar Para Produção Etanol. 35 (2012) 1004–1010. doi:10.1590/S0100-40422012000500025.

[45] P.L. Dhepe, A. Fukuoka, Cellulose Conversion under Heterogeneous Catalysis, ChemSusChem. 1 (2008) 969–975. doi:10.1002/cssc.200800129.

[46] L.P. Ramos, The chemistry involved in the steam treatment of lignocellulosic materials, Quim. Nova. 26 (2003) 863–871. doi:10.1590/S0100-40422003000600015.

[47] B.U. Stambuk, E.C.A. Eleutherio, L.M. Florez-Pardo, A.M. Souto-Maior, E.P.S. Bon, Brazilian potential for biomass ethanol: Challenge of using hexose and pentose cofermenting yeast strains, J. Sci. Ind. Res. (India). 67 (2008). http://sci-hub.cc/http://nopr.niscair.res.in/handle/123456789/2420.

[48] F. Peng, P. Peng, F. Xu, R.C. Sun, Fractional purification and bioconversion of hemicelluloses, Biotechnol. Adv. 30 (2012) 879–903. doi:10.1016/j.biotechadv.2012.01.018.

[49] M.S. BUCKERIDGE, W.D. SANTOS, A.P. SOUZA, As rotas para o etanol celulósico no Brasil, in: Bioetanol Da Cana-de-Açúcar P&D Para Prod. e Sustentabilidade, Sao Paulo, 2010: pp. 365–380.

[50] M. Ek, G. Gellerstedt, G. Henriksson, Pulp and Paper Chemistry and Technology - Volume 1 - Wood Chemistry and Wood Biotechnology, 2nd ed., Walter de Gruyter, Berlin, 2009.

[51] J. Ralph, K. Lundquist, G. Brunow, F. Lu, H. Kim, P.F. Schatz, J.M. Marita, R.D. Hatfield, S.A. Ralph, J.H. Christensen, W. Boerjan, Lignins: Natural polymers from oxidative coupling of 4-hydroxyphenyl-propanoids, Phytochem. Rev. 3 (2004) 29–60. doi:10.1023/B:PHYT.0000047809.65444.a4.

[52] S.P.S. Chundawat, G.T. Beckham, M.E. Himmel, B.E. Dale, Deconstruction of lignocellulosic biomass to fuels and chemicals, Annu. Rev. Chem. Biomol. Eng. 2 (2011) 121–45. doi:10.1146/annurev-chembioeng-061010-114205.

[53] Y. Zha, P.J. Punt, Exometabolomics approaches in studying the application of lignocellulosic biomass as fermentation feedstock., Metabolites. 3 (2013) 119–43. doi:10.3390/metabo3010119.

[54] Y. Pu, M. Kosa, U.C. Kalluri, G.A. Tuskan, A.J. Ragauskas, Challenges of the utilization of wood polymers: How can they be overcome?, Appl. Microbiol. Biotechnol. 91 (2011) 1525–1536. doi:10.1007/s00253-011-3350-z.

[55] R.D. Hatfield, J. Ralph, J.H. Grabber, Cell wall cross-linking by ferulates and diferulates in grasses, J. Sci. Food Agric. J Sci Food Agric. 79 (1999) 403–407. doi:10.1002/(SICI)1097-0010(19990301)79:3<403::AID-JSFA263>3.0.CO;2-0.

[56] F. Xu, R.C. Sun, J.X. Sun, C.F. Liu, B.H. He, J.S. Fan, Determination of cell wall ferulic and p-coumaric acids in sugarcane bagasse, Anal. Chim. Acta. 552 (2005) 207–217. doi:10.1016/j.aca.2005.07.037.

[57] Z. Xu, F. Huang, Pretreatment Methods for Bioethanol Production, Appl. Biochem. Biotechnol. 174 (2014) 43–62. doi:10.1007/s12010-014-1015-y.

[58] S. Niju, M. Swathika, Delignification of sugarcane bagasse using pretreatment strategies for bioethanol production, Biocatal. Agric. Biotechnol. 20 (2019) 101263. doi:https://doi.org/10.1016/j.bcab.2019.101263.

[59] S.C. Rabelo, N.A. Amezquita Fonseca, R.R. Andrade, R. Maciel Filho, A.C. Costa, Ethanol production from enzymatic hydrolysis of sugarcane bagasse pretreated with lime and alkaline hydrogen peroxide, Biomass and Bioenergy. 35 (2011) 2600–2607. doi:10.1016/j.biombioe.2011.02.042.

[60] N.N. Deshavath, V.V. Dasu, V. V Goud, P.S. Rao, Development of dilute sulfuric acid pretreatment method for the enhancement of xylose fermentability, Biocatal. Agric. Biotechnol. 11 (2017) 224–230. doi:https://doi.org/10.1016/j.bcab.2017.07.012.

[61] M. Ek, G. Gellerstedt, G. Henriksson, Pulp and Paper Chemistry and Technology - Volume 2 - Pulping Chemistry and Technology, Walter de Gruyter, Berlin, 2009.

[62] L.J. Jönsson, C. Martín, Pretreatment of lignocellulose: Formation of

inhibitory by-products and strategies for minimizing their effects, Bioresour. Technol. 199 (2016) 103–112. doi:10.1016/j.biortech.2015.10.009.

[63] D.B. Wilson, Cellulases, Encycl. Microbiol. (Third Ed. (2009) 252–258.

[64] D.B. Wilson, Cellulases and biofuels, Curr. Opin. Biotechnol. 20 (2009) 295–299. doi:10.1016/j.copbio.2009.05.007.

[65] J. Xiang, X. Wang, T. Sang, Cellulase production from Trichoderma reesei RUT C30 induced by continuous feeding of steam-exploded Miscanthus lutarioriparius, Ind. Crops Prod. 160 (2021) 113129. doi:https://doi.org/10.1016/j.indcrop.2020.113129.

[66] S.P. Faria, G.R. de Melo, L.C. Cintra, L.P. Ramos, R.S. Amorim Jesuino, C.J. Ulhoa, F.P. de Faria, Production of cellulases and xylanases by Humicola grisea var. thermoidea and application in sugarcane bagasse arabinoxylan hydrolysis, Ind. Crops Prod. 158 (2020) 112968. doi:https://doi.org/10.1016/j.indcrop.2020.112968.

[67] N. Srivastava, P.K. Mishra, S.N. Upadhyay, Microbial cellulase production, in: N. Srivastava, P.K. Mishra, S.N. Upadhyay (Eds.), Ind. Enzym. Biofuels Prod., Elsevier, 2020: pp. 19–35. doi:https://doi.org/10.1016/B978-0-12-821010-9.00002-4.

[68] B.P. Prajapati, R. Kumar Suryawanshi, S. Agrawal, M. Ghosh, N. Kango, Characterization of cellulase from Aspergillus tubingensis NKBP-55 for generation of fermentable sugars from agricultural residues, Bioresour. Technol. 250 (2018) 733–740.

doi:https://doi.org/10.1016/j.biortech.2017.11.099.

[69] L.F. Martins, D. Kolling, M. Camassola, A.J.P. Dillon, L.P. Ramos, Comparison of Penicillium echinulatum and Trichoderma reesei cellulases in relation to their activity against various cellulosic substrates, Bioresour. Technol. 99 (2008) 1417–1424. doi:10.1016/j.biortech.2007.01.060.

[70] W. Liu, W. Zhu, Y. Lu, J. Kong, G. Ma, Production, partial purification and characterization of xylanase from Trichosporon cutaneum SL409, Process Biochem. 33 (1998) 331–336. doi:10.1016/S0032-9592(97)00071-X.

[71] W. Liu, Y. Lu, G. Ma, Induction and glucose repression of endo-?-xylanase in the yeast Trichosporon cutaneum SL409, Process Biochem. 34 (1999) 67–72. doi:10.1016/S0032-9592(98)00071-5.

[72] A. Sunna, G. Antranikian, Xylanolytic Enzymes from Fungi and Bacteria, Crit. Rev. Biotechnol. 17 (1997) 39–67. doi:10.3109/07388559709146606.

[73] P. Bajpai, Xylanases, in: Encycl. Microbiol., 2009: pp. 600–612. doi:10.1016/B978-012373944-5.00165-6.

[74] P. Bajpai, Chapter 3 – Microbial Xylanolytic Systems and Their Properties, in: Xylanolytic Enzym., 2014: pp. 19–36. doi:10.1016/B978-0-12-801020-4.00003-2.

[75] K. Patel, P. Dudhagara, Optimization of xylanase production by Bacillus

tequilensis strain UD-3 using economical agricultural substrate and its application in rice straw pulp bleaching, Biocatal. Agric. Biotechnol. 30 (2020) 101846. doi:https://doi.org/10.1016/j.bcab.2020.101846.

[76] P.O. da Silva, N.C. de Alencar Guimarães, J.D.M. Serpa, D.C. Masui, C.R. Marchetti, N.V. Verbisck, F.F. Zanoelo, R. Ruller, G.C. Giannesi, Application of an endo-xylanase from Aspergillus japonicus in the fruit juice clarification and fruit peel waste hydrolysis, Biocatal. Agric. Biotechnol. 21 (2019) 101312. doi:https://doi.org/10.1016/j.bcab.2019.101312.

[77] A.C. da Costa, G.F. Cavalheiro, E.R. de Q. Vieira, J.R. Gandra, R.H. de T. e B. de Goes, M.F. da Paz, G.G. Fonseca, R.S.R. Leite, Catalytic properties of xylanases produced by Trichoderma piluliferum and Trichoderma viride and their application as additives in bovine feeding, Biocatal. Agric. Biotechnol. 19 (2019) 101161. doi:https://doi.org/10.1016/j.bcab.2019.101161.

[78] Z. Chen, A.A. Zaky, Y. Liu, Y. Chen, L. Liu, S. Li, Y. Jia, Purification and characterization of a new xylanase with excellent stability from Aspergillus flavus and its application in hydrolyzing pretreated corncobs, Protein Expr. Purif. 154 (2019) 91–97. doi:https://doi.org/10.1016/j.pep.2018.10.006.

[79] U.S.P. Uday, P. Choudhury, T.K. Bandyopadhyay, B. Bhunia, Classification, mode of action and production strategy of xylanase and its application for biofuel production from water hyacinth, Int. J. Biol.

Macromol. 82 (2016) 1041–1054. doi:https://doi.org/10.1016/j.ijbiomac.2015.10.086.

[80] A.F.A. Carvalho, F.C. de Figueiredo, T.S. Campioni, G.M. Pastore, P. de Oliva Neto, Improvement of some chemical and biological methods for the efficient production of xylanases, xylooligosaccharides and lignocellulose from sugar cane bagasse, Biomass and Bioenergy. 143 (2020) 105851. doi:https://doi.org/10.1016/j.biombioe.2020.105851.

[81] B.M. Brena, F. Batista-Viera, Immobilization of Enzymes, 2006. doi:10.1007/978-1-62703-550-7_2.

[82] W. Tischer, F. Wedekind, Immobilized Enzymes: Methods and Applications, in: W.-D. Fessner, A. Archelas, D.C. Demirjian, R. Furstoss, H. Griengl, K.-E. Jaeger, E. Morís-Varas, R. Öhrlein, M.T. Reetz, J.-L. Reymond, M. Schmidt, S. Servi, P.C. Shah, W. Tischer, F. Wedekind (Eds.), Biocatal. - From Discov. to Appl., Springer Berlin Heidelberg, Berlin, Heidelberg, 1999: pp. 95–126. doi:10.1007/3-540-68116-7_4.

[83] B. Miladi, A. El Marjou, G. Boeuf, H. Bouallagui, F. Dufour, P. Di Martino, A. Elm'selmi, Oriented immobilization of the tobacco etch virus protease for the cleavage of fusion proteins., J. Biotechnol. 158 (2012) 97–103. doi:10.1016/j.jbiotec.2012.01.010.

[84] D. Agyei, B.K. Shanbhag, L. He, Enzyme engineering (immobilization) for food applications, in: R.Y. Yada (Ed.), Improv. Tailoring Enzym. Food Qual. Funct., Woodhead Publishing, 2015: pp. 213–235.

doi:10.1016/B978-1-78242-285-3.00011-9.

[85] A.C. Puhl, C. Giacomini, G. Irazoqui, F. Batista-Viera, A. Villarino, H. Terenzi, Covalent immobilization of tobacco-etch-virus NIa protease: a useful tool for cleavage of the histidine tag of recombinant proteins, Biotechnol. Appl. Biochem. 53 (2009) 165–174. doi:10.1042/BA20080063.

[86] Q. Husain, β Galactosidases and their potential applications: a review, Crit. Rev. Biotechnol. 30 (2010) 41–62. doi:10.3109/07388550903330497.

[87] B.C. Brodie, On the atomic weight of graphite, Philos. Trans. R. Soc. London. 149 (1859) 249–259.

[88] W.S. Hummers, R.E. Offeman, Preparation of Graphitic Oxide, J. Am. Chem. Soc. 80 (1958) 1339–1339. doi:10.1021/ja01539a017.

[89] K.S. Novoselov, A.K. Geim, S. V. Morosov, D. Jiang, Y. Zhang, S. V. Dubonos, I. V. Grigorieva, A.A. Firsov, Electric Field Effect in Atomically Thin Carbon Films, 2004.

[90] S.C. Ray, Application and Uses of Graphene Oxide and Reduced Graphene Oxide, in: Appl. Graphene Graphene-Oxide Based Nanomater., Elsevier Inc., 2014: pp. 39–56. doi:10.1016/B978-0-323-37521-4.00002-9.

[91] K. Raidongia, A.T.L. Tan, J. Huang, Graphene Oxide : Some New Insights into an Old Material, in: Carbon Nanotub. Graphene, Second

Edi, Elsevier Ltd, 2014: pp. 341–374. doi:10.1016/B978-0-08-098232-8/00014-0.

[92] Y. Wang, Z. Li, J. Wang, J. Li, Y. Lin, Graphene and graphene oxide: Biofunctionalization and applications in biotechnology, Trends Biotechnol. 29 (2011) 205–212. doi:10.1016/j.tibtech.2011.01.008.

[93] H. Hashemi-Moghaddam, S. Kazemi-Bagsangani, M. Jamili, S. Zavareh, Evaluation of magnetic nanoparticles coated by 5-fluorouracil imprinted polymer for controlled drug delivery in mouse breast cancer model, Int. J. Pharm. 497 (2016) 228–238. doi:10.1016/j.ijpharm.2015.11.040.

[94] H. Jiang, D. Jiang, J. Shao, X. Sun, Magnetic molecularly imprinted polymer nanoparticles based electrochemical sensor for the measurement of Gram-negative bacterial quorum signaling molecules (N-acyl-homoserine-lactones), Biosens. Bioelectron. 75 (2016) 411–419. doi:10.1016/j.bios.2015.07.045.

[95] S. Rostamnia, E. Doustkhah, Synthesis of water-dispersed magnetic nanoparticles (H2O-DMNPs) of ?-cyclodextrin modified Fe3O4 and its catalytic application in Kabachnik?Fields multicomponent reaction, J. Magn. Magn. Mater. 386 (2015) 111–116. doi:10.1016/j.jmmm.2015.03.064.

[96] S. Rostamnia, B. Zeynizadeh, E. Doustkhah, A. Baghban, K.O. Aghbash, The use of κ-carrageenan/Fe3O4 nanocomposite as a nanomagnetic catalyst for clean synthesis of rhodanines, Catal. Commun. 68 (2015) 77–83. doi:10.1016/j.catcom.2015.05.002.

[97] K. Sbissi, V. Collière, M.L. Kahn, E.K. Hlil, M. Ellouze, F. Elhalouani, Fe doping effects on the structural, magnetic, and magnetocaloric properties of nano-sized Pr0.6Bi0.4Mn1−x Fe x O3 (0.1 ≤ x ≤ 0.3) manganites, J. Nanostructure Chem. 5 (2015) 313–323. doi:10.1007/s40097-015-0163-0.

[98] D. Li, M.B. Müller, S. Gilje, R.B. Kaner, G.G. Wallace, Processable aqueous dispersions of graphene nanosheets, Nat. Nanotechnol. 3 (2008) 101–105. doi:10.1038/nnano.2007.451.

[99] S. Park, R.S. Ruoff, Chemical methods for the production of graphenes, Nat. Nanotechnol. 4 (2009) 217–224. doi:10.1038/nnano.2009.58.